5-2003

CO2 Separation and Fuel Desulfurization Involving Room-Temperature Ionic Liquids

Benjamin Culbertson
University of Tennessee - Knoxville

To the Graduate Council:

I am submitting herewith a thesis written by Benjamin Culbertson entitled "CO2 Separation and Fuel Desulfurization Involving Room-Temperature Ionic Liquids." I have examined the final electronic copy of this thesis for form and content and recommend that it be accepted in partial fulfillment of the requirements for the degree of Master of Science, with a major in Chemical Engineering.

Dr. David DePaoli, Major Professor

We have read this thesis and recommend its acceptance:

Dr. R.M. Counce, Dr. Sheng Dai

Accepted for the Council:
Carolyn R. Hodges

Vice Provost and Dean of the Graduate School

(Original signatures are on file with official student records.)

To the Graduate Council:

I am submitting herewith a thesis written by Benjamin Culbertson entitled "CO_2 Separation and Fuel Desulfurization Involving Room-Temperature Ionic Liquids." I have examined the final electronic copy of this thesis for form and content and recommend that it be accepted in partial fulfillment of the requirements for the degree of Master of Science, with a major in Chemical Engineering.

Dr. David DePaoli
Major Professor

We have read this thesis
and recommend its acceptance:

Dr. R.M. Counce

Dr. Sheng Dai

Accepted for the Council:

Anne Mayhew
Vice Provost and
Dean of Graduate Studies

(Original signatures are on file with official student records)

CO_2 Separation and Fuel Desulfurization Involving Room-Temperature Ionic Liquids

A Thesis
Presented for the
Master of Science Degree
The University of Tennessee, Knoxville

Benjamin Culbertson
May 2003

Acknowledgements

I would like to thank the University of Tennessee and Oak Ridge National Laboratory for allowing me the opportunity to conduct this research. During the time I have spent at these institutions I have met many faculty and staff who have had a large impact on my progression through this work. Of the many people who have helped me through this project, four people stand out as having the greatest impact on my completion of this project. These people are:

Dr. Sheng Dai

Dr. R. M. Counce

Dr. Ruth Baltus

Dr. David DePaoli

Without the effort and support of these people I would not have been able to complete this project. Dr. Sheng Dai gave me confidence in myself as a researcher and was an endless source of wisdom in just about anything I questioned him. Dr. R.M. Counce helped me as a student and as a worker by extending the principles he taught in our classes to my work presented here. Dr. Ruth Baltus helped me maintain my focus and aided in developing laboratory problem solving. Dr. David DePaoli helped me realize the potential of the work I was conducting and helped me focus on the task at hand. The combined effort of these people through friendship and support have made this thesis possible.

Abstract

Imidazolium based room-temperature ionic liquids were used to investigate the technical and economic feasibility of energy-related chemical separations. The separations conducted for this work are sulfur-removal from fuels and carbon dioxide removal from flue gas emissions. In the sulfur-removal experiments, the sulfur-containing compound dibenzothiophene was removed from octane by liquid-liquid extraction, yielding partition coefficients with ionic liquid around 1.5. Attempts to regenerate the ionic liquid using vacuum filtration were not fully successful in removing dibenzothiophene; extractions with the regenerated ionic liquid had a 50% decreased capacity. For this process to become economically feasible in comparison to the currently used hydrotreating, the regenerability of the liquids will need to be further explored; in addition experiments with more realistic fuel mixtures will need to be conducted.

In the carbon dioxide removal experiments, a new quartz crystal microbalance (QCM) technique was developed and membrane studies were used to determine the solubility, diffusivity, and membrane permeability of carbon dioxide in various ionic liquids. The QCM techniques provide a rapid and inexpensive means of determining carbon dioxide solubility and diffusivity in thin ionic liquid layers. Many previously untested ionic liquids and ionic liquid mixtures were tested for carbon dioxide solubility. Of the liquids tested, most of the Henry's Law values were determined to be in the range of 35 to 50 atm. These values are in good agreement with recently published values for similar room-temperature ionic liquids. An ionic liquid containing an octyl-methyl-imidazolium cation in which 13 of the hydrogens on the octyl group were substituted with fluorine exhibited significantly greater solubility of carbon dioxide, yielding a Henry's Law value of 6 atm when combined with the Tf_2N (bis((trifluoromethyl)sulfonyl)amide) anion. CO_2 solubility in ionic liquids was also measured in the presence of water vapor. This test indicated that uptake of water at 40% relative humidity could not be said to have an impact on CO_2 solubility within the uncertainty of the QCM. The membrane studies involved measurement of the single-gas

permeance of nitrogen and carbon dioxide in a supported ionic liquid membrane (SILM). From these experiments the permeance values of CO_2 were found to be on the order of 4.06×10^{-9} mol/(atm·cm^2·s); for N_2 the permeance was on the order of 3.22×10^{-11} mol/(atm·cm^2·s). These permeance values were used to calculate a CO_2:N_2 selectivity of 127. Based on the single-gas permeance values measured for carbon dioxide and nitrogen, an economic comparison was made between amine scrubbing and ionic liquid membrane technology for use in flue gas treatment. The present preliminary values seem to indicate that the process could be competitive if the diffusivity for ionic liquid mixtures is much greater than that observed for the fluorinated liquid. Further studies with more accurate representations of flue gases and conditions are needed for a real feasibility determination; however, the preliminary values show some promise.

Table of Contents

List of Tables

List of Figures

1.0. Introduction

As environmental sustainability becomes a primary issue, newer technology is needed to replace existing inefficient processes. In an effort to pursue this goal, scientists have developed numerous instruments and chemicals to produce "greener" technology. One chemical group that has emerged from this pursuit is room-temperature ionic liquids (RTIL or IL). Room-temperature molten salts are a relatively new class of compounds that present new and exciting possibilities for restructuring our current separation technologies.

The discovery of the first RTIL, ethyl-ammonium nitrate, in 1914 by Walden did not initiate overwhelming interest in these low temperature molten salts, but with the advent of newer anions and stable imidazolium based cations, ionic liquid interest has reemerged (Gordon 2001). Two reasons RTILs have gained in interest are their versatility as solvents and their negligible vapor pressures, making them seemingly ideal substitutes for their organic counterparts. For these reasons, research has been conducted seeking to replace volatile organic solvents which typically have high vapor pressures, with low-vapor-pressure RTIL capable of performing the same tasks with little solvent loss or product contamination.

Some of the applications being studied for these ionic liquids include solvents for catalysis and biocatalysts (Lau et al 2000; Schofer et al 2001; Kim et al 2001; Cull et al 2000), media for electrodeposition of metals (Murase et al 2001), sensors for organic vapors (Liang et al 2002), materials extraction (Visser et al 2001; Bosmann et al 2001), and gas separation (Scovazzo et al 2002; Blanchard et al 2001). Most of the research conducted on ionic liquids so far has involved using the liquids for catalysis (Welton 1999). Studies of ionic liquids used for biphasic catalysis have shown that when accompanying certain reactions the reaction rate is enhanced, the selectivity is improved, and the catalyst (ionic liquid) can be reused (Gordon 2001). The studies involving organic vapor detection, materials extraction, and gas separations are all significant to the work presented here. Currently these ionic liquids are commercially available for purchase from companies such as Covalent Associates and Merck Chemical, which have

patented particular ions commonly used for ionic liquid experiments. The results of the studies to date have led to small-scale tests of RTILs in industry, however no large-scale uses have been reported. Through studying these applications it should not be difficult to discern many more potential uses for these compounds in industry.

The purpose of this project is to investigate potential uses for room-temperature ionic liquids in the field of separations. This study will focus on two categories of separations: (1) desulfurization of fuels by liquid-liquid extraction and (2) carbon dioxide separation from coal fired power plant flue gases. Both of these topics have been covered to some extent in previous literature; however, for all of the studies conducted in this project different ionic liquids have been used and alternative techniques were utilized to obtain the data (Bosmann et al 2001; Scovazzo et al 2002; Liang et al 2001). Emphasis will be focused on providing an engineering analysis into the technical feasibility of implementing ionic liquid technology in industry.

1.1. Properties of Room-Temperature Ionic Liquids

Room-temperature ionic liquids can vary in properties depending on their component anions and cations. RTILs are typically defined as salts molten below 100^{o}C. The following list outlines some general properties that have made ionic liquids an attractive solvent alternative.

1. RTILs have essentially zero vapor pressure. This property is useful in minimizing solvent losses through evaporation.
2. RTILs have a wide range of temperature stability. Ionic liquids are typically stable at temperatures below 300^{o}C. Above that temperature degradation occurs.
3. RTILs have densities and viscosities somewhat greater than water.
4. RTILs vary in hydrophobicity. Anion selection plays a large role in this property.

The characteristics of temperature stability, negligible vapor pressure, similar physical properties to traditional extraction media make room temperature ionic liquids a potential option to separation processes using organic or polymer solvents.

Organic solvents can be used in chemical synthesis or extraction reactions; however, those solvents often have high vapor pressure, thus requiring the experiments to be carried out in a closed system to prevent large solvent losses, or larger quantities of solvent to make up for evaporative losses. Solvent evaporation also poses a health risk to workers due to the carcinogenic nature of many organic solvents. Polymer solvents such as polyethylene are costly, sometimes require more planning, and are sometimes unpredictable (Stevens 1999). Cross-linking and unpredictable polymerizations can cause decreases in their separation abilities as well as add costs to replacing already expensive solvents (Stevens 1999). Ionic liquids have the potential to overcome the shortcomings of polymer and organic solvents based on the properties listed above. Using this information on the benefits of ionic liquids one could see how substituting these solvents for simple extractions utilizing organic solvents, or polymers might provide a safer and cheaper means of production.

Ionic liquids have been touted in the literature as environmentally friendly or "green" solvents. This statement is largely based on their negligible vapor pressure and not on knowledge that they interact benignly to humans or the environment when in contact. Material Safety Data Sheets (MSDS) have been posted for selected ionic liquids and can be obtained through a variety of sources, including the Merck Chemicals website. These sheets emphasize the point that little is known of the toxicity of ionic liquids. Few studies have been published in the literature explicitly stating the potential health effects of these liquids; however, the composition of many of the liquids tends to make one consider them a hazardous chemical. The toxicity studies conducted thus far seem to indicate that cation selection plays a larger role in toxicity than anion selection (Brennecke 2003). Preliminary tests conducted by Brennecke have shown the LC_{50} of BuMeIm PF_6 and BuMeIm Cl to be both approximately 25 mg/L (2003). The ionic liquids used in this project are imidazolium-based ionic liquids primarily accompanied with the bis((trifluoromethyl)sulfonyl)amide (Tf_2N) anion. By looking at the substituents

that make up these liquids we see that degradation of the cation could yield imidazole and various alkanes and degradation of the anion could yield sulfonated and fluorinated compounds. Imidazole is a carcinogen and the fluorinated compounds are highly reactive and can produce HF gas which in turn can induce asphyxia. Also, it is not known in what way these liquids might react in local ecosystems on account of the ionic nature of the liquids. The ions could deplete minerals in the soil by absorption in the same manner as acid rain acts to remove minerals from the soil to the water, thus causing plant growth reduction (Baird 1999). The potential of ionic liquid degradation may make RTILs look far from green; however, when this potential hazard is compared with the known hazards of conventional organic solvents the ionic liquid appears to be the less harmful solvent. But, keeping in mind the uncertainty of ionic liquid toxicity, the experiments conducted in this work and their proposed applications focused heavily on accounting for mass transfer of ionic liquids into solvent media and potential losses that would occur in process applications.

The class of RTIL this project focuses on is imidazolium-based ionic liquids, primarily with Tf_2N as the anion. These ionic liquids have proven to be the most popular for chemical interactions due to its ring-stabilized cation (Bonhote et al 1996). For this reason the imidazolium-based ionic liquids are used most frequently and appear more often in the literature. The basic structure of these ionic liquids can be seen in Figure 1.1. In this figure the R_1 and R_2 arms of the ionic liquid produce its versatility. The R groups can be simple alkyl chains or any number of complex branching ligands. These groups are a component in determining the stability, hydrophobicity, viscosity, and reactivity of the ionic liquid. The observed trend of the cation is that the longer the alkyl chain in the R group, the more stable the ionic charge, which has a direct effect on the liquid as an extractant (Gordon 2001).

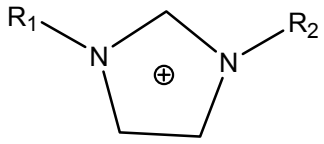

Figure 1.1: Imidazolium-Based Cation

The anion also determines these properties to a similar extent (Gordon 2001). This fact produces the possibility of an enormous amount of possible ligand, cation, and anion combinations. Several of these combinations could exhibit similar physical properties, yet have differing affinities towards certain target compounds. Using this logic one could design an ionic liquid to meet the physical demands of a process and simultaneously yield optimal separations of key compounds. The following is a list of the anions most commonly associated with imidazolium based ionic liquids based on stability and hydrophobicity (Bronco et al 2002):

Less Stable	Br,Cl < BF_4 < PF_6, Tf_2N, TfO	More Stable
Hydrophilic	Br,Cl < BF_4 < PF_6, Tf_2N, TfO	Hydrophobic

The RTIL used primarily in this project is 1-butyl-3-methyl-imidizolium Tf_2N (BuMeIm Tf_2N). Tf_2N is sparingly soluble in water and is inert in most media, thus making it an attractive anion for these studies (Seddon et al 2000). A more popular anion, PF_6, is also highly immiscible in water; however, studies have indicated a concern that HF could be produced from this anion under non-ambient conditions or on contact with water (Rogers et al 2002). Furthermore, most cations coupled with the PF_6 anion have higher viscosities than the same cations coupled with the Tf_2N anion. This increased viscosity would indicate a negative impact on the transport properties of the ionic liquids. There is also not as much published research with ionic liquids involving the Tf_2N anion as there is for other anions such as the PF_6 anion, so there is still a need for more research with these liquids. The cation BuMeIm has been studied extensively since the inception of imidazole based ionic liquids. The structure of BuMeIm Tf_2N and other ionic liquids included in this project can be found in Table 1.1. All of the ionic liquids in the table were synthesized at Oak Ridge National Laboratory by Huimin Luo. The bulk of the experiments were conducted using BuMeIm and PrMeIm Tf_2N. The remaining ionic liquids were synthesized to determine trends in removal with varying ligands and chain length. As can be seen in the gap of information in the physical properties of these liquids there is not much published data on these liquids.

Table 1.1. Structure and Properties of RTILs

1-methyl-3-propyl-imidazolium bis((trifluoromethyl)sulfonyl)amide PrMeIm Tf_2N

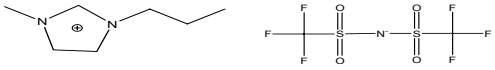

Properties: Cation MW = 125 amu, Anion MW = 280 amu, Decomposition Temperature = 452°C

1-methyl-3-butyl-imidazolium bis((trifluoromethyl)sulfonyl)amide BuMeIm Tf_2N

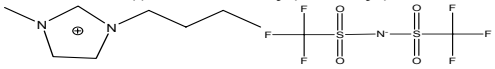

Properties: Cation MW = 139 amu, Anion MW = 280 amu, Decomposition Temperature = 439°C
Density (T=22°C) = 1.429 g/cm^2, Viscosity (T=20°C) = 52 cp, Surface Tension = 37.5 dyn/cm
Refractive Index (T=20°C) = 1.4271, Specific Conductivity (T=20°C) = 3.9 mS/cm
Saturation Water Content (T=20°C) = 1.4%

1-methyl-3-hexyl-imidazolium bis((trifluoromethyl)sulfonyl)amide HexMeIm Tf_2N

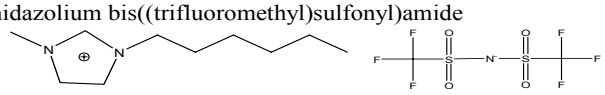

Properties: Cation MW = 167 amu, Anion MW = 280 amu

1-methyl-3-octyl-imidazolium bis((trifluoromethyl)sulfonyl)amide OctMeIm Tf_2N

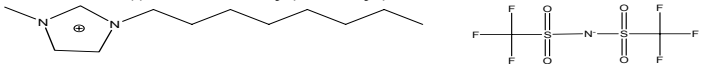

Properties: Cation MW = 195 amu, Anion MW = 280 amu

1-methyl-3-propyl-imidazolium hexafluorophosphate PrMeIm PF_6

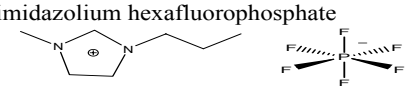

Properties: Cation MW = 139 amu, Anion MW = 145 amu

1-methyl-3-(3,3,4,4,5,5,6,6,7,7,8,8,8-tridecafluoro-octyl)-imidazolium bis((trifluoromethyl)sulfonyl)amide

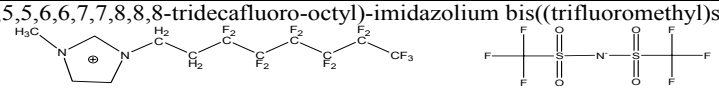

Properties: Cation MW = 432 amu, Anion MW = 280 amu

1,4-butyl-3-phenyl-imidazolium bis((trifluoromethyl)sulfonyl)amide BuPhBuIm Tf_2N

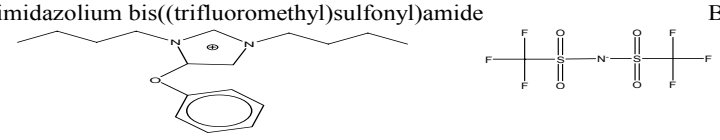

Properties: Cation MW = 497 amu, Anion MW = 280 amu

1-butyl-3-phenyl-imidazolium bis((trifluoromethyl)sulfonyl)amide BuPhIm Tf_2N

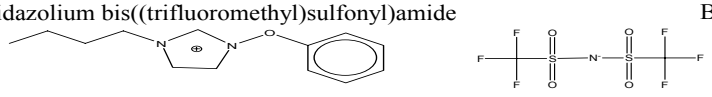

Properties: Cation MW = 217 amu, Anion MW = 280 amu

The primary reason for this data deficiency is the newness of these liquids. New cation, anion, and ligand arrangements are discovered daily. Even though the physical properties have not been quantified for many of the ionic liquids tabulated, general observations can be made based on their appearance. The following trends were observed for the ionic liquids used in this work:

1. The density and viscosity increase slightly as the alkyl chains on the cation are increased. The fluorinated cation is the most viscous of the liquids, with a consistency similar to syrup.
2. The liquids are all clear with a greenish yellow tint for the alkyl substituted cations and clear and dark red for the fluorine substituted cation.
3. The liquids seem to act similar to oils in contact with aqueous solution.

In some cases these liquids were combined with additives in an attempt to increase the desired separations. These mixtures are described in more detail in the desulfurization and carbon dioxide separation sections.

2.0. Desulfurization of Fuels

In this section, the work conducted on desulfurization of fuels using ionic liquids is presented. The first section discusses current desulfurization technology and the need for more productive desulfurizing agents to meet the new standards posed by EPA. The second section discusses experiments conducted to observe the technical feasibility of an ionic liquid desulfurization process. The third section discusses the findings of these experiments and their implications.

2.1. Summary of Modern Desulfurization Technology

Desulfurization of fuels has become a topic of recent concern with the increased environmental hazards sulfur emissions are having on the atmosphere, such as photochemical smog and acid rain. In the case of acid rain, the sulfurous gases mix with water vapor in clouds and condense with them in the form of rain as the atmosphere in the cloud becomes saturated. The resultant acid rain can irreversibly damage ecosystems by disturbing the pH of the groundwater and absorption by plants (Baird 1999). In the case of photochemical smog, the sulfurous gases accumulate in the troposphere thus blocking sunlight from reaching the earth's surface which is needed for plant photosynthesis (Baird 1999). The combustion of fuels typically used in automobiles is a large contributor to SO_x production. Sulfur in the form of compounds such as dibenzothiophene become SO_x compounds upon combustion. The simplest solution for minimizing this emission is removing the sulfur-containing compounds from the fuels prior to combustion. The Environmental Protection Agency (EPA) is decreasing the allowable sulfur standard in response to more information on the SO_x problem (EPA website 2003). The new allowable sulfur content in fuels will be 50 ppm sulfur which will be set nationally by EPA in 2005 (EPA website 2003). It is hoped that by using ionic liquid technology in this instance the ionic liquid will absorb sulfur-containing compounds without contamination of the fuels or ionic liquid solvent loss, such that

combustion of the fuels produces a negligible concentration of SO_x emissions to the atmosphere and fuel meets the DBT standard set by EPA. This measure would minimize the largest anthropogenic producer of sulfonated gases and in turn allow the recovery of ecosystems not already occupying land near natural SO_x producers such as around volcanoes (Baird 1999). In attempting to tackle this problem several mechanisms of sulfur extraction have been proposed, including standard thermochemical treatement (hydrotreating) and biodesulfurization (Kaufman et al 1998; Kim et al 2001).

Hydrotreatment is the most commonly used process for sulfur extraction prior to combustion. In this process the petroleum fuel is contacted with the Ru^{2+} compound (L)Ru(H_2O) at temperatures between $560< T(K)<670$ (Angelici et al 2001). L in this compound is a ligand which solubilizes ringed sulfur containing structures in the fuel such as thiols, thioethers and dibenzothiophenes (Kaufman et al 1998). The resultant complex (L)Ru(DBT) is then pressurized to remove the DBT for incineration or sonochemical decomposition (Kim et al 2001). This step regenerates the Ru, thus enabling large quantities of low-sulfur fuel feedstock for a small amount of extractant. The major problem with this system is that the ligands required to successfully complex with the DBT are fairly expensive and unstable. The ligands typically used in this complex include: cyclopentadiene, phosphines, and carbon monoxide. Any losses within the fuel are not only costly to replace, but can also add worse chemicals to the fuels than those targeted for removal. Furthermore, the instability of these compounds guarantees some contamination to occur. Work has been conducted to try more stable and less expensive ligands, however these results have not yielded similar removals as their currently used less stable counterparts (Angelici et al 2001). Due to this lack of information, much emphasis has been placed on finding a replacement process capable of removing large quantities of sulfurous compounds without contaminating the fuel (Angelici et al 2001).

Biodesulfurization is a relatively new approach to sulfur treatment that utilizes enzymes to decompose and remove dibenzothiophene. In this process, the sulfur-containing fuel feedstock is fed into a tank, oxidized, and decomposed using *Rhodococcus* biocatalysts (Kaufman et al 1998). The advantage this process has over

hydrotreating is that this process can be carried out at ambient temperature which reduces the operating costs. The removal involves partially oxidizing the fuel and decomposing the DBT with liquid-liquid extractions, which can take up to 8 hours for full sulfur-removing efficiency (Kaufman 1998). The sulfur reduction potential of this process seems to match that of the hydrotreatment process. However, its lack of fuel contamination and ability to be run at ambient conditions is not enough to offset the increased equipment cost and longer treatment times (Kaufman 1998).

Since neither of these methods has proven to be economically efficient in complete sulfur removal, there is still a need for alternative mechanisms. Utilization of RTIL provides one potential solution. Desulfurization of fuels using ionic liquids has been attempted by Bosmann and coworkers (2001). In their experiments they tested a number of ionic liquid cation and anion variations as well as multistage dibenzothiophene removal. The major drawbacks they have encountered are that their average error is too great for accurate partition coefficient calculations at their target DBT concentrations, that they achieve their greatest removal rates with chlorinated ionic liquid mixtures such as BuMeIm $AlCl_3$, which are not only expensive but highly unstable at high temperatures, they are not able to regenerate the ionic liquid after extraction, and they have not identified an ionic liquid with exceptional removal capabilities. Based on their results they have shown that ionic liquids can remove DBT from fuel, that as ion size increases so to does extraction ability, and that multistage-extractions could accomplish the goal of 50 ppm S. The best partitioning they received was a distribution coefficient of 2.25 with a .35/.65 BuMeIm $Cl/AlCl_3$ molar mixture; however, most of their results were closer to 0.84 as achieved by BuMeIm BF_4. These numbers represent the partition or distribution coefficient observed in the liquid-liquid extractions. The distribution coefficient, which represents the rate of concentration ratios of DBT in the ionic liquid and organic phases after equilibration, is calculated using the Equation (2-1):

$$K_D = \left(\frac{(C_i)}{(C_f)} - 1 \right) \frac{V_{Oct}}{V_{IL}} \qquad (2\text{-}1)$$

The derivation of this equation can be found in Appendix E. In this equation the concentration of DBT in the initial octane solution and the concentration of DBT in the octane after contact with the ionic liquid are C_i and C_f respectively. The volume of DBT containing octane that is contacted ionic liquid is V_{Oct} and the volume of ionic liquid is V_{IL}. The higher the distribution coefficient (K_D), the more DBT is absorbed by the ionic liquid in a single equilibrium step. Through stepwise extractions Bosmann and coworkers (2001) were able to remove their target amount of sulfur; however, as the concentration of DBT decreased in the fuel so to did the partitioning of the ionic liquid. In each stage of the process fresh ionic liquid was used. At the highest concentration of DBT in the fuel (500 ppm) they tested, the partition coefficient was calculated to be 1.25, however when the concentration in the fuel was lowered to 100 ppm the partition coefficient was only 0.25. The fact that they were not able to come up with any means of regenerating the liquid coupled with their inability to come up with a standout stable ionic liquid extractant leaves much room for more work in this area. The research they conducted proves that ionic liquids can be used to remove dibenzothiophene, but they have yet to fully address all of the technical implications of such a process.

The research presented in this section attempts to tackle some of the unresolved issues left by Bosmann and coworkers (2001) on utilization of ionic liquid technology in desulfurization. Through their use we could potentially increase worker conditions, decrease solvent waste costs, and reduce atmospheric sulfur emissions.

2.2. Desulfurization Experiments

In order to test the possibility of implementing ionic liquid technology for industrial desulfurization processes a few questions need to be answered. The following list identifies those questions and provides short answers. The experiments and results sections following these questions provide a more in depth analysis on how these questions are being addressed.

1. Can ionic liquids separate sulfur-containing compounds from fuels, and if so to what extent? The question of whether or not ionic liquids can separate sulfur-containing compounds from alkanes has been affirmed by Bosmann et al (2001). The extent to which separation of sulfur can occur is still unknown. Bosmann showed distributions in the ionic liquid of sulfur to be slightly greater than in the fuel; however, their uncertainties and the wide range of ionic liquid alternatives preclude answering the question with respect to extent of separation (2001). In this project this question was addressed using liquid-liquid extractions involving pure octane as the fuel, dibenzothiophene as the sulfur-containing compound, and many of the ionic liquids tabulated earlier.
2. What is the solubility of octane in ionic liquid and ionic liquid in octane? Ideally for these purposes octane and ionic liquid would be insoluble in each other; however, in reality this is not the case. It is important to know the extent of their solubilities in order to determine how much octane can be expected to dissolve into the ionic liquid and how much ionic liquid will be lost to the octane over time.
3. How can the ionic liquid be regenerated after becoming saturated with sulfur-containing compounds? Bosman et al (2001) addressed the issue of regeneration, but were unable to unsuccessfully regenerate the liquids. In order for an ionic liquid process to compete with modern technology then the ionic liquid must be able to be regenerated.
4. How would an ionic liquid-desulfurization setup appear in the fuel refinery industry? Knowing the answers to questions 1-3 provides insight into addressing this problem. At this time it is unknown how impurities in the fuel will affect the ionic liquids, therefore an ionic liquid-desulfurization process would probably be most effective after the fuel has been processed.

The following experiments were set up keeping the above questions in mind. The ionic liquid extraction of DBT in fuel experiments discusses the extent of separation and the regeneration questions. The solubility of organics and ionic liquids experiments

addresses the solvent and fuel solubility question. The ionic liquid process schematic provides a general design of a proposed ionic liquid process in fuel processing, which addresses the appearance in industry question.

Ionic Liquid Extraction and Regeneration of DBT in Fuel

In this experiment liquid/liquid extractions were carried out to determine the partition coefficient of various ionic liquids to dibenzothiophene in fuel. To conduct the extraction experiments solid DBT was dissolved in a surrogate fuel (for most of the experiments 99% pure octane was used as fuel). The concentration of DBT in solution was held to between 0 and 60 ppm due to the calibration stability of the gas chromatography (GC) which was used to analyze the samples. The GC used for this series of experiments is a HP 5890 Series II GC. The detector used is a flame ionization detector (FID). The column used is a J&W Scientific 125-1012 DB-1 with length of 15 meters, inner diameter of 0.53 mm, film of 1.5 micro-meters, and temperature limits from –60^{o}C to 320^{o}C. The GC was calibrated with DBT and octane solutions and was found to have a linear correlation from 0 to 70 ppm DBT. For these experiments, a HP 7673 auto-injector was used. Samples were run using HP Chemstation software with the following parameters:

Injector Temperature: 250^{o}C
Oven Temperature: 180^{o}C
Detector Temperature: 300^{o}C
Pressure: 8.67 psi @ oven temperature of 180^{o}C
Air Pressure: 42 psi
Hydrogen Pressure: 16 psi
Helium Pressure: 75 psi

0.500 mL of the DBT standard was injected into a GC vial for concentration identification. 0.050 mL of ionic liquid was mixed with 0.350 mL DBT standard in a 2 mL GC vial to produce a 1:7, ionic liquid: DBT/octane ratio. The sample was then mixed for 5 minutes and then centrifuged for 15 minutes at a speed of 2500 rpm and allowed to stand for 40 minutes thus allowing 1 hour of contacting the liquid phases before testing the octane for DBT. This amount of time of equilibration was determined by contacting the ionic liquid and octane containing DBT overnight and receiving the same partitioning as in the one hour experiments. 1μL samples of organic phase were run in the GC and the resultant spectra were compared to the standard DBT/Octane spectrum to discover the DBT removed by the ionic liquid and thus determine the distribution coefficient. Using these parameters the octane eluted almost immediately and the DBT had a retention time of 6.8 minutes. DBT peaks were compared for DBT in pure octane to DBT in octane with ionic liquid to determine the amount of DBT removed from the octane phases. Contacting the ionic liquid with the octane did not produce any unusual peaks in the GC analysis. The experiments were reproducible and standard deviations in peaks yielded uncertainties in the partition coefficients of $D \pm 0.2$.

For the GC experiments only the organic layer was tested for DBT concentration changes, so there is no closure on the mass balance. It is assumed that the decrease in concentration of DBT in the octane after contacting with the ionic liquid is equivalent to the amount of DBT entering the ionic liquid during contact with the octane. It has been proposed that high performance liquid chromatography (HPLC) could be used to measure the amount of DBT in the ionic liquid phase to close the material balance on this system. This experimental check has not been conducted at this time.

Economical regeneration of these samples was tested by low vacuum pumping the sample tested in the GC and then rerunning the sample to see the difference in size of the DBT peak. In the vacuum filtration the ionic liquid sample was heated to $70^{o}C$ for 12 hours to remove the DBT. The vacuum filtration experiments were conducted by Huimin Luo.

Solubility of Ionic Liquids and Organics

A method using a quartz crystal microbalance (QCM) was developed to determine the solubility of ionic liquids in organic solvents and the solubility of organics in ionic liquid. QCMs measure changes in frequency of a quartz crystal to changes in its environment. These changes in frequency can be correlated to mass, density, and viscosity effects on the quartz crystal using the Sauerbrey equation, which is shown in Equation (2-2) (Liang et al 2002).

$$\Delta f = \frac{-2 \cdot \Delta m n f_o^2}{A\sqrt{\mu_q \rho_q}} \tag{2-2}$$

In this equation A corresponds to the electrode surface area, ρ_q is the density of the quartz and μ_q is the shear modulus of the quartz, m is the mass, n is the liquid thickness, and f_o is the clean quartz frequency. Figure 2.1 illustrates the size and appearance of a QCM.

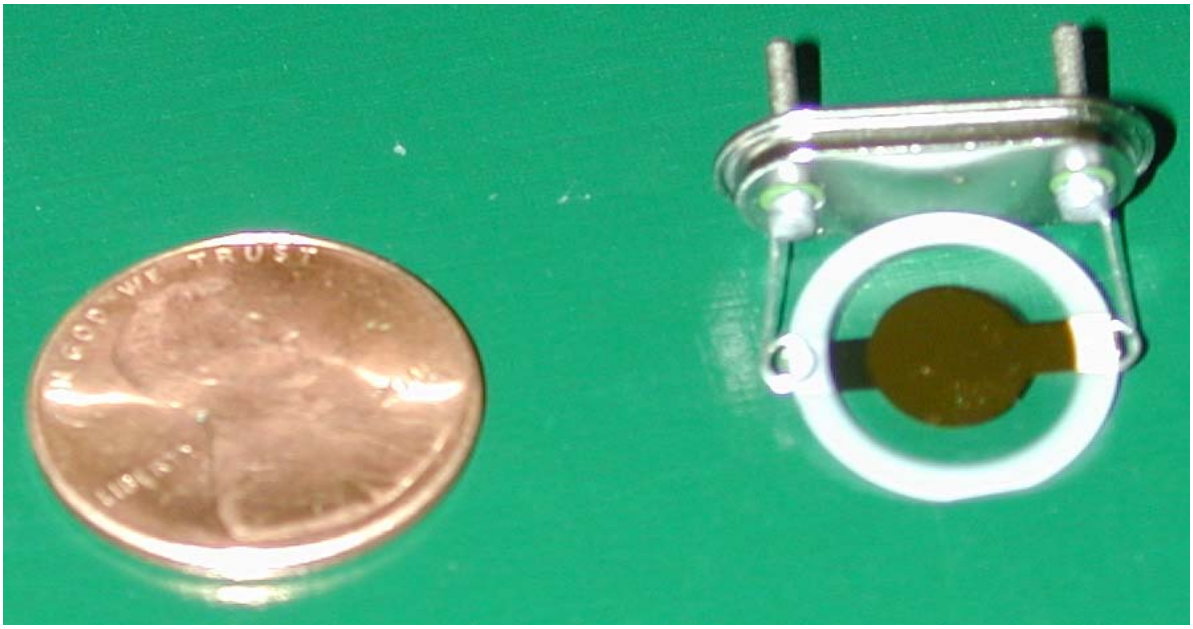

Figure 2.1: Appearance of the QCM Used in These Experiments

In Figure 2.1, the gold electrodes on each face of the quartz crystal can be seen. The electrodes are connected to a holder which can be connected to a frequency counter to measure changes in frequency when the QCM is exposed to various media. QCMs have traditionally been used to measure adsorption in polymer layers from the gas phase (Tsionsky et al 1994; Ricco et al 1998). Liang and coworkers (2002) have shown that the QCM can be used for ionic liquid measurements in the same manner as polymer films or ceramic coatings. The method used for these solubility experiments is an adaptation of a method for using ionic liquid coated quartz crystals as organic vapor sensors determined by Liang and coworkers (2002).

To test the organic solubility, organic vapors were passed over ionic liquids on a quartz crystal microbalance (QCM). Figure 2.2 shows the setup for these experiments. An ICM Lever Oscillator, depicted as a black box in Figure 2.2, was used to induce resonant oscillations of the QCM. HP 53131 Universal Counter was used to measure frequency flux. HP Benchmark software was used to control the system and record data. Two MKS mass flow controllers were setup to flow dry nitrogen through organic solutions past the QCM.

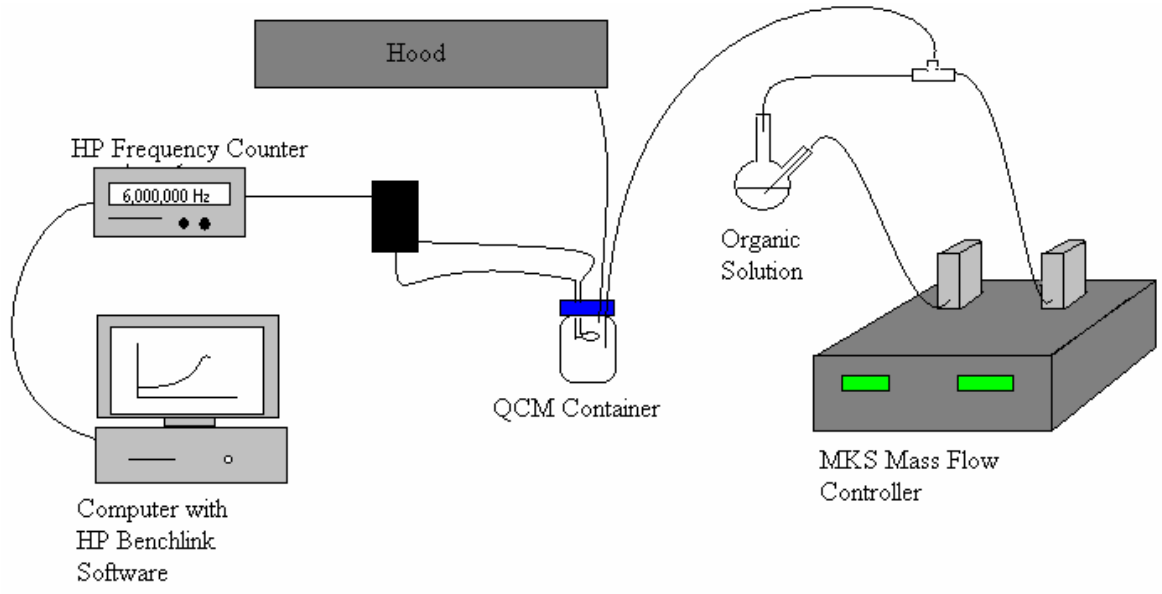

Figure 2.2: QCM Setup for Vapor Solubility Studies

The QCM is used to analyze the absorption of gas organic phases onto an ionic liquid layer or organics evaporation from the crystal. 6.0 MHz AT cut etched quartz crystals (received by ICM – International Crystal Manufacturers) were used for these experiments. Etched crystals were used because they seemed to facilitate an even distribution of the ionic liquid on the crystal surface versus the smooth crystals, and the etched crystals allowed the ionic liquid to act more like a solid on the crystal surface for the thin layer experiments, which is needed for mass determination. A sparger was used to bubble organic solvents to create a gas stream nearly saturated with organic vapor. The ionic-liquid-coated crystal was equilibrated by passing dry nitrogen through the QCM container for a period of time necessary to achieve a steady baseline, typically twenty minutes prior to starting the experiment. Saturated organic vapors are flowed into the QCM cell to observe organics absorption into the ionic liquid by either a frequency increase or decrease depending on the vapor. Figure 2.3 shows data obtained from the QCM for octane vapor exposure to BuMeIm Tf_2N, to better illustrate this point.

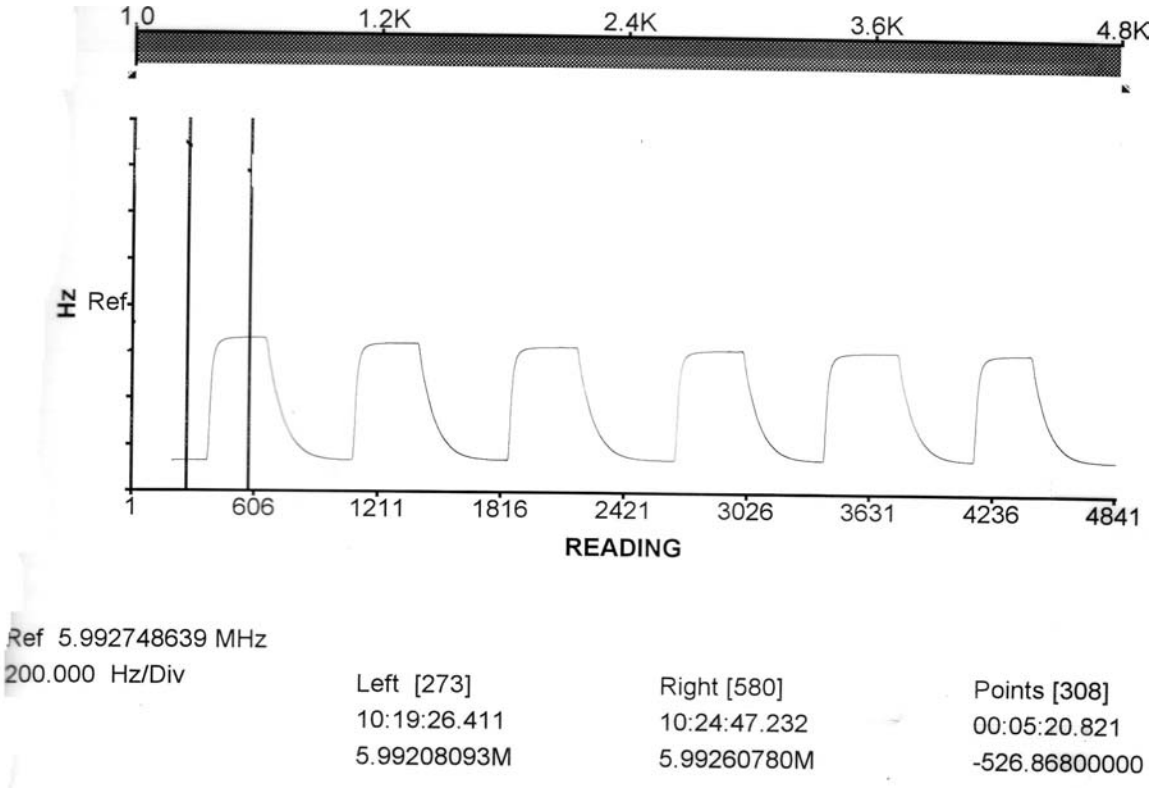

Figure 2.3: QCM Response of Ionic Liquid to Octane Vapor

The y-axis shows the frequency (Hz) and the x-axis is time (sec). The Ref value on the bottom left is the frequency of the quartz crystal with ionic liquid on it. The scale of the y-axis is 200 Hz per division. The Left and Right values indicate the location of the markers on the graph. In this case the left marker is at the equilibrated frequency of the ionic liquid on the QCM before coming in contact with organic vapor. At around 350 seconds the saturated octane was flowed over the ionic liquid until the frequency stabilized again and then it is cutoff to observe the absorption and desorption of the vapor. The absorption and desorption occur rapidly as the organic vapors are switched on and off of the QCM cell. The five peaks following the initial absorption peak show the reproducibility of these measurements. The frequency shift of the first peak is given in the lower right corner (527 Hz). This shift corresponds to mass, viscosity, and density changes in the ionic liquid thus indicating absorption of the organic vapors. The QCM does not distinguish between these properties; however, so steps have to be taken in order to extrude useful information from this instrument. The following list details the method used to distinguish between those properties and how other problems associated with the QCM were dealt with.

1. The amount of ionic liquid placed on the QCM determines the response observed when it is exposed to organic vapor. In Liang's experiments two drops of ionic liquid are applied to the clean quartz surface (Liang et al 2002). When using a larger volume of ionic liquid, such as in Liang's experiments and the experiment shown on the previous page, the corresponding frequency shift of the QCM corresponds to viscosity, density, and to a small extent mass increase. This method allows for qualitative determination of organics solubility in ionic liquid. For a quantitative means of determining the organics solubility in ionic liquid or ionic liquid in organics, very thin layers of ionic liquid need to be applied to the QCM. According to the Sauerbrey equation if the ionic liquid is applied in thin layers on the QCM, then the liquid will act as a rigid solid on the crystal surface. With the liquid acting like a solid, the density and viscosity effects are eliminated,

so the frequency shift corresponds to only mass changes. This mass can be calculated from the Sauerbrey equation to determine the solubility.

2. The QCM is sensitive to water vapor so the system was flushed with dry nitrogen for 20 minutes prior to and during the experiments to minimize water effects. Water vapor effects were measured by pumping nitrogen saturated with water vapor past the QCM at various relative humidity, which was measured by an ALNOR APM 360 RH meter at the outlet of the QCM cell. By increasing the relative humidity, the frequency decreased a few Hz. Slight fluctuations in the relative humidity may be the cause for baseline drift that was observed in a few of the experiments, however since the system is flushed prior to and during experiments it is unlikely this is a source of significant error. In some of the experiments there is a constant noticeable drift that can vary in ranges of $\pm$ 1 Hz per hour. This drift is accounted for by calculating frequency shifts by averaging 150 points from the baseline and absorption frequencies and then taking the difference and by using relatively short exposure times.
3. The QCM is sensitive to changes in gas density. This buoyancy effect causes the bare quartz crystal to change in frequency when it is exposed to organic vapors. Organic vapors change the frequency with respect to pure nitrogen because the vapors have different densities than nitrogen. This effect has been observed to shift the frequency a few Hz. This small shift has little effect on larger layer studies, however in thin ionic liquid layer studies this shift can have a large impact on the observed solubility. To account for this shift, the QCM was run without ionic liquid using the same organic vapor concentrations to determine the clean quartz frequency shift. These clean quartz frequency shifts were subtracted from the frequency shifts with ionic liquid to determine the effects only caused by the ionic liquid and not the quartz crystal.

The frequency of the crystal was measured before and after the ionic liquid was applied to determine the amount of liquid applied to the quartz. For thick layers of ionic liquid, the liquid was applied to the center of the QCM with a cotton swab. For thin

layers, the ionic liquid was applied by placing approximately 1 μL of an ionic liquid-acetone solution to the center of both sides of the gold surfaces of the crystal. Because the crystal is cleaned with pure acetone in between tests, applying the ionic liquid in an acetone solution spreads the ionic liquid visually uniformly on the gold electrode surface. Acetone was chosen to create the ionic liquid solutions because prior tests of ionic liquid solubility with acetone vapor showed that while acetone will dissolve in ionic liquid, it will not remain in the liquid after the solution is exposed to room temperature dry nitrogen. This volume of ionic liquid is used because it covers the entire gold surface without spilling to the outer arc of the crystal, where mass effects can not as easily be determined thus propagating more error (Ullevig et al 1982). The acetone-ionic liquid solutions were prepared such that the resultant solution yielded approximately 0.00250 g of ionic liquid per mL of acetone. This amount means that approximately 10 ng of ionic liquid or less was needed for each of the experiments. Using the Sauerbrey equation and assuming that the ionic liquid spreads evenly on the surface of the crystal, the thickness of the layers was approximated to be 90 nm thick (Rodahl et al 1996). Experiments conducted using smaller thicknesses yielded the same results as the 90 nm thickness, so this is thought to be thickness at which the ionic liquid begins to act like a solid on the QCM surface. Using thicker films (approximated thickness of 200 nm) the solubility appears to be less because viscosity and mass affects are observed simultaneously.

The experiments discussed to this point involved applying ionic liquid to the QCM to determine the solubility of the organics in the liquid. An experiment that was used to test the solubility of the ionic liquid in the organics was to contact the ionic liquid in a flask and then pull off the organic solvent over a period of time. These organic solvents were then applied to the QCM crystal. If the baseline of the crystal did not return to its original position then this indicates that ionic liquid was probably dissolved in the organic phase. Pure organic solvent was also applied to the QCM as a blank to insure impurities in the organic were not responsible for the frequency not returning to the baseline. The frequency change can also be used to calculate the amount of IL dissolved in the organic using the same logic described in the first solubility experiments.

2.3. Desulfurization Results

In this section the results of the desulfurization experiments are given. The results are arranged in the order of (1) the DBT partition and regeneration results, (2) the solubility results, and (3) the significance of these results to utilization of ionic liquids in the desulfurization industry.

Distribution Coefficient and Regeneration Results

The distribution coefficient was defined in equation 1. As discussed in the experimental section, various ionic liquids and ionic liquid mixtures were contacted with DBT-containing octane and the resultant distribution coefficient was measured using GC analysis. The results of these extractions are given in Table 2.1.

Table 2.1: Measured Distribution Coefficients for DBT in Ionic Liquid/Octane System

Contact Liquid	Distribution Coefficient	Standard Dev. (+/-)
[BuMeIm]Tf_2N	1.7	0.1
[ImPrCO2Et]Tf_2N	1.5	0.2
[ImMeCO2Et]Tf_2N	0.1	0.4
Ethylene Diamine	2.2	0.3
[ImPrCO2Et]Tf_2N + TOPO	0.8	0.2
[BuMeIm]Tf_2N + Ethylene Diamine	3.2	0.3
[BuMeIm]Tf_2N + Ethylene Diamine + Zinc Acetate	3.4	0.4
[BuMeIm]Tf_2N + Ethylene Diamine + Zinc Chloride	1.6	0.2
[BuMeIm]Tf_2N + Zinc Acetate	1.6	0.2
[BuMeIm]Tf_2N + Zinc Chloride	1.3	0.3
[BuMeIm]Tf_2N + Cadmium Chloride	1.8	0.2
[BuMeIm]Tf_2N + Cadmium Acetate	2.9	0.4
[BuMeIm]Tf_2N/Dodecane	1.2	0.3

The ionic liquids and additives listed in the table were equimolar mixtures. The errors were determined through GC peak measurement differences between multiple runs of the same sample. Most of the experiments seen above were carried out using BuMeIm Tf_2N as the ionic liquid, which has a DBT partition coefficient of 1.7 with octane. This value means that the concentration of DBT in the ionic liquid phase is 1.7 times that in the octane phase at equilibrium. Of the various pure ionic liquids tested, the BuMeIm Tf_2N liquid provided the largest DBT partition. Pure ethylene diamine and a mixture of it with ionic liquid were run in an attempt to increase the partitioning. The zinc and cadmium chlorides and acetates were run based on the success Bosmann and coworkers (2001) had using aluminum chloride mixtures with ionic liquids in increasing the partitioning. The experiment conducted in dodecane was run to see how different organics affect the partitioning of DBT with ionic liquids.

When considering partition coefficients you either want them to be very large or above or around unity. In the case of very high partitioning, more target compounds can be removed per extractant, however it might also be more difficult to remove the key compounds from the extractant. In this case regeneration of the solvent might not be possible. In the alternate case where the partition coefficient is close to unity, the target compound is not held too tightly by the extractant, thus regeneration is possible, but it may take much longer or require larger solvent ratios to remove the same amount of the compound as the solvent with a greater distribution. The highest distribution value was achieved with a equimolar mixture of BuMeIm Tf_2N and ethylenediamine and also with a small amount of zinc acetate. Even though these values are higher, the presence of additives such as ethylenediamine and zinc acetate increase the hazards associated with running a process with these chemicals. Ethylenediamine has a low flash point of 43^{o}C and is very volatile (Merck Index). Since the distribution coefficients for most of the samples lie between 1 and 3, it shows that there is little difference between which of these extractants is chosen. For this reason the purest and most stable sample BuMeIm Tf_2N would seem to be the best candidate for industrial applications. Its partitioning of DBT is slightly higher than that of octane which could be advantageous in that it will

remove DBT from octane without holding the DBT so tightly that regeneration of the ionic liquid becomes implausible.

In two tests the regenerability of the liquids was studied and it was determined that the ionic liquids were capable of being reused for extraction after regenerating it through vacuum pumping the DBT rich ionic liquid sample and through contacting it with organic media such as toluene. These tests have not proven to be completely effective in regenerating the ionic liquid which can be discerned from lower partitioning when contacted with more DBT-containing octane. This indicates that not all of the DBT has been removed from the ionic liquid prior to secondary contacting. In the vacuum filtration the ionic liquid sample was heated to 70^{o}C for 12 hours to remove the DBT. These values were chosen to see if the DBT could be removed economically without excessive heating or pumping. Because this liquid is stable at higher temperatures these vacuum pumping experiments could be conducted at higher temperatures to try to increase the DBT-IL separation; however, unless an ionic liquid with greater partitioning can be found, the amount of time and energy required for ionic liquid regeneration might make current processes seem like better alternatives. Other potential means of regeneration that could be tried such as pervaporation, super critical CO_2 extraction, or even dissolution of the ionic liquid could be attempted in place of the attempted before mentioned processes (Blanchard & Brennecke 2001; Schafer et al 2001; Swatloski et al 2001).

Solubility of Ionic Liquids and Organics

In the desulfurization experiments ionic liquids are contacted with organics containing DBT in order to determine the distribution of DBT between the two phases. In order to accurately characterize this distribution it is important to know whether or not any of the ionic liquid is dissolving in the organics or if the organics are dissolving in the liquid. To test the solubility of ionic liquid in organics, BuMeIm Tf_2N was contacted with octane for a day. A drop of the resulting octane phase was applied to a clean quartz

yielding the data in Figure 2.4. In this figure, the left bar represents the baseline frequency of the clean quartz crystal. The dip in frequency represents the application of octane that was contacted with BuMeIm Tf_2N for 24 hours. The drop in frequency corresponds to an increase in mass on the crystal. As the octane evaporates from the crystal, the frequency increases, which corresponds to decreasing the mass present on the crystal. After the octane is applied it evaporates off the crystal, restoring the frequency to within 4 Hz of the crystal's initial frequency. Measurements with pure octane achieved similar results, thus indicating that no ionic liquid can said to be dissolved in the octane within the given QCM uncertainty. With this uncertainty, approximately 0.3 ppb by weight ionic liquid could potentially be dissolved in the octane; however, this baseline shift was observed for several experiments not involving ionic liquids, so the actual residual ionic liquid in the octane is probably much less. At this concentration, assuming 1 million gallons of fuel per day were contacted with ionic liquids, then only 350 grams ionic liquid per year would be expected to be lost due to solubility.

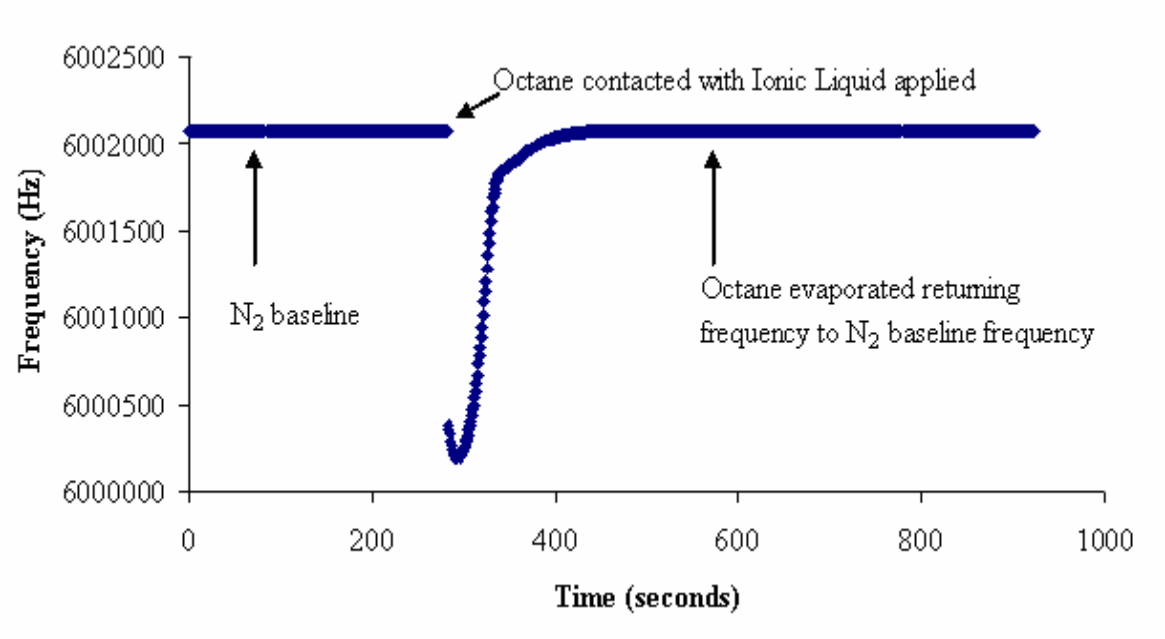

Figure 2.4: Ionic Liquid Solubility in Octane

The second solubility experiment looked at octane solubility in ionic liquids. Octane vapor was passed over ionic liquid on a QCM at various vapor fractions. The fraction of octane absorbed into the ionic liquid was recorded and there was no discernable amount of octane remaining in the ionic liquid after exposure. Figure 2.5 illustrates these findings. The octane peaks here correspond to exposing the ionic liquid to decreasing concentrations of octane vapor. The first peak is nitrogen saturated with octane. As the octane vapor concentration is decreased, the corresponding frequency shift decreases. When the octane is absorbed and released from the ionic liquid the frequency returns to the baseline frequency of the ionic liquid. This occurrence indicates that within the limits of the QCM no octane can said to be remaining in the ionic liquid after exposure.

Based on these two sets of tests, no conclusive evidence was found that ionic liquids permanently dissolve in octane or octane in ionic liquids. Contacting the ionic liquid with octane did show that, for given concentrations of octane a certain amount of the octane would be absorbed by the ionic liquid; however, removing the presence of octane from the surroundings caused the octane to quickly leave the liquid.

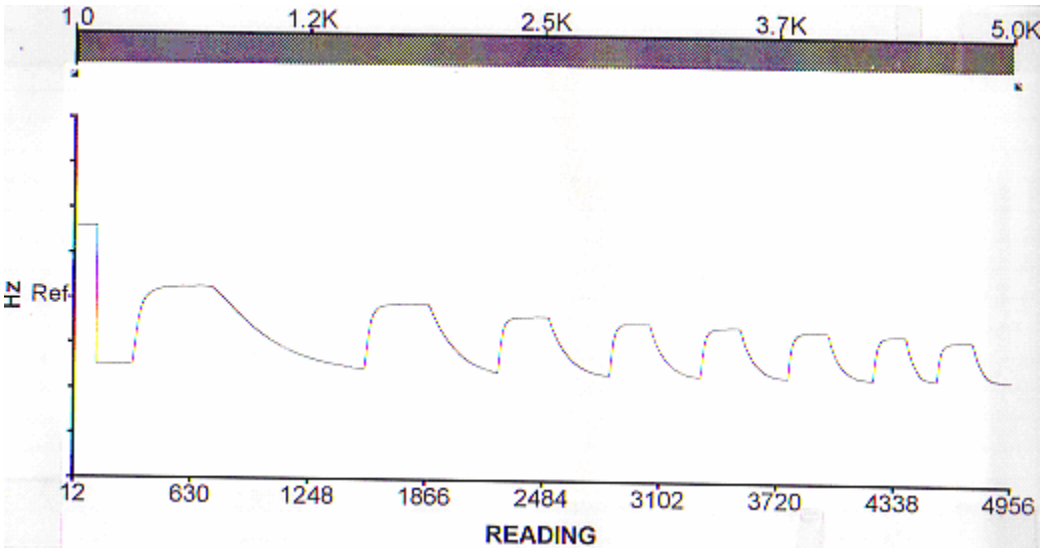

Figure 2.5: Octane Solubility in Ionic Liquid at Various Vapor Concentrations

This result might add more complexity to the system and affect the DBT separation because, some of the DBT removed could be due to DBT-containing octane being dissolved in the ionic liquid and not just DBT. The ionic liquid solubility test indicated that at most ppb levels of ionic liquid would be dissolved in the octane. It is unknown how this might affect the gas and whether an additional removal step would be needed to recapture this ionic liquid.

Ionic Liquid Process Schematic

Figure 2.6 shows a general schematic of how ionic liquids might be used in industrial extractive process for desulfurization of fuels. In this proposed ionic liquid setup, sulfur-containing fuel would be contacted countercurrently with an ionic-liquid extractant.

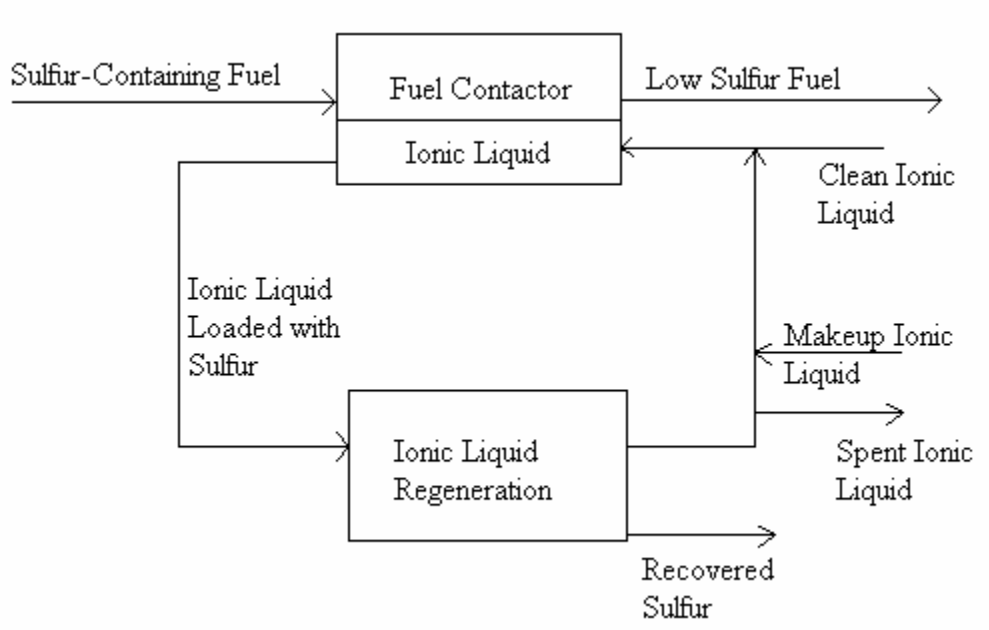

Figure 2.6: Conceptual Schematic of Ionic-Liquid-Based-Desulfurization-Process

Due to the quick transport of DBT into the ionic liquid and the low distribution coefficient of the ionic liquids, a relatively high ionic liquid to fuel flow ratio would be needed to desulfurize the fuel. The problems with this setup are the potential ionic liquid losses associated with contacting the fuel at a large flow rate, the potential high solubility of aromatics in the fuel, and the lack of an efficient means of regenerating the ionic liquid. Ionic liquid can be expensive, so any loss of these liquids via contact loss or aromatic contamination could result in a major potential cost. Studies conducted to this project have not shown large contamination with the ionic liquid and octane, but the presence of aromatics in real fuel might change these observations. Also, the tests conducted for this project were not flow measurements, so the losses due to high flow contacting are unknown. Since an effective means of regenerating the ionic liquids has not been found yet, the desulfurization process can only be as fast as the regeneration process. At the lengths of time required as of now to regenerate the ionic liquid, the hydrotreatment and biodesulfurization techniques appear to be more practical desulfurization alternatives. If the time of regeneration decreases to minutes instead of hours, then the ionic liquid process may prove to be more beneficial. Also, the bench-scale tests have not indicated organics or ionic liquids dissolving in each other; however, in bulk experiments some dissolution or losses into the solvents might be expected. It is unknown how these impurities might affect the fuel.

3.0. Carbon Dioxide Separation from Coal Fired Power Plant Flue Gases

In this section, the work conducted on CO_2 removal from flue gases is presented. The first section discusses current CO_2 capture technology proposed for use in treating power plant flue gases. The second section discusses experiments conducted to measure quantities need to evaluate the technical feasibility of an ionic liquid membrane capable of capturing CO_2 from flue gases. The third section discusses the findings of these experiments and their implications.

3.1. Background for Carbon Dioxide Capture from Power Plant Flue Gases

Carbon dioxide has sparked the attention of many scientists due to its probable link to global warming. Our economy is primarily fueled by fossil fuel combustion. Power plant coal combustion is the single greatest anthropogenic source of atmospheric CO_2. Although pure CO_2 is not toxic to people, it accumulates below the ozone layer and essentially traps outgoing photons of light for longer periods of time between the stratosphere and the earth's crust thus potentially contributing to a gradual temperature increase (Baird 1999). Additional hazards from flue gases are posed by traces of acid gases and mercury that can be mixed in the gas. Since the debate of carbon dioxide as a factor in global warming is ongoing, there is presently little or no economic incentive for CO_2 reduction. In the near future it appears as though tax incentives will be given to production involving reduced CO_2 emissions; however, without knowing the exact figures there is no certain confirmation that a CO_2 reduction process will be economically profitable. CO_2 capture would only be economical if there is a use for it, such as in enhanced oil recovery or if a carbon tax is levied (Chapel et al 1999). Carbon dioxide can be captured and resold for commercial uses; however, CO_2 is so abundant that very few geographical areas are in need of this chemical (EPA 2003). For these reasons the current incentives for utilizing a CO_2 capture process are for potential environmental benefits, improved customer perception, and the hope of future tax incentives for CO_2

reduction. Currently work is being conducted to find new media that could accompany driers, CO_2 compressors, and scrubbers to decrease the carbon dioxide output from power plants (Simbeck 2001). Power plant flue gases consist of about 70% N_2, 6% H_2O, and 24% CO_2 (Simbeck 2001). In order to curb CO_2 emissions from coal fired power plant flue gases, several processes have been proposed. Two of the more attractive processes are amine scrubbing and revised power plant systems such as hydrogen fired coal gasification combined cycle (H_2-CGCC).

Amine scrubbing is the most widely accepted process for CO_2 removal from flue gases. This technology is relatively new for flue gas treatment, but has been used for many years for acid gas scrubbing (Chapel et al 1999). One company that has taken the lead in developing this technology is Fluor Daniel Inc. which has created the Econamine process (Chapel et al 1999). In that and similar processes the flue gas from the boiler is passed through an aminated solvent in a scrubber. The amines extract the CO_2 and are then depressurized to remove the CO_2. After depressurization the amines can be reused for more CO_2 removal. The benefits of this amine scrubbing process are: the low cost of the solvent, the high separations that are achievable, and relatively simple implementation with existing power plant technology. The disadvantages of this process are: it consumes a significant amount of power, it requires corrosive, degradable, and volatile extractive chemicals, and it requires a new backpressure steam generator, CO_2 scrubber/stripper, and CO_2 compressor/dryer. In order to operate the CO_2 scrubber and compressor additional energy is needed, which is approximately 30% of the power plant output (Simbeck 2001). Currently, amine scrubbing appears to have the most promise for industrial scale CO_2 removal; however, the extra cost leaves room for improvement.

The hydrogen fired coal gasification combined cycle process (H_2-CGCC) involves coal gasification and water shift to produce hydrogen in order to produce a cleaner flue gas and to actually increase the power produced. A significant element of this process is an H_2/CO_2 separator on the high-pressure product of the shift reactor. An economic evaluation indicated that the hydrogen fired process would cost $25 per metric ton of CO_2 avoided as opposed to $33 per metric ton for amine scrubbing of the gas in a conventional system (Simbeck 2001). Calculations conducted by the SEEN corporation

estimate that an average power plant produces 7,947 metric tons of CO_2 annually, thus what may seem like a small difference of \$8/mt CO_2 is actually \$220/MWe produced (SEEN 2002). A drawback of this system is that it does not use existing power plant technology. In order to implement this system entirely new equipment would need to be purchased.

Supported ionic liquid membranes (SILMs) are a potential alternative to amine scrubbing in these processes. It is hoped that by using ionic liquid technology in power plants to treat flue gases that the concentration of anthropogenic CO_2 emitted will be minimized. Ionic liquids have potential in achieving these decreased emission goals. The wide range of temperature stability of ionic liquids such as BuMeIm Tf_2N (-4 to 400^oC) and their versatility as an extractant could allow introduction of the species to CO_2 treatment facilities already at the plants without incurring massive instrument changes (Simbeck 2001). This low volatility is also an attractive property in that it minimizes potential losses through volatilization. Work has previously been conducted to determine the solubility of gases present in flue gas emissions into ionic liquids (Scovazzo et al 2002; Blanchard et al 2001; Blanchard & Brennecke 2001; Kamps et al 2003; Bates et al 2002; Anthony et al 2001). This work is important in that it provides an idea of the extent of separations one might expect for CO_2 removal. Table 3.1 provides the solubility data that has been reported that might be of relevance to flue gas removal. All of the values reported in this table were obtained at standard pressure and temperature. Most of the solubility studies were conducted with BuMeIm PF_6. The exceptions to this observation are the ethyl-methyl-imidazolium Tf_2N and the task-specific ionic liquid reported by Bates et al (2002).

The results reported by Scovazzo et al show very different solubilities for the same solutes than a later study by this group and Anthony et al (2002; 2001). This disparity is most likely due to the means by which the solubility was determined and the water content of the liquids. The solubilities determined by Anthony et al were determined by gravimetric measurements, where the mass of the ionic liquid was measured as it was exposed to various solutes over a period of time (2001).

Table 3.1: Reported Henry's Constants for RTIL

Solvent	Solute	Henry's Law Value bar
BuMeIm PF_6[a]	CO_2	11.3
BuMeIm PF_6[b]	CO_2	58
EtMeIm Tf_2N[b]	CO_2	38
BuMeIm PF_6[a]	O_2	154
BuMeIm PF_6[a]	N_2	109
BuMeIm PF_6[c]	H_2O	0.17
BuMeIm PF_6	CO_2	53.4
BuMeIm PF_6[c]	C_2H_4	173
BuMeIm PF_6[c]	C_2H_6	355
BuMeIm PF_6[c]	CH_4	1690
BuMeIm PF_6[c]	O_2	8000
BuMeIm PF_6[c]	Ar	8000
BuMeIm PF_6[c]	CO	>20,000 (nondetect)
BuMeIm PF_6[c]	N_2	>20,000 (nondetect)
BuMeIm PF_6[c]	H_2	>1,500 (nondetect)
BuMeIm PF_6[d]	CO_2	57
1-butyl-3-propylaminylimidizolium BF_4[e]	CO_2	2

[a] Scovazzo et al 2002, [b] Scovazzo et al 2003, [c] Anthony et al 2001, [d] Kamps et al 2003
[e] Bates et al 2003

These measurements involved the use of a sensitive, specialized piece of equipment to measure the mass uptake for solubility determination. In Scovazzo's 2002 studies, the solubilities were determined by flowing gases through a SILM and determining the solubility from the permeance. Since permeance is affected by more than just solubility the methods used could be a large reason for the disparity in solubilities. Another reason for the solubility differences between Scovazzo et al and Anthony et al could be the water content of the BuMeIm PF_6 used in the studies. As discussed previously, the PF_6 anion is hydrophobic, so one would not expect to find more than 2 to 3 % water content in the liquid (Bonhote et al 1995). Scovazzo et al attributes the disparity in solubilities to the

presence of water in his liquids and the lack thereof in Anthony's (2002). Scovazzo et al avoided drying the liquids as Anthony had done, to prevent breakdown of the PF_6 anion into hydrogen fluoride by prolonged vacuum drying. Scovazzo et al conjecture that the presence of water in the liquid could have possibly facilitated a faster transport of CO_2 across the membrane. The PF_6 anion is more viscous than water, so the presence of water in the liquid would make the liquid less viscous, which might make mass transport of gases through the membrane easier. Anthony indicated that the presence of water might decrease the CO_2 solubility (2001). This decrease in solubility Anthony et al mentions is most likely offset by the increase in permeance of Scovazzo's studies, which is another reason why Scovazzo et al has reported higher solubilities than Anthony et al. For the purposes of the flue gas separations studied in this project both solubility findings are useful. Anthony's solubilities provide a reference for comparison for typical gas solubilities. Scovazzo's 2002 measurements lend insight into factors that can affect solubility and permeance.

The most interesting solubility reported in the previous table is that achieved with the CO_2 task specific ionic liquid (TSIL) reported by Bates et al(2002). This liquid incorporates an amine group on the cation. Amines are known for their strong affinity for CO_2 capture, so it is understandable why this TSIL is so successful in removing CO_2 (Chapel et al1999). The two major drawbacks of this separation is the time it takes for maximum CO_2 uptake and it requires regeneration. For the membrane and gravimetric studies, the CO_2 absorption and desorption in the ionic liquid occurred within seconds of exposure and removal from the gas (Scovazzo et al 2002; Anthony et al 2001). For the TSIL, CO_2 solubility approaches a Henry's Law value of 2 atm over a three hour exposure period. After absorbing the gas, the ionic liquid has to be regenerated by heating it to 80-100^{o}C for several hours. Bates proposes that this liquid could be used in industry as an ionic liquid scrubber; however, Bates notes that with its present viscosity it is not currently practical for such purposes. The high viscosity and regeneration needed would also preclude this TSIL for use with SILMs, because the high viscosity would limit the diffusion of gas through the membrane and the need for regeneration would cause additional problems. Membrane permeance is directly proportional to the

solubility and diffusion. Diffusion decreases as viscosity of the liquid increases, so unless the TSIL viscosity is decreased this liquid would not be a competitive option for SILMs.

Along with gas solubility studies, some permeance and selectivity studies have been conducted with reference to SILMs (Scovazzo et al 2002; Branco et al 2002; Anthony et al 2001). In the Scovazzo study the permeance and selectivity of CO_2 with respect to N_2 was measured for supported ionic liquid membranes consisting of polyvinylidene fluoride and polyethersulfone membranes. In the Anthony study the CO_2/N_2 selectivity was predicted from Henry's Law values and experimentally determined. Table 3.2 illustrates their findings. Scovazzo reports that the data illustrated above is competitive with polymer coated membranes, which typically have CO_2/N_2 selectivities of 15 to 35 (2002). As with the solubility results, there is a discrepancy between Anthony's and Scovazzo's predicted selectivities. These differences can again possibly be attributed to using different techniques to determine the selectivity and water content of the ionic liquids. The selectivities determined by Anthony were found by dividing the Henry's Law value of CO_2 by the Henry's Law value for N_2 (2001). The selectivities determined by Scovazzo were found by dividing the permeance of CO_2 by the permeance of air through a SILM (2002). It is unknown how their experimental selectivities compare; however it would be interesting to see if the selectivities are different because of water content. Both of these results are useful in that they illustrate a high selectivity for separation of CO_2 from other gases using SILMs.

Table 3.2: Reported Permeance and Selectivity Values for Supported Ionic Liquid Membranes

Ionic Liquid	Gas	Permeance (mol/atm*cm^2*sec)	Predicted Selectivity of CO_2 to N_2	Experimental Selectivity of CO_2 to N_2
BuMeIm PF_6[a]	CO_2	4.60E-09	1	---
BuMeIm PF_6[a]	Air	1.58E-10	10	≥ 29
BuMeIm PF_6[b]	N_2	---	> 400	very high
BuMeIm PF_6[b]	CH_4	---	34	8.5

[a] Scovazzo et al 2002, [b] Anthony et al 2001

The studies conducted up to this point in the literature have indicated the possibility of separating CO_2 from other gases using SILMs. The limitations of the work conducted to date is that they have only studied the solubilities and permeances of the BuMeIm PF_6 ionic liquid (2001; 2002). Also, the selectivity of CO_2 to N_2 has not been well characterized such that a real technical or economic evaluation can be constructed for using this technology in industry. The purpose of the CO_2 study conducted here is to test the solubility and permeance of untested ionic liquids in order to provide a more complete image of how SILM technology compares to modern CO_2 capture processes. In measuring the solubilities a new QCM technique was developed for rapid and inexpensive data collection.

3.2 Carbon Dioxide Removal Experiments

In this section carbon dioxide separation experiments are discussed for use with SILMs. These experiments were set up to answer some of the questions one encounters when trying to test the technical feasibility of a new process. The following are the questions addressed in this project.

1. What is the solubility of CO_2 in ionic liquids? The solubility of CO_2 is important in determining which ionic liquids might be the best candidates for membrane separations. The solubility shows how much CO_2 can be absorbed by the ionic liquid. Studies by Anthony et al, Scovazzo et al, and Bates et al have determined this solubility for certain ionic liquids (2001, 2002, 2002). A selective separation will require an ionic liquid with a high CO_2 solubility and low solubility of other gases such as N_2 and H_2O.
2. What is the diffusivity of CO_2 in ionic liquids? The diffusivity of CO_2 is important in that it can provide a prediction for the permeance of CO_2 through a membrane. The diffusivity multiplied by the solubility equals the membrane permeance (Hines & Maddox 1985).

3. What is the permeance of CO_2 through a supported ionic liquid membrane? The permeance of CO_2 through a membrane determines the rate at which CO_2 could be removed. The permeance is affected by the physical characteristics of the ionic liquid as well as the solubility.
4. What is the selectivity of CO_2 to other flue gases through a supported ionic liquid membrane? The selectivity of CO_2 determines the extent of separation that can be achieved for a membrane. Studies by Scovazzo et al (2002) indicate a high selectivity of CO_2 to N_2 ($\geq$ 29). This selectivity is important to know because power plant flue gases are mostly composed of N_2 and CO_2 (Simbeck 2001).
5. To what extent can supported ionic liquid membranes be used in flue gas treatment? It is important to know what percent of CO_2 could technically be removed and how the costs associated with such a removal compares to modern technology. Simbeck conducted an economic analysis of amine scrubbing for both conventional flue gas treatment and for H_2-CGCC (2001). The models he constructed should provide a solid basis for comparison with ionic liquid membrane technology.
6. What membrane properties are needed for the best separations? The properties of the membrane from membrane material, to thickness, to pore size, to volume needed for filling, to area needed, all impact the separation and economics of the system.

The following experiments were setup keeping the above questions in mind. The solubility of CO_2 in ionic liquids experiments address the extent of solubility and diffusivity questions. The supported ionic liquid membrane experiments address the permeance questions, which can be used to calculate the selectivity. The economic analysis of a supported ionic liquid system in industry addresses the questions of membrane properties and to what extent can ionic liquid membranes be used in CO_2 removal from flue gases.

Solubility of Carbon Dioxide in Ionic Liquids

A QCM technique was developed to measure the solubility of CO_2 and other gases in ionic liquids. Figure 3.1 illustrates the setup. This setup uses the same instrumentation as the desulfurization experiments except now CO_2 is passed over the QCM at various concentrations to measure the solubility of it in ionic liquids. Figure 3.2 is representative of the responses observed for the QCM measurements of CO_2. The primary difference between these QCM experiments and the organics experiments is that for CO_2 solubility thin ionic liquid layers were used and for the organic experiments thick layers were mostly used (Kanazawa et al 1985). The magnitude of the QCM frequency shifts is much smaller for the thin layer measurements than for those with thick layers. When exposed to CO_2 the frequency decreases on the order of 1 to 6 Hz. This frequency shift is linear with concentration of CO_2 exposed to the ionic liquid.

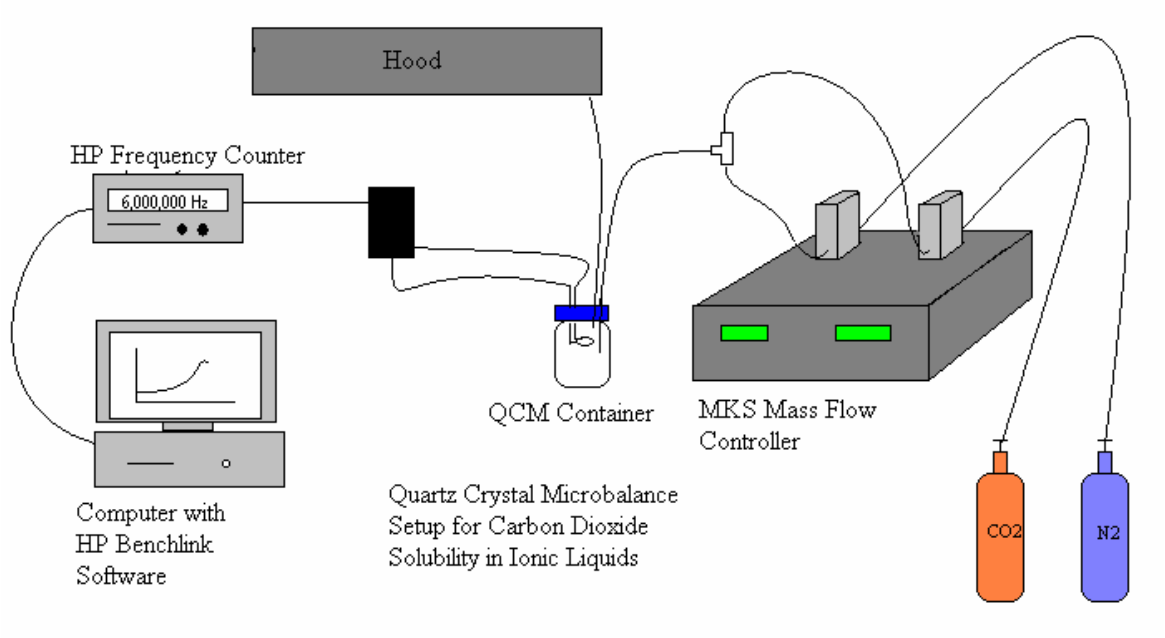

Figure 3.1: QCM Setup for CO_2 Solubility Studies

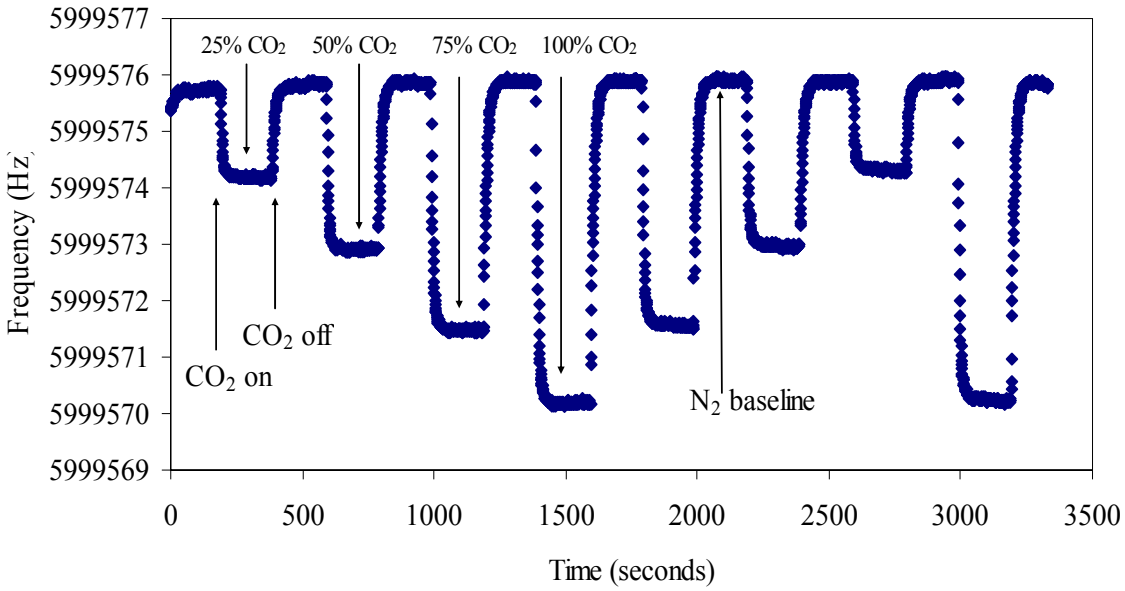

Figure 3.2: Transient QCM Response to Varying CO_2 Levels in CO_2/N_2 Gas Mixtures

This characteristic is important in determining the Henry's Law value of the liquid to CO_2. The transient times during exposure of the ionic liquid to CO_2 is well recorded by the QCM. Absorption and removal of the gas from the ionic liquid occurs within seconds of adding and removing the flow of the gas past the QCM. As in the desulfurization studies baseline shift was accounted for here by averaging 150 points of the N_2 baseline and 150 points of the CO_2 frequency shift to determine the average frequency shift.

Since thin layers were used and measuring the conditions that might affect gas solubility in these CO_2 experiments, the following issues were addressed.

1. Thin ionic liquid layers (< 100 nm) were used to observe only mass uptake of CO_2 into ionic liquids at various CO_2 concentrations.
2. Buoyancy effects were accounted for, because they have a greater impact on thin layer measurements than on thick layers.
3. Relative humidity effects were studied to determine how the presence of water affects CO_2 solubility.

Thin layer QCM experiments were used to measure the mass of CO_2 absorbed in the ionic liquid. As discussed in the desulfurization experiments, thin layers make the ionic liquid act like a rigid solid on the QCM surface such that changes in frequency of the QCM correspond to changes in mass alone. These changes in mass can then be used to calculate the solubility and diffusivity of CO_2 in the ionic liquid. In order to compare these experiments to results obtained by others (Anthony et al 2001; Scovazzo et al 2002; Bates et al 2002), the solubility was expressed in terms of Henry's Law values. Equation (3-1) was used to calculate these values, which is an adaptation of the Sauerbrey equation:

$$H = \left(1 + \frac{\Delta f_{IL}\ MW_g}{(f_{IL} - f_{CC})\ MW_{IL}}\right) P \qquad (3\text{-}1)$$

The derivation of this equation can be found in Appendix F. In this equation f_{IL} and f_{CC} are the averages of the frequency change versus mole fraction of CO_2 present in the space surrounding the QCM for the ionic liquid on the quartz and the clean quartz respectively. MW_g is the molecular weight of the gas or carbon dioxide and MW_{IL} is the molecular weight of the given ionic liquid. Δf_{IL} is the frequency shift observed when the ionic liquid is applied to the clean quartz crystal in dry nitrogen. P is the pressure in the cell. From the equation it can be seen that the lower the Henry's Law value, the greater the amount of carbon dioxide that is absorbed by the ionic liquid. This equation yields the Henry's Law value in units of atmospheres. Most of the experiments were conducted at 1 atm; however, experiments were run up to 4 atm and still exhibited linear solubility of CO_2 into the ionic liquid, as can be seen in Figures 3.3 and 3.4. In Figure 3.3 data obtained from the QCM for CO_2 solubility in OctMeIm Tf_2N is shown, for similar data tables for other ionic liquids refer to Appendix D. This data was used to calculate H using Equation (3-1). The uncertainty was determined by 95% confidence analysis. Graphing this data shows the linear response one would expect for Henry's Law value determinations. Figure 3.4 is the graphical representation of Figure 3.3.

Mole Fraction CO_2	Partial P_{CO2} atm	f_{IL}	$(f_{IL}-f_{CC})/\Delta f_{IL} * MW_{IL}/MW_g + 1$
0.256	0.256	1.650	0.013
0.488	0.488	2.840	0.018
0.745	0.745	4.160	0.024
1.000	1.000	5.530	0.032
0.745	0.745	4.150	0.024
0.488	0.488	2.810	0.018
0.256	0.256	1.510	0.010
1.000	1.000	5.550	0.032
0.256	0.256	1.570	0.011
0.488	0.488	2.910	0.019
0.745	0.745	4.250	0.025
1.000	1.000	5.520	0.030
0.745	0.745	4.240	0.025
0.488	0.488	2.870	0.018
0.256	0.256	1.590	0.011
1.000	1.000	5.590	0.032
0.256	0.256	1.570	0.013
0.488	0.488	2.570	0.015
0.745	0.745	3.860	0.021
1.000	1.000	5.200	0.028
0.745	0.745	3.950	0.023
0.488	0.488	2.740	0.019
0.256	0.256	1.400	0.009
1.000	1.000	5.420	0.033
1.000	2.361	8.100	0.073
1.000	2.361	8.300	0.077
1.000	2.361	8.500	0.080
1.000	3.042	11.900	0.106
1.000	3.042	11.500	0.099
1.000	3.042	11.100	0.092
1.000	3.723	14.800	0.123
1.000	3.723	14.000	0.110
1.000	3.723	14.500	0.118

H (atm)	**error (+/-)**
31.9	**1.0**

SUMMARY OUTPUT

Regression Statistics

Multiple R	0.996192189
R Square	0.992398878
Adjusted R Square	0.992153681
Standard Error	0.003229257
Observations	33

ANOVA

	df	*SS*	*MS*	*F*	*Significance F*
Regression	1	0.042206114	0.042206114	4047.34545	2.03197E-34
Residual	31	0.000323271	1.04281E-05		
Total	32	0.042529385			

	Coefficients	*Standard Error*	*t Stat*	*P-value*	*Lower 95%*	*Upper 95%*
Intercept	0.001708132	0.000845533	2.020183009	0.052077576	-1.63455E-05	0.003432609
X Variable 1	0.031340374	0.000492628	63.61875077	2.03197E-34	0.030335653	0.032345096

Figure 3.3: QCM Data for CO_2 Solubility in OctMeIm Tf_2N

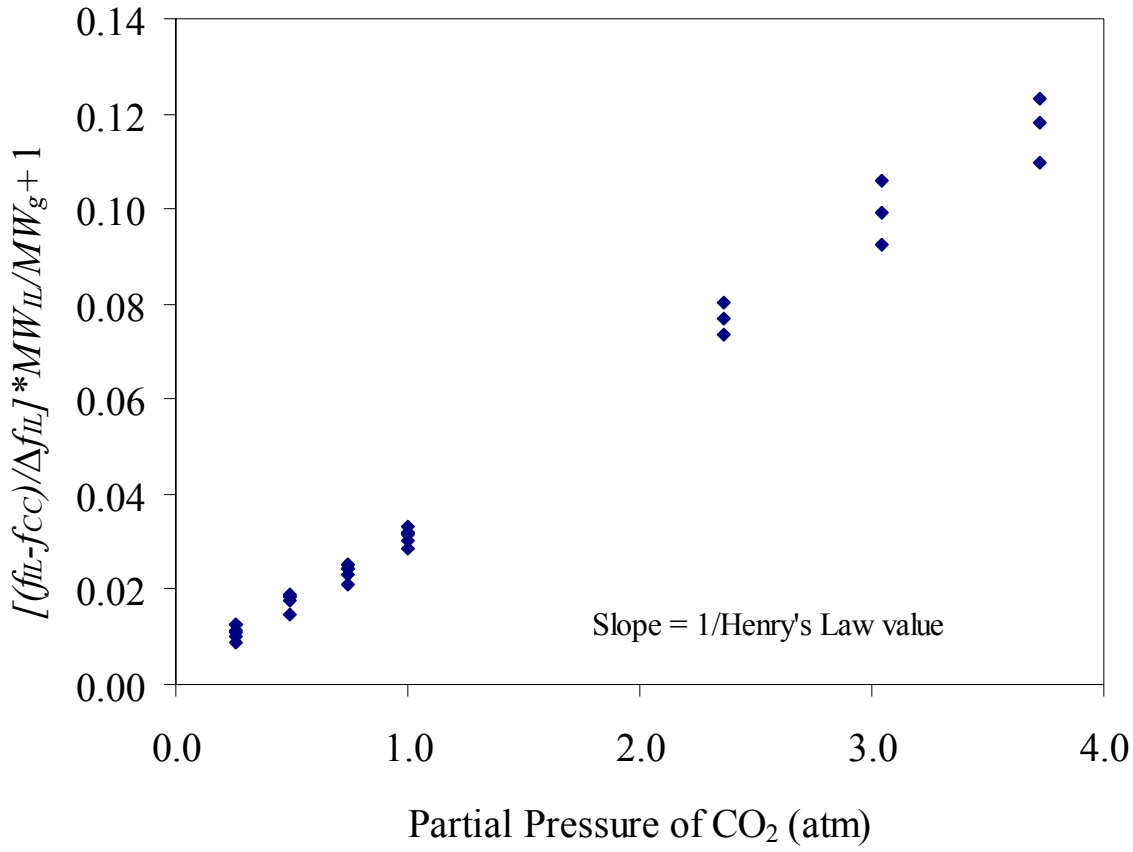

Figure 3.4: Low Pressure Effects on Solubility of CO_2 in OctMeIm Tf_2N

Figure 3.3 shows a linear solubility response at low pressures. It has been observed by others (Anthony et al 2001) that above these pressures (5-50 atm) the solubility increases nonlinearly. These findings are important in that Figure 3.4 shows that the solubilities measured by the QCM are unaffected by small pressure variations, but that one could expect greater solubility with increased pressure for high pressure CO_2 collection from flue gases. Also these results show that at low pressures CO_2 solubility can be readily measured by the Henry's Law value

Temperature is also known to have an effect on solubility (Anthony et al 2001). No temperature studies have been conducted in this project; however, studies in the literature have documented the effects of temperature and pressure with regard to CO_2 solubility in ionic liquids (Anthony et al 2001). Anthony et al has observed a linear CO_2

solubility increase with increased pressure for the BuMeIm PF_6 ionic liquid and that solubility decreased as the ionic liquid is heated. Anthony's data indicates that pressure plays a larger role in gas solubility than temperature effects. This information is important in that the ionic liquids will be partitioning CO_2 in a high temperature and possibly high pressure.

The diffusivity was also determined along with the solubility. Since thin layers only measure mass uptake on the QCM, the mass transfer of CO_2 into the ionic liquid could be measured over time. Figure 3.5 shows the transient response of the QCM with uptake of CO_2 as gas is changed from N_2 to CO_2 in the presence of the fluorinated OctMeIm Tf_2N ionic liquid.

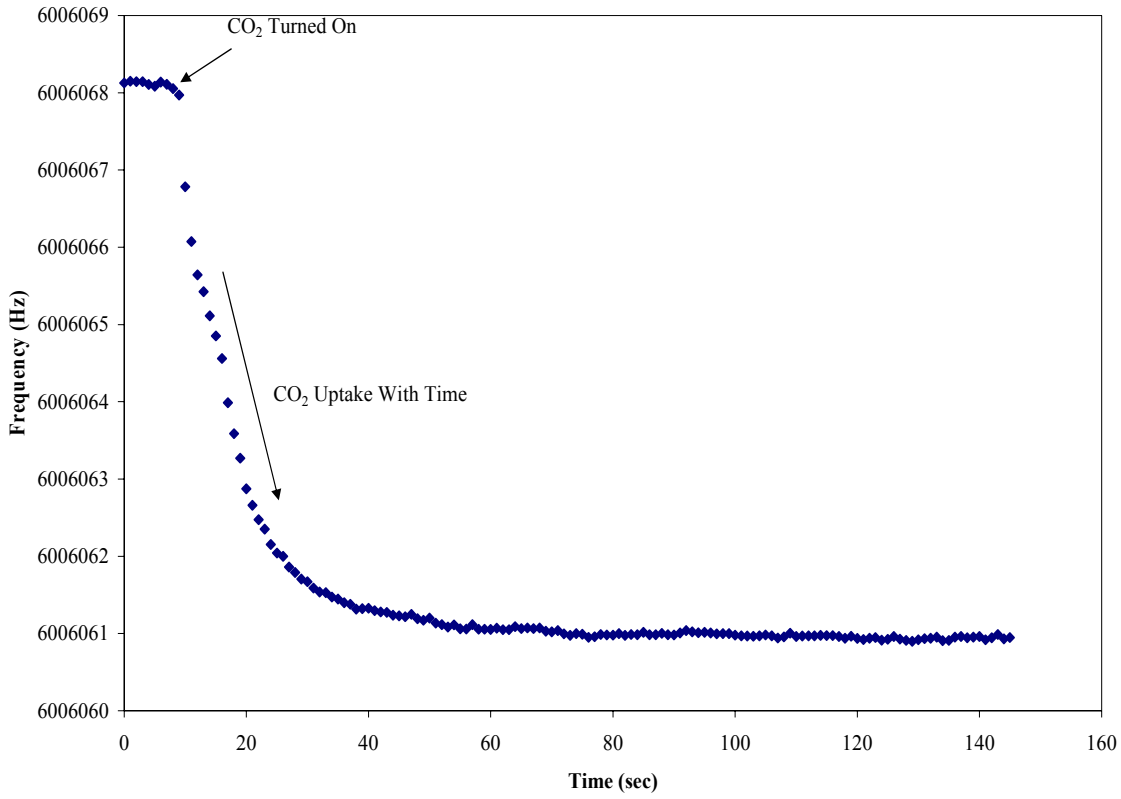

Figure 3.5: Transient Response to Changing Gas from N_2 to CO_2 for a QCM Loaded with Ionic Liquid

These measurements were fit to diffusion curves and the diffusivity was determined from them. This modeling is described in detail in the results section. Diffusivity measurements have not been reported for ionic liquids with CO_2, but permeance measurements could be used to test the validity of the diffusion measurements obtained here. If the diffusion and solubility measurements are in agreement with the permeance, then it would be possible to predict permeance with using just the QCM.

The effects of gas density on the QCM have been mentioned previously in the desulfurization section. In the CO_2 experiments the gas density or buoyancy effect was accounted for similarly in that CO_2 was flowed over a clean quartz crystal at various concentrations to measure the change in frequency of the quartz with respect to nitrogen. Then the same concentrations of CO_2 were flowed past the QCM with ionic liquid on it to determine the amount of CO_2 absorbed into it. The frequency response of the ionic liquid on the quartz to the CO_2 subtracted by the frequency response of the quartz crystal to CO_2 at the same CO_2 concentration gives the amount of CO_2 absorbed by the ionic liquid. Figure 3.6 shows the frequency responses of the clean quartz and ionic liquid to CO_2 to better illustrate this buoyancy effect. The response to CO_2 for both the quartz coated with ionic liquid and the clean quartz is linear. In this plot the region between the two lines is the frequency shift associated with just absorption of CO_2 in the ionic liquid. As expressed in Equation (3-1), this response f_{IL}-f_{CC} is what is used in the calculation of the value for Henry's Law value for gas solubility. From this plot, the importance of accounting for gas density effects in thin layer measurements is apparent. Pure CO_2 causes a 4 Hz frequency shift with respect to N_2 on the QCM. Without accounting for the density effect, the Henry's Law constant would erroneously be determined to be 11 atm, while the density-corrected value is 37 atm.

Relative humidity studies were conducted to observe how the presence of water impacts CO_2 solubility. Scovazzo et al observed that the presence of water in the ionic liquid may have increased the solubility of CO_2 in the ionic liquids (2002). Based on this observation and the fact that industrial uses such as flue gas treatment will expose SILMs with very high water concentrations, studies were conducted to observe the effects of relative humidity on the ionic liquid.

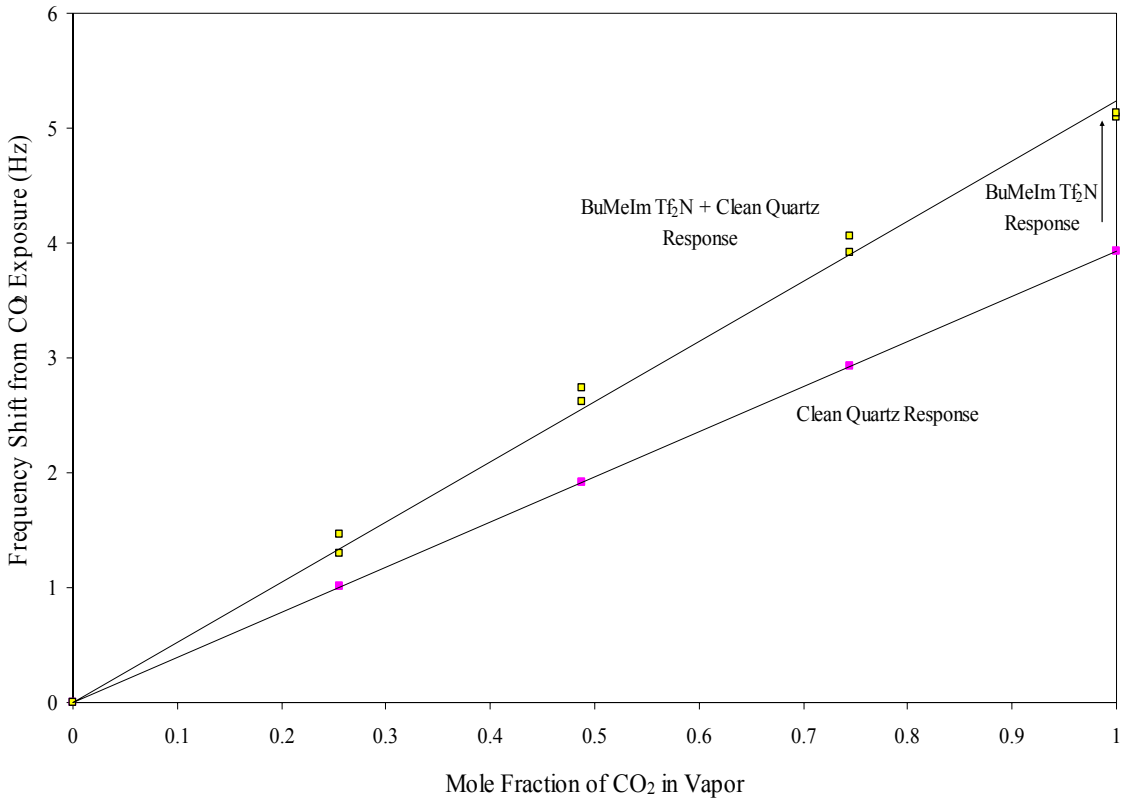

Figure 3.6: Blank Subtraction for CO_2 Solubility Measurements

These tests were conducted with the QCM by first observing the effect relative humidity had on the clean quartz, as in the gas density studies, and then comparing the frequency responses to those of the ionic liquid exposed to various relative humidities. After determining the amount of water the ionic liquid would uptake at each relative humidity, CO_2 was exposed to the ionic liquid at those same humidities to observe the effect of water on CO_2 solubility.

Supported Ionic Liquid Membrane Separation of Carbon Dioxide

Single-gas permeation tests were conducted to measure the permeance of gases through supported ionic liquid membranes. The tests measured the amount gas passing

through the membrane into a fixed volume as a function of driving force and time. In these tests supported ionic liquid membranes were prepared and sealed in a gastight membrane apparatus in order to observe the diffusion of carbon dioxide through the membrane over time. The membranes used are 47 mm diameter alumina Whatman Anodisc 47 filters with 0.02 and 0.2 μm pores. The ionic liquid was applied to the discs by cotton swabs and Kimwipes were used to remove any excess liquid. The membrane was then spun in a spin-coater at 3000 rpm for five minutes to produce a visually uniform surface. The membranes were weighed before and after the addition of ionic liquid to measure the amount of ionic liquid in the membrane. The setup for these experiments can be seen in Figure 3.7. The pressures of the upstream and downstream gases are measured using a Sensotec SC series equipped with two model TJE/0713-01TJA sensors. The downstream fixed volume is 78.5 cm^3. As shown in Figure 3.8 the membrane is held in a membrane cell supported by a metal screen and sealed by o-rings. The permeance experiments were run by: (1) checking the system for leaks, (2) evacuating the system and purging several times with test gas, (3) creating a pressure difference (typically <5 psi) across the membrane with a single-gas, (4) keeping the upstream pressure constant and measure the changes in downstream pressure over time, (5) check for leaks again after measurements are complete, and (6) calculate the permeance.

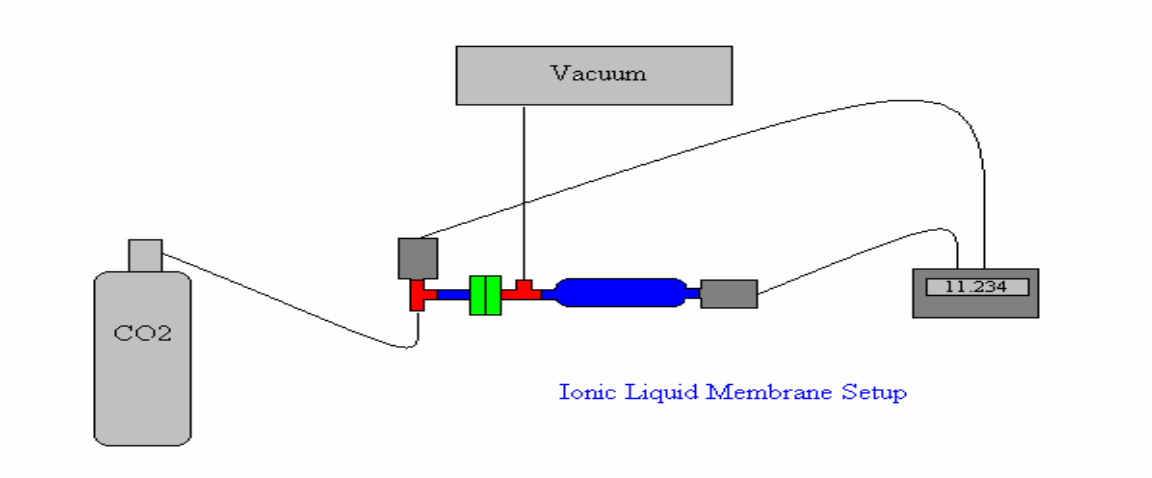

Figure 3.7: SILM Setup for Single-Gas Permeation Experiments

Figure 3.8: Supported Ionic Liquid Membrane Cell

The pressure of the gas in the upstream side was held below 20 psi due to the calibrated limits of the pressure probe. The pressures of both sides were recorded periodically until the cell approached equilibrium (the pressures were within 0.2 psi of each other). By measuring the pressure changes of the downstream side over time, the single-gas permeance can be determined for the SILM. Ionic liquids with strong affinities for CO_2 removal as measured by QCM were employed in these membrane tests. In conducting these single-gas experiments the following questions were addressed.

1. What is an appropriate pore size for the membrane? Previous SILM studies indicate 0.02 μm pore sizes were used for the membranes (Scovazzo et al 2002). 0.2 μm pore sized membranes were initially used for the work presented here; however, the results of those initial studies seemed to indicate that the pore size may have been too large. The permeance appeared to increase as the experiment progressed and leak checks and membrane observation seemed to indicate that the ionic liquid was being pushed through the membrane pores, thus allowing more gas to pass through. Later experiments conducted with 0.02 μm pore sized membranes did not have this problem, which shows how pore size selection can affect the measurements.
2. How can the system be checked for gas leaks? The system was checked for leaks by pulling a vacuum on the system and observing whether or not it could hold the

vacuum. This check was conducted before and after membrane experiments to ensure that the permeance values were unaffected by leakage. The area where leakages were most commonly found was around the membrane encasement.

3. What is an appropriate method for evacuating other trace gases from the system, so that only the single-gas permeance can be observed? In order to run single-gas measurements, it is important to minimize traces of other gases from the system, other than that being analyzed. The permeance is determined by measuring the downstream pressure over time, so the addition of any other gases in the upstream or downstream sides of the membrane would make it impossible to measure the driving force for gases to pass through the membrane simply from pressure measurements and would thus lead to errors in the permeance. To evacuate the system both sides of the system were vacuumed to approximately 2 psi. Then the vacuum was shut off and both sides of the membrane were pumped with pure gas for five minutes. This step was repeated three more times. This amount of time might not be adequate for removing gases trapped in the ionic liquid; however, tests involving evacuation periods much longer yielded the same permeance results as those with shorter evacuation periods. To check this result the amount of other gases that could be present on the downstream side was estimated based the solubility of gas in the ionic liquid and the number of purgings to be <350 ppm. This concentration should provide a negligible gas driving force across the membrane.

Through answering the above questions and getting accurate pressure change measurements with respect to time, the permeance can be calculated. A general equation for membrane permeance is given in Equation (3-2).

$$Permeance = \frac{CO_2\ Flux}{\Delta P_{CO_2}} \tag{3-2}$$

Using this general equation a new equation (Equation (3-3)) was determined for calculating the permeance. The derivation of Equation (3-3) can be found in Appendix G. The permeance was found by plotting the following equation as a function of time (t) and solving for permeance from the slope.

$$\ln\left(\frac{P - P_{up} - P_o}{-P_{up}}\right) = \left(\frac{A \cdot R \cdot T \cdot Permeance \cdot t}{V}\right) \tag{3-3}$$

In this equation P_{up} is the constant CO_2 pressure on the upstream side of the membrane, P_o is the initial pressure of the downstream side, P is the downstream CO_2 pressure as a function of time t, A is the area of the membrane, R is the ideal gas constant, T is temperature which was held at room temperature, and V is volume of the downstream side.

3.3. Carbon Dioxide Separation Results

In this section the results of the CO_2 separation are given. The results are arranged in the order of (1) the solubility of CO_2 in ionic liquids, (2) the diffusivity of CO_2 in ionic liquids, (3) the SILM single-gas permeances, and (4) the significance of these results to utilization of SILMs in flue gas treatment.

Solubility of CO_2 in Ionic Liquids

As mentioned before the Henry's Law constant is a measure of the solubility of one species in another in the dilute media. Thin layers of ionic liquids were used on the QCM to determine the amount of CO_2 absorbed by the ionic liquid at differing molar percentages of CO_2 in the atmosphere. As in the organic vapor study, the solubility is

measured by changes in frequency of the ionic liquid when exposed to CO_2. Table 3.3 illustrates the Henry's Law values determined for various ionic liquids and Appendix B contains examples of the QCM data produced for each of the ionic liquids from which these values were derived. All of the ionic liquids tested for CO_2 solubility utilized the Tf_2N anion except PrMeIm PF_6. This ionic liquid was used to compare Henry's Law values measured with the QCM to other values observed in the literature by Scovazzo et al and Anthony et al (2002; 2001). The propyl, butyl, hexyl, and octyl ionic liquids were used to observe trends in cation alkyl chain length on CO_2 solubility. The BuMeIm Tf_2N + polyimide mixture was an equimolar solution aimed at increasing the CO_2 solubility. The OctMeIm Tf_2N with a fluorinated cation was used to observe the effects on solubility of fluorine which is known to have a strong affinity for CO_2. The PrMeIm Tf_2N gas density check was obtained as a check for the method used for correcting the solubility measurements for buoyancy effect on the QCM. The BuPhIm Tf_2N and BuPhBuIm Tf_2N liquids were used to see the effects of phenol and phenol in a tri-alkyl substituted imidazolium cation respectively.

Table 3.3: Solubility of CO_2 in Ionic Liquids

Ionic Liquid	Molecular Weight g/mol	Henry's Law Value atm	Error (+/-)
PrMeIm Tf_2N	405	36.8	7
BuMeIm Tf_2N	419	37	3.4
HexMeIm Tf_2N	447	34.2	5.1
OctMeIm Tf_2N	475	30.7	1.4
PrMeIm PF_6	260	47.6	7.8
BuMeIm Tf_2N + polyimide	460	37.6	2.7
OctMeIm w/ 13 F in place of H	712	6.1	1.2
BuPhBuIm Tf2N	554	62.1	7.5
BuPhIm Tf2N	497	178.2	17.2
PrMeIm Tf_2N: Gas Density Check	405	38.3	1
OctMeIm Tf_2N: 20% Relative Humidity	475	29.7	2.2
OctMeIm Tf_2N: 40% Relative Humidity	475	26.3	4.1
OctMeIm Tf_2N: 70% Relative Humidity	475	12.7	9.3
NonFluorinated: Fluorinated OctMeIm Tf2N Mixture (58 mole %: 42 mole %)	575	14.5	1.2

The OctMeIm Tf_2N experiments with humid gas were conducted to observe CO_2 solubility trends in the presence of water. The fluorinated and non-fluorinated OctMeIm Tf_2N mixture was used to observe the miscibility of ionic liquids an to see how mixing affects the solubility measurements and the ionic liquid physical properties.

From this data we can extract a number of trends. For one, it can be observed that as the length of the alkyl groups on the cation is increased, the solubility of CO_2 seems to increase. The mechanism of separation is not fully understood at this point, but one possible explanation for this phenomenon is as follows: Carbon dioxide is removed by the interaction of the cation of the ionic liquid and the free unbound electrons of the oxygens on the carbon dioxide molecule. The two factors that contribute to the removal of carbon dioxide are the strength of the cation and the weakness of the anion. If the anion is too tightly associated to the cation, then the net positive charge of the ionic liquid will be less and it will not attract free electrons of the CO_2 as well. Carbon is an electron-donating chemical, thus as the chain length of the cation is increased the extra carbons on the chain help stabilize the net positive charge in the imidazole ring. This stabilization creates a smaller net positive effect thus it does not interact as strongly with the CO_2 and the gas separation is lower.

A second phenomenon that can be observed from the data is that when ligands of the same chain length have their substituents changed from neutral to electron-withdrawing or CO_2 philic, the net effect yields a lower Henry's Law value and thus a greater absorbance of CO_2 (Singh et al 2002; Broeke et al 2002). Following the logic of the first observed trend, the presence of fluorine in the OctMeIm cation would pull more electrons from the cation ring and thus cause a greater net positive effect. In this case thirteen fluorines are used in place of hydrogens. Fluorine has about twice the electro-negativity of hydrogen, thus it is more electron withdrawing. By comparing the values of the OctMeIm with and without the fluorinated cation we see that the presence of fluorine increases the absorbance of CO_2 removal by decreasing the Henry's Law value from 30.7 to 6.1 atm. This finding is very significant in that this value is about 5 times smaller than previously found Henry's Law values, and that it lends positive insights into how to

increase the separation even further.

A third phenomenon that can be observed from the data is the effect of anion selection in CO_2 absorbance. The physical characteristics of the PF_6 and Tf_2N anions were discussed earlier. The PrMeIm cations coupled with PF_6 and Tf_2N anions yield Henry's values of 47.6 and 36.8 atm respectively. The difference in these values could be due to the instability of the PF_6 anion in comparison to the Tf_2N. This characteristic could be the sole purpose for the greater absorbance of CO_2 by ionic liquid coupled with the Tf_2N anion; however, there could be an additional purpose for this increased selectivity. The PF_6 anion is a hexafluoro species. As just discussed fluorine is a strongly electron-withdrawing substituents, thus they tend to pull most of the electrons from the phosphorus to the surrounding fluorine. This movement of electrons to the outer shell of the molecule would induce a greater net negative charge than that of the Tf_2N anion. The greater negative charge of the anion will compete with the carbon dioxide for pairing with the cation of the ionic liquid. Due to this competition in pairing, less carbon dioxide is absorbed by the ionic liquid.

A fourth phenomenon that can be observed from the data is the effectiveness of determining the Henry's Law values of ionic liquids with the QCM when the buoyancy effect is accounted for. The molecular weight of the gas was held constant flowing past the QCM by mixing argon, carbon dioxide, and helium. By conducting the experiment in this manner, the buoyancy does not have to be accounted for using the clean quartz subtraction method. Figure 3.9 show an example of the three gas measurements. Mixing the three gases created a flat baseline frequency response to the clean quartz crystal. The response of the ionic liquid on the QCM is measured by subtracting the ionic liquid on the QCM response with the baseline clean quartz response. The results of this determination yielded a Henry's Law value of 38.3 as opposed to the value of 36.8 as determined by the subtraction method. This agreement in the solubilities confirms the method of correcting for gas density effects in the other measurements.

A fifth phenomenon that can be observed from the data is the effect of CO_2 solubility in ionic liquids in the presence of water.

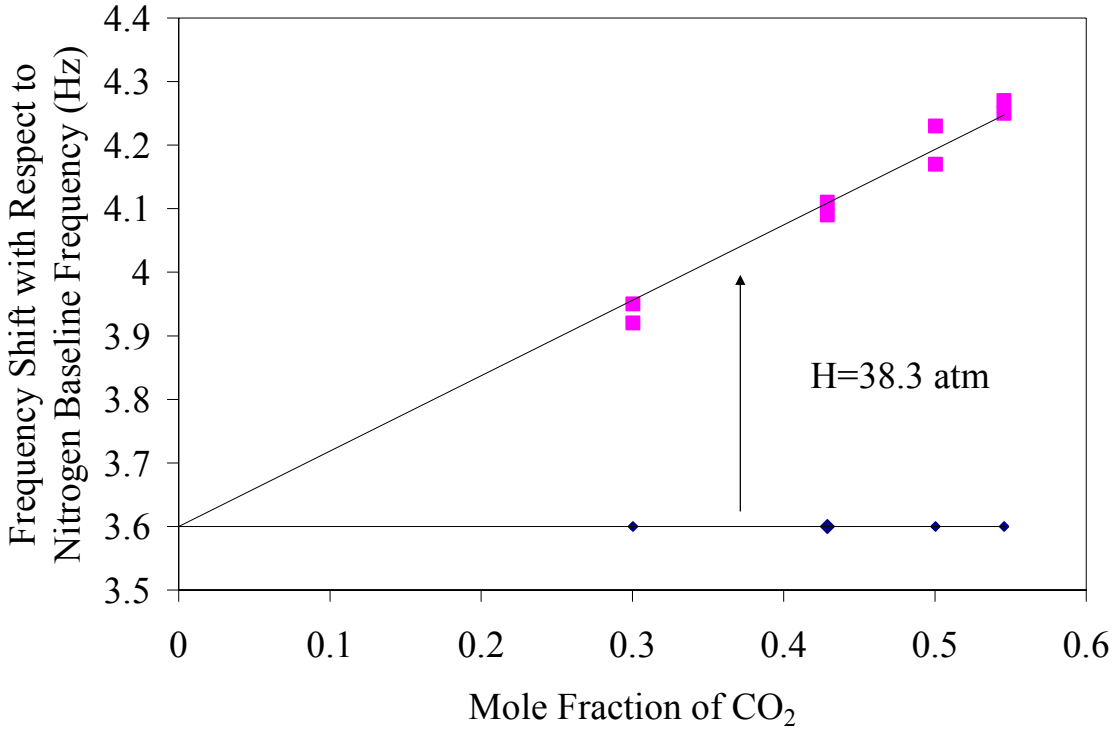

Figure 3.9: Results of QCM Tests Conducted with CO_2-Containing Gas Mixtures with Constant Gas Density

Saturated water vapor was passed over the QCM with no ionic liquid loaded at various concentrations and then this experiment was repeated for an ionic liquid coated QCM. The difference in the clean quartz response and the ionic liquid response is assumed to be the response of the ionic liquid. Figure 3.10 illustrates the QCM response to relative humidity and CO_2 when coated with ionic liquid. Figure 3.10 shows that for a given relative humidity the ionic liquid and QCM shows a greater response when CO_2 is added. When the ionic liquid was removed from water vapor most of the water evaporated from the ionic liquid within seconds; however, each successive run built up a small amount of water in the liquid. Pumping the liquid with dry nitrogen for an hour after contact removed the remaining traces of water.

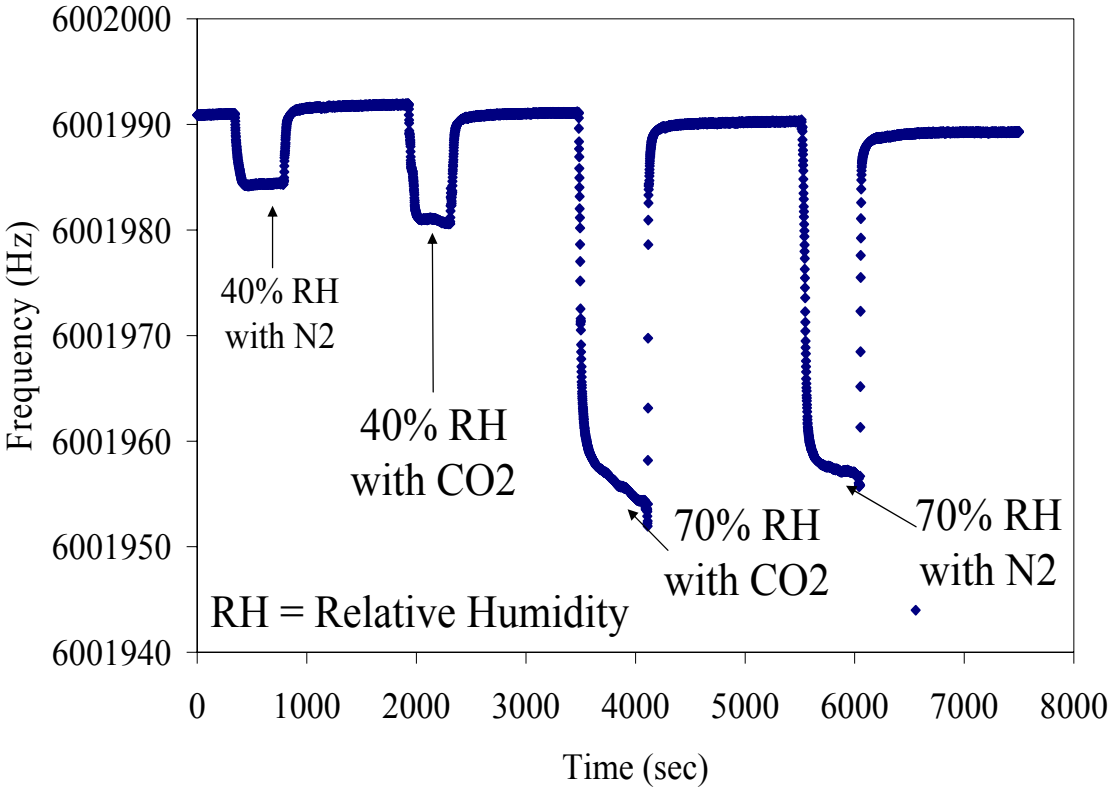

Figure 3.10: Water Effects on CO_2 Uptake in Ionic Liquids

The 40% relative humidity readings appear to have reached equilibrium with the ionic liquid; however, the 70% relative humidity readings seem to indicate that the liquid is approaching equilibrium with the water vapor, but equilibrium frequency shift was not measured. This lack of equilibrium measurement creates error in the CO_2 solubility calculations. Based on the solubilities in Table 3.3, water can not be said to have an effect on solubility measured by the QCM up to around 40% relative humidity. This finding is significant in that small fluctuations in the relative humidity of the QCM cell should not have an impact on the solubilities measured. The relative humidity measurements also allowed for the solubility of water in ionic liquids to be observed. Figure 3.11 shows the concentration of water absorbed at different mole fractions of water in air.

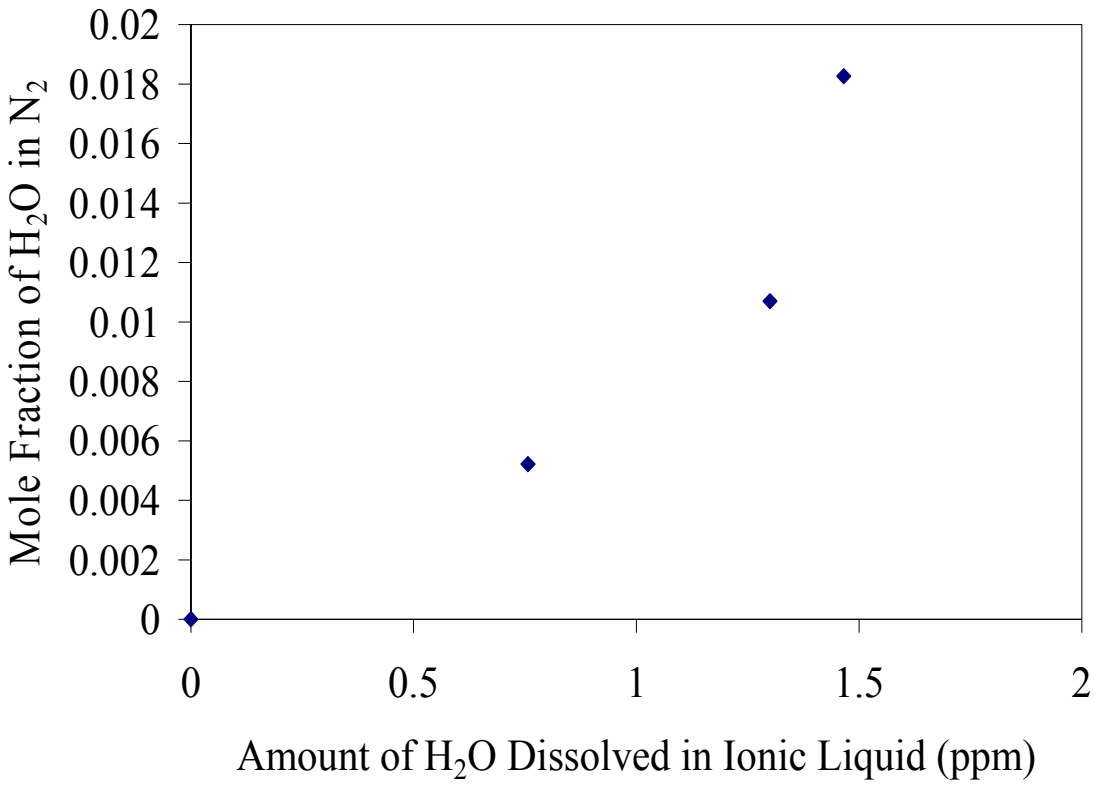

Figure 3.11: Water Solubility in Ionic Liquids at Different Mole Fractions of Water

Figure 3.11 shows a linear response up to 1.2 ppm of water absorbed in the ionic liquid. Beyond this point the solubility decreases asymptotically towards approximately 1.6 ppm. These findings are lower than those observed in the literature. The saturated water content of BuMeIm Tf_2N was approximated to be <100 ppm (or 2% of the ionic liquid) (Bonhote et al 1996). Also the linear region of Figure 3.11 can be used to calculate a Henry's Law value for water in ionic liquids. Based on Figure 3.11 the Henry's Law value for water in OctMeIm Tf_2N is 7000 atm. This value is much higher than those observed using ionic liquids with the PF_6 anion (Blanchard et al 2001). This difference is attributed to a lack of hydrogen bonding of water with the Tf_2N anion (Bonhote et al 1996).

A sixth phenomenon that can be observed from the data is the effect of mixing ionic liquids. Mixing the fluorinated and non-fluorinated OctMeIm Tf_2N liquid showed

the ionic liquids to be fully miscible in each other. The solubility of CO_2 in the ionic liquid mixture was measured in the same manner as the other ionic liquids on the QCM. The mixture produced a Henry's Law value of 14.5 atm. Based on this finding, Figure 3.12 was made to show what solubility might be expected for a given ionic liquid mixture. More ionic liquid mixtures would need to be tested before real projections of CO_2 solubility in mixtures can be established. Another factor to consider for the mixtures is how the physical properties of the ionic liquids change by mixing. No studies have been conducted on the physical properties of ionic liquid mixtures.

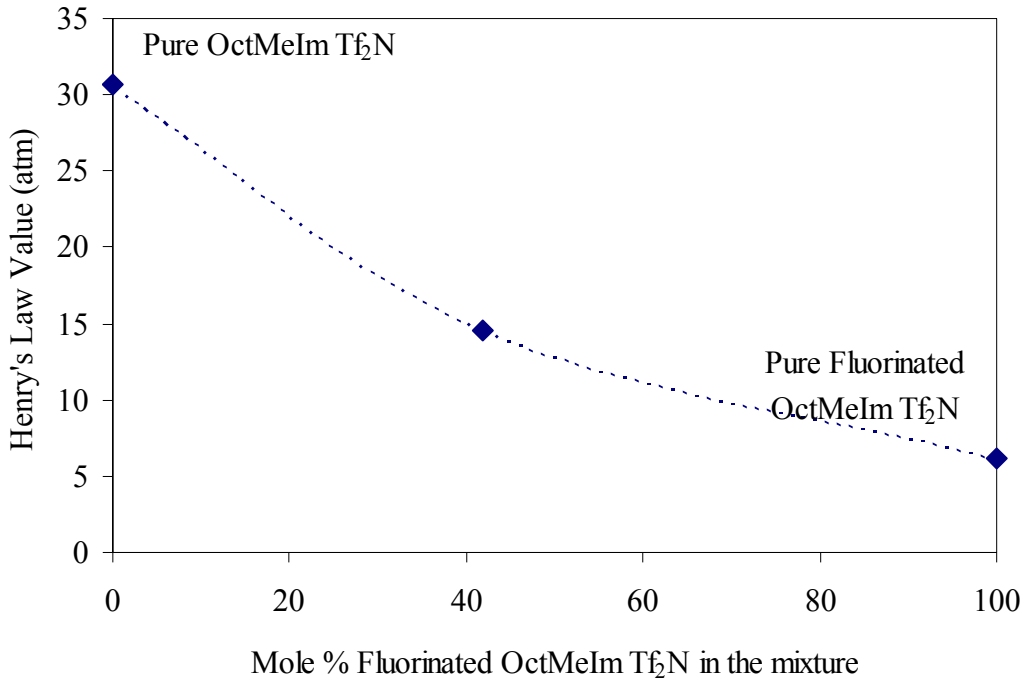

Figure 3.12: CO_2 Solubility Projection for Ionic Liquid Mixtures

Carbon Dioxide Diffusivity in Ionic Liquids

The diffusivity of CO_2 in ionic liquids was determined using the mass uptake over time data obtained from the QCM. This technique of determining the diffusivity on microbalance has been used for polymeric films (Von Solms et al 2003). In order to determine the diffusivity the ionic liquid on the QCM was modeled with the diffusion of gas into a slab. In this model diffusion is only considered to occur in the *Z* direction such that the following second order partial differential equation (PDE), Equation (3-4), applies.

$$D\frac{\partial^2 C_A}{\partial Z^2} = \frac{\partial C_A}{\partial t} \tag{3-4}$$

In this equation *D* is the diffusivity, C_A is the concentration of CO_2 in the ionic liquid, *Z* is the distance into the ionic liquid layer, and *t* is the time. In order to solve the PDE for diffusivity the following boundary conditions were used.

$$\text{Boundary Condition 1: } \frac{\partial C_A}{\partial Z} = 0 \text{ at } Z = 0 \text{ for all } t$$

$$\text{Boundary Condition 2: } C_A = C_{A1} \text{ at Z = d for } t > 0$$

$$\text{Initial Condition: } C_A = 0 \text{ at t = 0 for } Z < d$$

In these conditions *d* is the thickness of the ionic liquid layer and C_{A1} is the concentration at distance *d* at any point beyond time zero, equal to the liquid concentration equilibrated with the gas. Using this PDE and boundary conditions Hines and Maddox (1985) have shown the analytical solution for this PDE yields Equation (3-5) for fractional mass uptake:

$$\frac{M_t}{M_\infty} = 1 - \frac{8}{\pi^2}\sum_{n=0}^{\infty}\frac{1}{(2n+1)^2}\exp\left[-\frac{(2n+1)^2\pi^2 Dt}{4d^2}\right] \tag{3-5}$$

In this equation M_t/M_∞ is the mass transferred divided by the maximum mass uptake and n is the number of iterations. This equation is further simplified by grouping terms to yield as shown in Equation (3-6).

$$t^* = \frac{Dt}{d^2} \tag{3-6}$$

Using these equations the experimentally obtained mass uptake can be fit to the model of the predicted mass uptake to determine the diffusivity. The fractional uptake (g^*) was calculated from experimental data, because g^* equals M_t/M_∞. Equation (3-7) defines g^*.

$$g^* = \frac{(f_o^{IL} - f_o^{CQ}) - (f^{IL} - f^{CQ})}{(f_o^{IL} - f_o^{CQ}) - (f_\infty^{IL} - f_\infty^{CQ})} \tag{3-7}$$

In this equation f_o^{IL} and f_o^{CQ} are the frequency of the ionic liquid and the clean quartz before it has been exposed to CO_2 respectively, f^{IL} and f^{CQ} are the frequency of the ionic liquid and clean quartz at any time during the exposure, and f_∞^{IL} and f_∞^{CQ} are the asymptotic frequency values of the ionic liquid and clean quartz. Since in thin layer measurements mass is directly proportional to frequency and mass uptake is directly proportional to concentration, then g^* is equal to the fractional uptake of CO_2 in the liquid. In Figure 3.13 g^* is plotted with time for experimental data to show the mass uptake of CO_2 observed on the QCM coated with ionic liquid. This curve shows mass uptake of CO_2 with time. Since g^* equal to M_t/M_∞, then by plotting Equation 3-5, g^* will be known with respect to t^*. Values for M_t/M_∞ were calculated by truncating the series to $n = 150$. Figure 3.14 shows the experimental relationship observed between g^* and t^* and the models predicted behavior. In this plot the solid line is the model results and the dotted line are the QCM measured results. The experimental results were fit to the model at 80% CO_2 uptake, which fits well from $t^* = 0.6$ to 0.9, so this value can be used to determine the diffusivity.

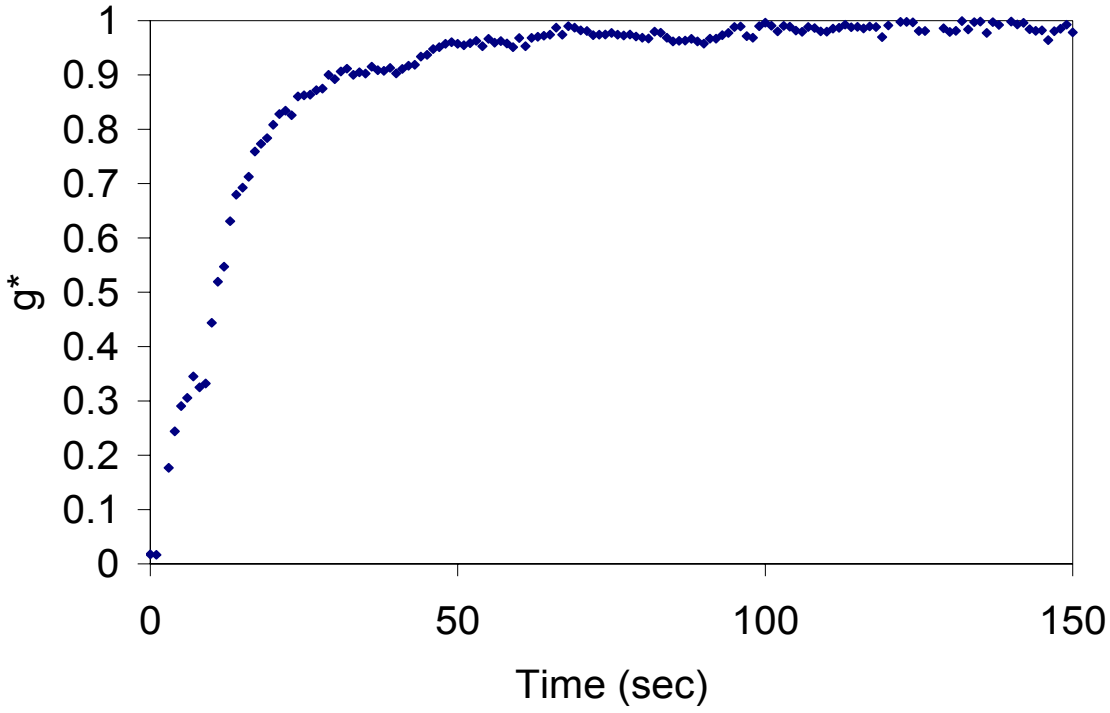

Figure 3.13: Mass Transfer of CO_2 into Ionic Liquid

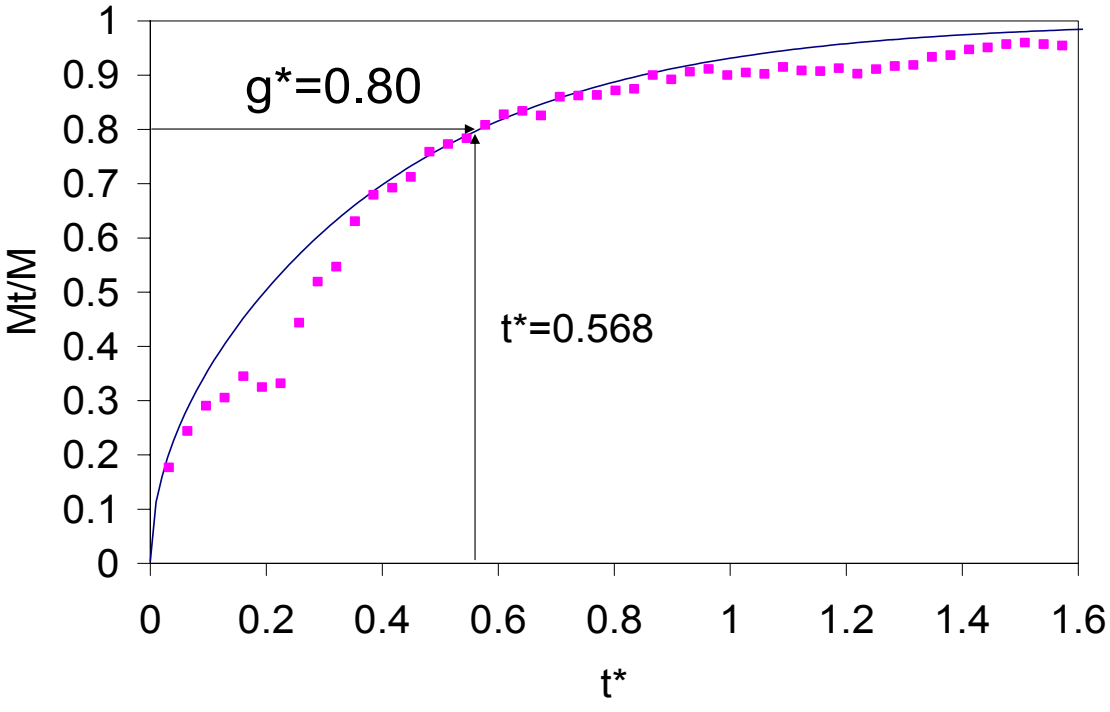

Figure 3.14: Modeled Diffusion of CO_2 into Ionic Liquid

At g^* equals 0.8, t^* equals 0.568, and t equals 17.7 seconds (Figure 3.13). The ionic liquid film thickness for these particular measurements is estimated to be 93 nm. Using equation 3.6 and these values the diffusivity of the fluorinated OctMeIm Tf_2N was determined to be $2.78\times10^{-12}cm^2/sec$. This diffusivity is much lower than one would expect for a gas entering a liquid. In high-density polyethylene (HDPE) Von Solms determined the diffusivity of CO_2 to be $1.15\times10^{-6}cm^2/sec$ (2003). The much lower diffusivity of the ionic liquid might be due to the following factors.

1. The thickness is an approximation based on the assumption that the ionic liquid deposits uniformly on the quartz crystal surface. The frequency shift of the ionic liquid when it is coated on the QCM provides the mass of ionic liquid applied. For liquids of known density the volume of ionic liquid can be determined. For unknown liquids of unknown densities, the density is estimated for volume calculation. This volume of ionic liquids is divided by the area the liquid occupies on the QCM to determine the thickness of the layer. Diffusivity is directly proportional to thickness, so variations in the thickness of the ionic liquid layer would cause some error in the calculations. This error would not account for the large deviation in diffusivity observed from what might be expected for gaseous diffusion into a liquid. The thickness would have to be off by a factor of 1000 (92,000 nm thickness) in order to receive an expected diffusion of 2.78×10^{-6} cm^2/sec
2. The selection of a point where g* equals M_t/M_∞ can change the value calculated for diffusivity since the experimental data does not perfectly fit the modeled curve. This error would also create small variations in the diffusivity similar to the thickness error, but does not account for such a lower diffusivity than expected.
3. The basis of the mass uptake measurements on the QCM is that the ionic liquid is acting like a solid on the quartz surface such that density and viscosity effects are not changed with gas uptake. The diffusivity calculated for the ionic liquid is similar to that which would be expected for gas diffusion in a solid.

Diffusivity was measured for non-fluorinated OctMeIm Tf_2N which has a much lower viscosity than the fluorinated liquid to determine if the diffusivity would increase. The diffusivity of the non-fluorinated OctMeIm Tf2N was determine to be $4.16\times10^{-11}cm^2/sec$. The results of the g* curve with time indicate that both of the liquids have very similar mass uptakes with time. Figure 3.15 shows this finding. The non-fluorinated ionic liquid appears to have a slightly greater diffusivity than the fluorinated liquid. Diffusion calculations of other CO_2 response curves indicate good agreement in values; however, due to the similarity of diffusion in the thin layers it is difficult to say anything about trends in diffusivity with different ionic liquids within the diffusion uncertainty. The thicknesses of these two ionic liquid layers were similar so there diffusivity was of the same magnitude. This indicates that the ionic liquid layer is most likely acting like a solid and thus the transport properties of the gas entering the ionic liquid are similar to those observed with gas entering a solid.

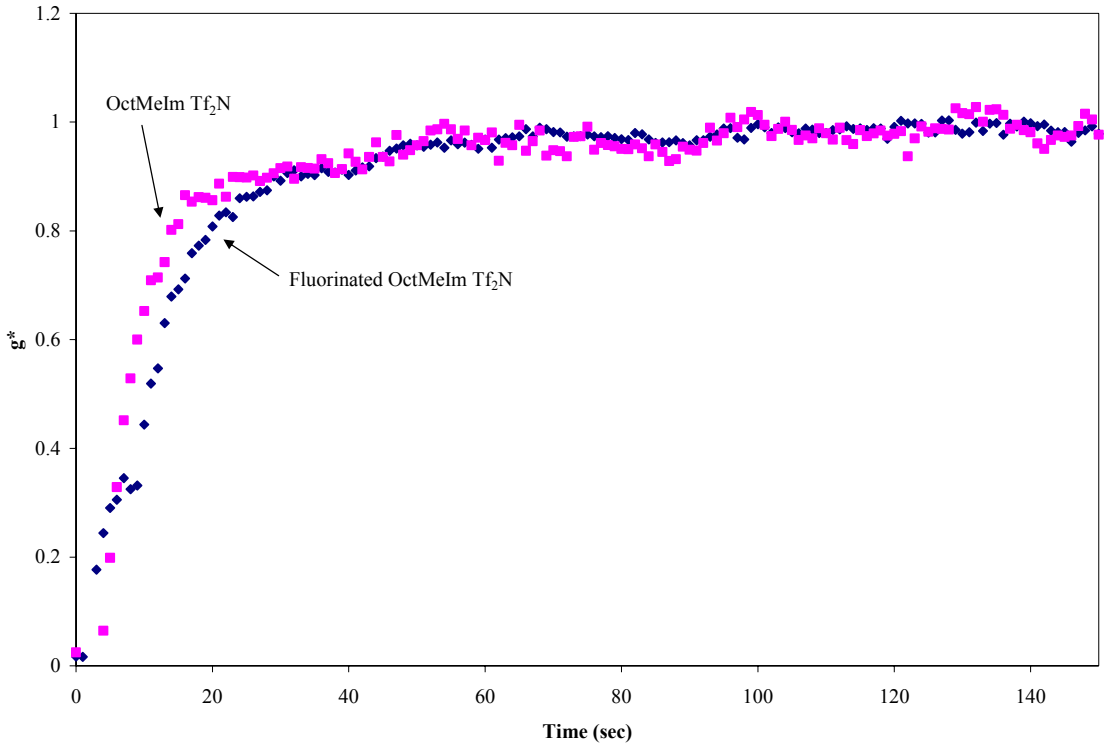

Figure 3.15: Mass Uptake in Different Ionic Liquids

This diffusion value is significant in that it indicates the speed in which CO_2 is entering the ionic liquid on the QCM; however, this diffusion may not be the same that would occur for CO_2 going into the membrane. For this reason the solubility multiplied by the diffusivity may not yield the expected permeance of the membrane.

Carbon Dioxide Membrane Permeance

Using the apparatus given in Figure 3.7, carbon dioxide pressures were measured and the permeance of CO_2 through a SILM was calculated. Figures 3.16 and 3.17 are representative of data obtained from these experiments. This data was recorded for single-gas permeance of a BuMeIm Tf_2N SILM. The data was plotted such that the slope is directly proportional to the permeance. CO_2 crosses through the membrane at a constant rate which can be observed by the linearity of the plots with respect to time.

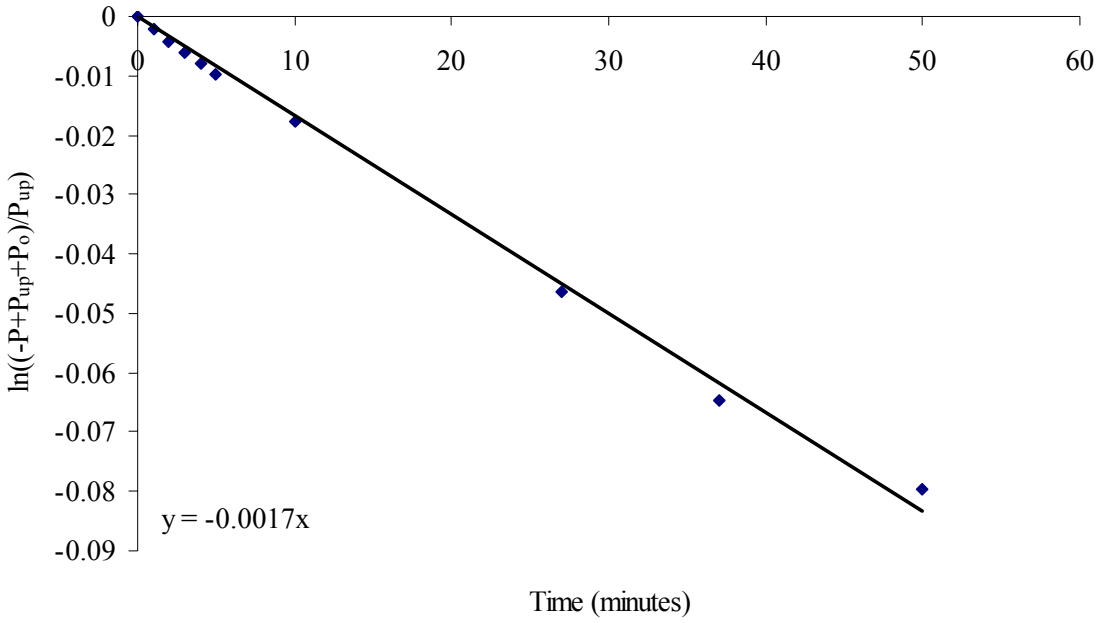

Figure 3.16: CO_2 Single-gas Permeance through a BuMeIm Tf_2N Coated SILM

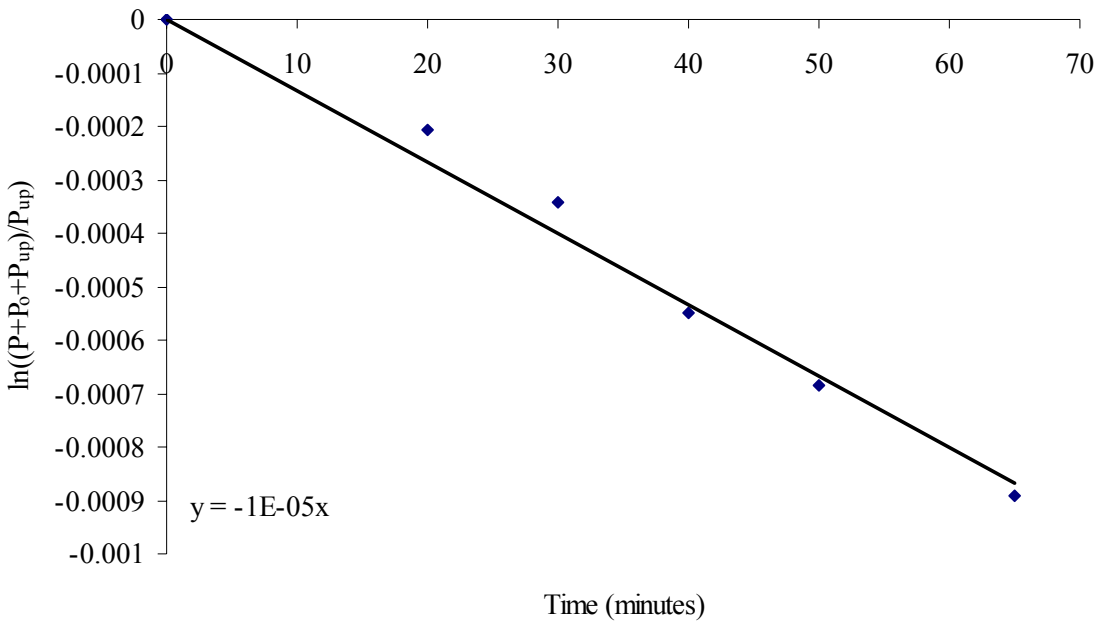

Figure 3.17: N_2 Single-gas Permeance through a BuMeIm Tf_2N Coated SILM

These experiments were conducted with 0.02 µm pore sized membranes. At this pore size the permeance is constant; however, at larger pore sizes (0.20 µm) this was not found to be the case. At larger pore sizes the permeance increased with time thus possibly indicating a leak in the system or the pores becoming unfilled with ionic liquid over time. As expressed in Equation (3-2) the permeance can be determined from plots of the ln(($P + P_o + P_{up}$)/P_{up}) versus time; the slope is defined by Equation (3-8).

$$\left(\frac{A \cdot R \cdot T \cdot Permeance}{V}\right) \tag{3-8}$$

In the data shown, the slope of the SILM in the presence of CO_2 is greater than that with N_2. Using Equation (3-2) these slopes correspond to permeances for CO_2 and N_2 of 4.06×10^{-9} mol/(atm*cm^2*sec) and 3.20×10^{-11} mol/(atm*cm^2*sec) respectively. These permeances can be used to estimate the selectivity of CO_2 to N_2 through the SILM with Equation (3-9).

$$Selectivity = \left(\frac{Permeance_{CO_2}}{Permeance_{N_2}} \right) \tag{3-9}$$

Using this equation the selectivity of CO_2 to N_2 can be found to be 127. This value indicates that CO_2 will pass through the SILM 127 times faster than N_2 with the same driving force. Table 3.4 lists more permeance and selectivities measured through different SILMs. The BuMeIm Tf_2N permeance values are an average of five runs. Only one run has been completed for the fluorinated OctMeIm Tf_2N membrane. From these measurements one can see the importance of knowing the solubility as well as the diffusivity to determining the permeance. In the solubility study the fluorinated OctMeIm Tf_2N ionic liquid had a much higher solubility of CO_2 than the BuMeIm Tf_2N; however, due to the greater viscosity of the fluorinated ionic liquid the mass transfer of CO_2 occurs more slowly than for the BuMeIm Tf_2N. Only preliminary measurements have been made for the fluorinated ionic liquid but the results of a permeance similar to BuMeIm Tf_2N is not unusual, because one might expect the mass transfer limitations of the fluorinated ionic liquid to offset its increased solubility.

Table 3.4: Measured Permenace and Selectivity for Supported Ionic Liquid Membranes

Ionic Liquid	Gas	Permeance (mol/atm*cm^2*sec)	Selectivity with Respect to N_2
BuMeIm Tf2N	CO_2	4.06E-09	127
BuMeIm Tf2N	N_2	3.20E-11	---
Fluorinated OctMeIm Tf2N	CO_2	1.52E-09	72
Fluorinated OctMeIm Tf2N	N_2	2.11E-11	---

Economic Feasibility of CO_2 Removal with Ionic Liquid Membranes

The measurements obtained so far for CO_2 separations using ionic liquids can be used to provide a general preliminary economic assessment of their potential use in industry and to determine if their known properties make them economically competitive with modern technology. The QCM measurements were used to determine the solubility of CO_2 in various ionic liquids. These solubilities were used to determine which ionic liquids might be the best candidates for SILM separations. The permeance measurements obtained from the SILM experiments provide insights into the technical feasibility of using a SILM process for CO_2 separation from flue gases. With these values it is possible to design a model for comparison with present technologies to determine the economic feasibility of SILMs in industry.

As mentioned before, there are currently two leading popular approaches to carbon dioxide separation in coal-fired power plants: amine scrubbers and H_2-CGCC (hydrogen-fired coal gasification combined cycle) with acid gas scrubbers (Simbeck 2001). Of these processes the amine scrubber is the most widely accepted CO_2 recovery operation, but the H_2-fired CGCC appears to be the cheapest means of separating the carbon dioxide (Simbeck 2001). Currently no process is an economically viable one due to the low cost of CO_2 disposal; however, as more government restrictions are levied on power companies the need for a low cost CO_2 removal system will become imperative.

Amine scrubbing works by spraying the resultant flue gas produced by the steam boilers and separating the CO_2 from the other gases. The CO_2 is absorbed by the amine droplets while the flue gas flows through the system unperturbed (Chapel 1999). This system is thought to be the most reliable procedure for removing CO_2 due to the low cost of amine solvents and their CO_2 extraction efficiency (Singh 2000). Through use of the same design and basis of coal usage, an ionic liquid membrane process could be used to replace the existing carbon dioxide scrubbing units. By calculating the change in cost of the energy and materials requirement, one can show an estimate of the economic feasibility of ionic liquid membrane technology in flue gas cleanup. In order to do this analysis, economic analysis conducted on the amine and hydrogen fired processes by

Simbeck were used. Figure 3.18 illustrates the amine scrubbing design and economics as presented by Simbeck (2001). This setup is for 90 percent removal of CO_2 from a 290 MWe process based on the combustion of 0.48 metric tons of raw coal per metric tons of CO_2 produced and 0.08 metric tons of natural gas per metric ton of CO_2 produced. The retrofit amine scrubbing system required an additional boiler, steam generator, scrubber/stripper, and gas compressor/dryer. The economics calculated for this process by Simbeck are shown in Figure 3.19.

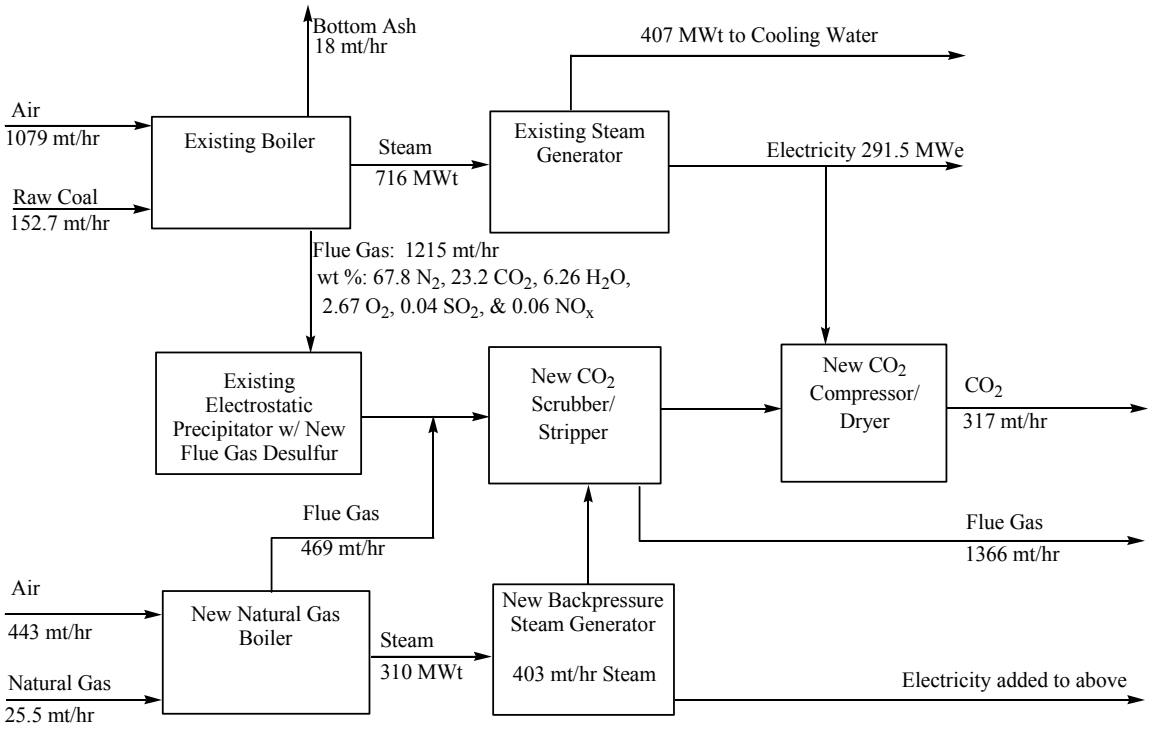

Figure 3.18: Amine Scrubbing Process from Simbeck (2001)

Capital Costs		Units	$ MM	$/kW net
	Existing Solids Handling	$/mt/d raw coal	29	101
	Existing PC Boiler	$/lb/hr reheat steam	122	420
	Existing ST/ gen	$/kWe gross	62	212
	New FGD-caustic wash	$/mt/hr PC flue gas	18	63
***	New SCR	$/mt/hr PC flue gas	-	-
	Existing ESP	$/mt/hr PC flue gas	5	17
	New NG Boilers	$/lb/hr no RH steam to boiler	13	46
	New Extraction ST/gen	$/kWe ST	19	64
	New CO2 Scrubber	$/mt/hr PC+NG flue gas	42	144
	New CO2 Stripper	$/mt/hr CO2	42	141
	New CO2 Drying & Compress	$/kWe power	46	159
	General Facilities	% of process unit capital	36	123
	Eng. Fees & Contingencies	% of process unit capital	18	62
	New Capital		**452**	**1552**
	Payoff Existing PC	% of original capital	28	97
	Retrofit Outage Power	$/MWhr for 0.10 year	7	22
	Total Capital		**487**	**1671**
Electricity Cost		% annual capacity factor		
	Capital Charges	% of capital per year	68	27
	Payoff Existing PC	% of PC capital per year	4	2
	Retrofit Outage Power	% of power cost per year	1	0.4
	O&M	% of capital per year + PC	21	8
	CO2 Emissions Tax	per mt CO2	-	-
	CO2 Disposal or Use	per mt CO2	24	11
	Natural Gas	per MM btu LHV	38	18
	Coal	per MM btu LHV	11	5
	CO2 Retrofit of Existing PC + New NGB		**167**	**70**
Baseline Existing PC Reference				12
	Net Change			28
CO2 Retrofit of Existing PC + New NGB Relative to existing PC			%	581
Marginal Load Dispatch Cost		% of O&M + fuel & CO2 costs		
	CO2 Retrofit of Existing PC + New NGB			16.5
	Baseline Existing PC Reference			7.5
		CO2 Emissions mt/MWh		
		0.121		
		0.971		
		-0.85		
	Percent CO2 Removal	-90	%	
	Cost for mt of CO2 Captured	**33.00**	$/mt CO2 avoided	
	Cost for mt of C Captured	**121**	$/mt carbon avoided	

Figure 3.19: Amine Scrubbing Economics from Simbeck (2001)

The most important values to note from this spreadsheet are the percent CO_2 removal (90%) and the cost per metric ton of CO_2 recovered ($33.00/mt CO_2). The capital and electricity costs are broken down into key unit costs, millions of dollars per year, and dollars per kilowatt produced.

In order to compare the economic feasibility of the ionic liquid membrane process, the Simbeck design and economic calculations were modified. By using the same assumptions a comparable economic evaluation can be made and we can see under which conditions an ionic liquid membrane would be profitable over amine scrubbing. Figure 3.20 is the proposed design for this process. The major changes in this setup are that a new flue gas compressor and ionic liquid membrane cartridge have been added in place of the amine scrubber/stripper, natural gas boiler, and steam generator. The new compressor is needed to sufficiently pressurize the gas so that it has a driving force for passing through the membrane. The membrane permeance was based on laboratory results.

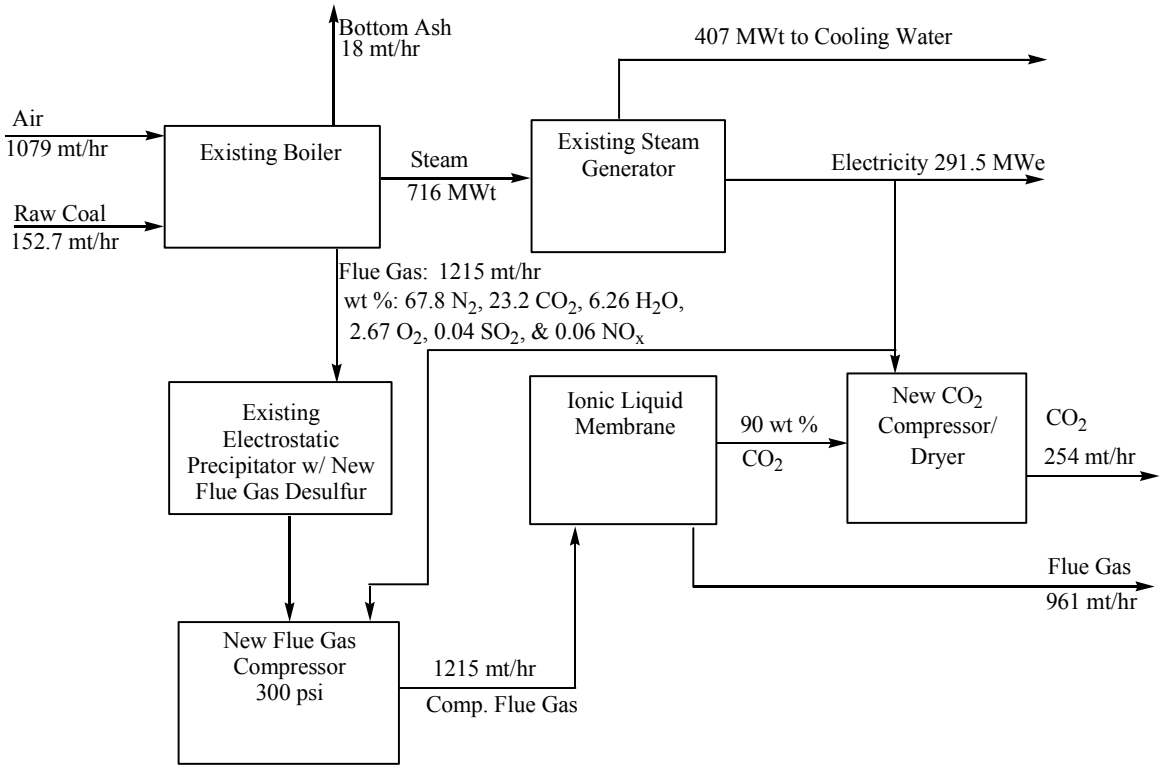

Figure 3.20: SILM Process

These results were coupled with personal communications from Fluor Daniel and Air Products to estimate membrane cartridge size and condenser properties. The following assumptions and parameters were used in doing the economic comparison.

Assumptions and Parameters:

1. The ionic liquid used for this design is BuMeIm Tf_2N.
2. The permeance and Henry's law values were both determined in the lab to be 4.06×10^{-9} mol $CO_2/(cm^2*sec*atm)$ and 37 atm respectively. The selectivity with N_2 was determined to be 127. Since no water vapor studies have been conducted with the SILM, the selectivity of CO_2 to N_2 under dry conditions was used to estimate the amount of ionic liquid needed for the separation.
3. In order to increase the permeance the membrane thickness was estimated to be 5 times thinner than those used in the laboratory, thus increasing the permeance by a factor of 5, making the permeance 2.03×10^{-8} mol $CO_2/(cm^2*sec*atm)$.
4. The amount of ionic liquid needed to coat the membrane was scaled based on the amount of ionic liquid measured on the membranes used in the lab (0.080g). This mass indicates that 0.056 cm^3 of ionic liquid is in the membrane. The area of the membranes used in the experiments was 15.2 cm^2.
5. The membrane cartridge was designed based on specifications given by Bill Pope from Air Products (2002). The membrane area needed was calculated using the single-gas permeance of BuMeIm Tf_2N and assuming 90% of the CO_2 would be removed from the flue gas. This would require about 30,000,000 m^2 membrane area which would cost approximately \$55,000,000/mt CO_2 removed/hr according to Air Products.
6. The ionic liquid BuMeIm Tf_2N is commercially available from Covalent Associates Inc. Based on a price quote a gallon of this solvent would cost \$18,000. To fully coat the membrane 350,000 gallons of ionic liquid would be needed, so the total cost of the solvent equals \$22,000,000. The lifetime of these liquids in the membrane is unknown.

7. In order to supply sufficient driving force for the gas to pass through the membrane Bill Pope indicated that the gas would need to be compressed to 300 psi. A compressor capable of this work was estimated to cost $16,000,000 for the membrane setup designed.
8. In order to power the compressor a new boiler will be needed. The power gained from not needing a backpressure steam generator is assumed to be offset by the increased power needed for the new boiler.

Based on these assumptions an economic evaluation was produced, which is shown in Figure 3.21. The ionic liquid process is $8.60 more per metric ton of CO_2 captured. This corresponds to $21,200,000 more per year than the amine scrubbing process. Based on these assumptions and results, a projection can be made to determine the breakeven Henry's Law constant needed to reduce the cost of the ionic liquid membrane process to that of the amine scrubber. In order to do this projection the Henry's Law constant is assumed to be directly proportional to the permeance, such that I am assuming that the diffusivity of the liquids is the same as that for BuMeIm Tf_2N. Figure 3.22 illustrates the breakeven point and the savings that could be produced by using ionic liquids with greater CO_2 separation. As can be seen in Figure 3.22, an ionic liquid with a Henry constant of 14 atm or below would make the membrane system more economical than the amine technology at the diffusivity of BuMeIm Tf_2N. On the graph the Henry constants of the fluorinated OctMeIm Tf_2N and a 55% non-fluorinated OctMeIm Tf_2N, 45% fluorinated OctMeIm Tf_2N mixture are listed. As seen from the permeance of the fluorinated ionic liquid, this value of solubility is not going to produce the savings one would expect based on this projection. This liquid was mixed with a non-fluorinated ionic liquid, which has a lower viscosity, in order to try to increase the diffusivity while maintaining a high solubility. The mixture produced a Henry's Law value of 14.3 atm and has not been tested for permeance values. If the mixture diffusivity is close to BuMeIm Tf_2N, then ionic liquid mixtures might be the key to creating real economic savings over amine scrubbing.

Capital Costs	Units	$ MM	$/kW net
Existing Solids Handling	$/mt/d raw coal	29	101
Existing PC Boiler	$/lb/hr reheat steam	122	420
Existing ST/ gen	$/kWe gross	62	212
New FGD-caustic wash	$/mt/hr PC flue gas	18	63
New Ionic Liquid Membrane Cartridge	$/mt/hr PC flue gas	55	122
Existing ESP	$/mt/hr PC flue gas	5	17
Ionic Liquid Solvent Cost	$/mt/hr PC flue gas	22	90
New CO2 Drying & Compress	$/kWe power	46	159
New Natural Gas Boiler	$/lb/hr no reheat steam	13	46
New Compressor	$/mt/hr PC flue gas	16	65
Subtotal of New and Retrofit		**388**	**1296**
General Facilities	% of process unit capital	78	259
Eng. Fees & Contingencies	% of process unit capital	39	130
New Capital		**504**	**1684**
Payoff Existing PC	% of original capital	28	98
Total Capital		**533**	**1782**
Electricity Cost	% annual capacity factor		
Capital Charges	% of capital per year	76	35
Payoff Existing PC	% of PC capital per year	4	2
O&M	% of capital per year + PC	21	10
CO2 Emissions Tax	per mt CO2	-	-
CO2 Disposal or Use	per mt CO2	24	11
Natural Gas	per MM btu LHV	38	18
Coal	per MM btu LHV	11	5
CO2 Retrofit of Existing PC + New NGB		**174**	**81**
Baseline Existing PC Reference			12
Net Change			69
CO2 Retrofit of Existing PC + New NGB Relative to existing PC		%	671
	CO2 Emissions mt/MWh		
	0.160		
	1.596		
	-1.436		
Percent CO2 Removal	-90 %		
Cost for mt of CO2 Captured	**41.60**	$/mt CO2 avoided	
Cost for mt of C Captured	**152.54**	$/mt carbon avoided	

Figure 3.21: SILM Economics

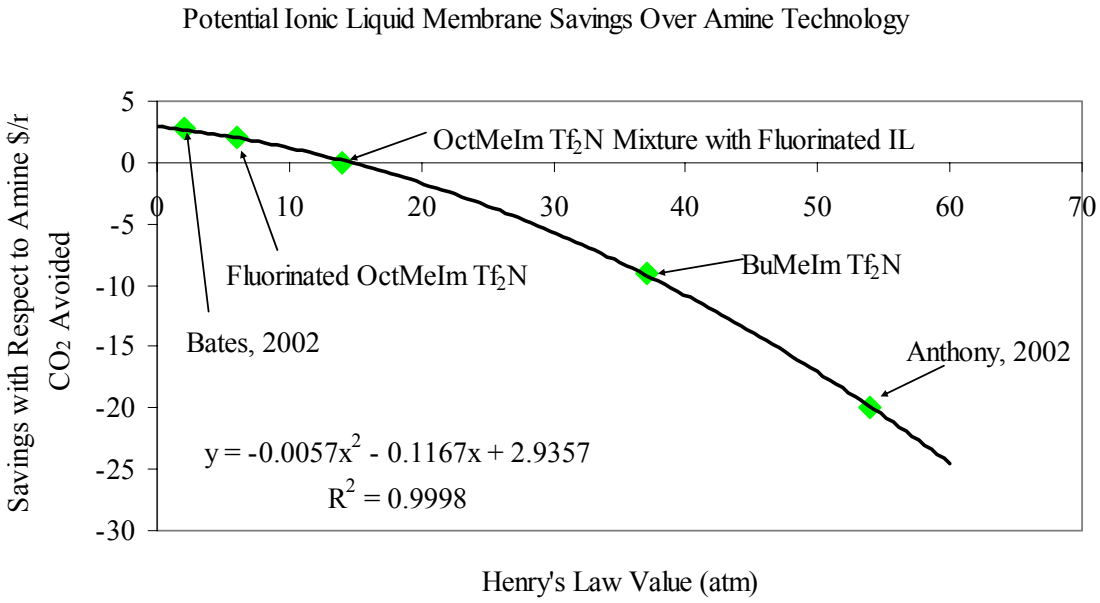

Figure 3.22: Potential Ionic Liquid Savings

Amine scrubbing is the most popular proposed method for CO_2 capture; however, H_2-CGCC coupled with amine scrubbing is an alternative to this process. Simbeck designed and provided economics to compare this H_2-CGCC process to amine scrubbing (2001). Since this method is not as widely accepted, only a quick economic comparison of this process was made with substituting ionic liquid membrane technology. In this substitution the acid gas scrubber/stripper in that process was replaced with an ionic liquid membrane column. The economic comparison centered on the reduced equipment cost of a scrubber/stripper and the increased cost of the membrane system. The assumptions used for the ionic liquid in the amine process were used here as well for direct comparison. Using these assumptions it appears as though the ionic liquid membrane, \$39 per metric ton of CO_2 avoided, is slightly more profitable than the value calculated for the comparison with the amine scrubbing process, but far from comparable to the H_2 fired process, \$25 per metric ton of CO_2 avoided. Table 3.5 summarizes these and the amine scrubbing findings.

Table 3.5: Comparison of CO_2 Removal Costs to SILMs Costs

CO_2 Removal Process	\$/mt CO_2 Avoided
Amine Scrubbing on Flue Gas	33
Amine Scrubber with H_2-Fired CGCC	25
SILM (New Boiler-BuMeIm Tf_2N)	42
SILM (Substituting AG Scrub/Strip)	39

In considering this comparison keep in mind that many untested assumptions were used. However, even if some of the assumptions do not hold, these designs provide a model in which it can be seen that ionic liquids could play a role in future CO_2 sequestration from flue gas emissions.

4.0. Conclusions

The study of separations is constantly changing. As novel chemicals are produced, separations become more advanced with better results. The novel chemicals presented here are no exception to this rule. In this project it was shown how room-temperature ionic liquids can be used in desulfurization and CO_2 removal processes. Furthermore these processes could be competitive alternatives to the separation processes of today. In addition to similar separations, the ionic liquids provide the enhanced benefit of their desirable physical properties, thus making them desirable alternatives to commonly used solvents. Since this is a relatively new class of compounds the possibilities for new applications of these solvents is nearly limitless. The point of this project was to explore a few of these possibilities and to show the real potential for these chemicals in an industrial setting. By extending values such as the Henry's Law constants which are commonly found in the literature, to real life applications, one can see the real potential benefits for ionic liquids in industry. To further develop the potential implementation of these liquids in industry the following items would be useful for further study.

1. Humidity Effects: Preliminary experiments indicate that the presence of large amounts of water has an impact on the CO_2 solubility. Further studies are needed for solubility measurements as well as applying relative humidity to the SILMs to see the water affects on permeance.
2. More Membrane Tests: Only a few membrane tests have been conducted on a limited number of liquids. More liquids need to be tested to determine a real correlation between solubility and permeance.

References

1. Abraham, Michael H.; Zissimos, Andreas M.; Huddleston, Jonathon G.; Willauer, Heather D.; Rogers, Robin D.; Acree, William E. Jr. Some Novel Liquid Partitioning Systems: Water-Ionic Liquids and Aqueous Biphasic Systems. *Ind. Eng. Chem. Res.*, **2003**, 42, 413-418.

2. Adam, David. Clean and green…but are they mean? *Nature*, **2000**, 407, 938-940.

3. Aki, Sudhir N.V.K.; Brennecke, Joan F.; Samanta, Anunay. How polar are room-temperature ionic liquids? *Chem. Commun.*, **2001**, 413-414.

4. Allen, Donald; Baston, Graham; Bradley, Antonia E.; Gorman, Tony; Haile, Andy; Hamblett, Ian; Hatter, Justine E.; Healey, J.F.; Hodgson, Brian; Lewin, Robert; Lovell, Kevin V.; Newton, Bill; Pitner, William R.; Rooney, David W.; Sanders, David; Seddon, Kenneth R.; Sims, Howard E.; Thied, Robert C. An investigation of the radiochemical stability of ionic liquids. *Green Chemistry*, **2002**, 4, 152-158.

5. Anderson, Jared L.; Ding, Jie; Welton, Thomas; Armstrong, Daniel W. Characterizing Ionic Liquids On the Basis of Multiple Solvation Interactions. *J. Am. Chem. Soc.*, **2002**, Vol. 124, No. 47, 14247-14254.

6. Angelici, Robert J.; McKinley, Scott; Alvarez. Sulfur Reduction in Gasoline and Diesel Fuels by Extraction/Adsorption of Refractory Dibenzothiophenes. Web journal available at: www.netl.doe.gov/publications/proceedings/01/ucr-hbcu/angilici.pdf, **2001**.

7. Anthony, Jennifer L.; Maginn, Edward J.; Brennecke, Joan F. Solution Thermodynamics of Imidazolium-Based Ionic Liquids. *J. Phys. Chem. B* **2001**, 105, 10942-10949.

8. Baird, Colin. Environmental Chemistry: 2nd Edition. W. H. Freeman and Company, **1999**.

9. Baker, Sheila N.; Baker, Gary A.; Bright, Frank V. Temperature-dependent microscopic solvent properties of 'dry' and 'wet' 1-butyl-3-methylimidizolium hexafluorophosphate: correlation with ET(30) and Kamlet-Taft polarity scales. *Green Chemistry*, **2002**, 4, 165-169.

10. Bates, Eleanor D.; Mayton, Rebecca D.; Ntai, Ioanna; Davis, James H Jr. CO_2 Capture by a Task Specific Ionic Liquid. *J. Am. Chem. Soc*, **2002**, Vol. 124, No. 6, 926-927.

11. Berger, Alexsandro; de Souza, Roberto F.; Delgado, Marcelo R.; Dupont, Jairton. Ionic liquid-phase asymmetric catalytic hydrogenation: hydrogen concentration effects on enantioselectivity. *Tetrahedron: Asymmetry*, **2001**, 12, 1825-1828.

12. Blanchard, Lynnette A.; Brennecke, Joan F. Recovery of Organic Products from Ionic Liquids Using Supercritical Carbon Dioxide. *Ind. Eng. Chem. Res.* **2001**, 40, 287-292.

13. Blanchard, Lynnette A.; Gu, Zhiyong; Brennecke, Joan F. High-Pressure Phase Behavior of Ionic Liquid/CO_2 Systems. *J. Phys. Chem. B* **2001**, 105, 2437-2444.

14. Bonhote, Pierre; Dias, Ana-Paula; Papageorgiou, Nicholas; Kalyanasundaram, Kuppuswamy; Gratzel, Michael. Hydrophobic, Highly Conductive Ambient-Temperature Molten Salts. *Inorg. Chem.,* **1996**, 35, 1168-1178.

15. Bosmann, A.; Datsevich, L.; Jess, A.; Lauter, A.; Schmitz, C.; Wasserchеid, P. Deep desulferization of diesel fuel by extraction with ionic liquids. *Chem. Commun.*, **2001**, 2494-2495.

16. Branco, Luis C.; Crespo, Joao G.; Afonso, Carlos A.M. Highly Selective Transport of Organic Compounds by Using Supported Liquid Membranes Based on Ionic Liquids. *Angew. Chem. Int. Ed.*, **2002**, Vol. 41, No. 15, 2771-2773.

17. Brennecke, Joan F. Presentation given at Oak Ridge National Laboratory, Nuclear Science and Technology Division, on CO_2 separations involving room temperature ionic liquids. March 2003.

18. Brennecke, Joan F.; Maginn, Edward J. Ionic Liquids: Innovative Fluids of Chemical Processing. *AIChE Journal*, **2001**, Vol. 47, No. 11, 2384-2389.

19. Broeke, Joep van den; Winter, Ferry; Deelman, Berth-Jan; Koten, Gerard van. A Highly Fluorous Room-Temperature Ionic Liquid Exhibiting Fluorous Biphasic Behavior and Its Use in Catalyst Recycling. *Org. Lett.*, **2002**, Vol. 4, No. 22, 3851-3854.

20. Chapel, Dan; Ernest, John; Mariz, Carl. Recovery of CO_2 from Flue Gases: Commercial Trends. Paper no. 340 presented at Canadian Society of Chemical Engineers annual meeting, October 4-6, **1999**, 1-18.

21. Cull, S.G.; Holbrey, J.D.; Vargas-Mora, V.; Seddon, K.R.; Lye, G.L. Room-Temperature Ionic Liquids as Replacement for Organic Solvents in Multiphase Bioprocess Operations. *Biotechnology and Bioengineering*, **2000**, Vol. 69, No. 2, 227-233.

22. Douglas, James M.; Woodcock, Duncan C. Cost Diagrams and the Quick Screening of Process Alternatives. *Ind. Eng. Chem. Process Des. Dev.*, **1985**, 24, 970-976.

23. Fadeev, Andrei G.; Meagher, Michael M. Opportunities for ionic liquids in recovery of biofuels. *Chem. Commun.*, **2001**, 295-296.

24. Gannon, Thomas J.; Law, George; Watson, Philip R. First Observation of Molecular Composition at the Surface of a Room-Temperature Ionic Liquid. *Langmuir* **1999**, 15, 8429-8434.

25. Gordon, Charles M. New Developments in Catalysis using Ionic Liquids. *Applied Catalysis A: General,* **2001**, 222, 101-117.

26. Grate, Jay W.; Patrash, Sammuel J.; Abraham, Michael H. Method for estimating polymer-coated acoustic wave vapor sensor responses. *Anal. Chem.*, **1995**, 67, 2162-2169.

27. Hanke, C.G.; Price, S.L.; Lynden-Bell, R.M. Intermolecular potentials for simulations of liquid imidazolium salts. *Molecular Physics*, **2001**, Vol. 99, No. 10, 801-809.

28. Hawk, G. G.; Aulbaugh. High vacuum indirectly-heated rotary kiln for the removal and recovery of mercury from air pollution control scrubber waste. *Waste Management*, **1998**, 18, 461-466.

29. Hines, Anthony L.; Maddox, Robert N. Mass Transfer Fundamentals and Applications. *Prentice Hall*, **1985**.

30. Howarth, Joshua; James, Paraic; Dai, Jifeng. Immobilized baker's yeast reduction of ketones in an ionic liquid, [bmim]PF6 and water mix. *Tetrahedron Letters*, **2001**, 42, 7517-7519.

31. Huddleston, Jonathan G.; Visser, Ann E.; Reichert, W. Matthew; Willauer, Heather D.; Broker, Grant A.; Rogers, Robin D. Characterization and comparison of hydrophilic and hydrophobic room temperature ionic liquids incorporating the imidazolium cation. *Green Chemistry*, **2001**, 3, 156-164.

32. Huddleston, Jonathan G.; Willauer, Heather D.; Swatloski, Richard P.; Visser, Ann E.; Rogers, Robin D. Room temperature ionic liquids as novel media for 'clean' liquid-liquid extraction. *Chem. Commun.*, **1998**, 1765-1766.

33. Kamps, Alvaro Perez-Salado; Tuma, Dirk; Xia, Jianzhong; Maurer, Gerd. Solubility of CO_2 in the Ionic Liquid [bmim][PF_6]. *ACS Published on the Web*. **2003**.

34. Kanazawa, K.K.; Gordon, J.G., III. Frequency of a Quartz Crystal Microbalance in Contact with Liquid. *Anal. Chem*. **1985**, *57*, 1770.

35. Karmakar, Rana; Samanta, Anunay. Solvation Dynamics of Coumarin-153 in a Room-Temperature Ionic Liquid. *J. Phys. Chem. A*, **2002**, Vol. 106, No. 18, 4447-4452.

36. Kaufman, Eric N.; Harkins, James B.; Borole, Abhijeet. Comparison of Batch-Stirred and Electro-Spray Reactors for Biodesulferization of Dibenzothiophene in Crude Oil and Hydrocarbon Feedstocks. *Appl. Biochemistry and Biotechnology*, **1998**, 73, 127-144.

37. Kim, Il-Kyu; Huang, Chin-Pao; Chiu, Pei C. Sonochemical Decomposition of Dibenzothiophene in Aqueous Solution. *Wat. Res.*, **2001**, Vol. 35, No. 18, 4370-4378.

38. Kim, Kwang-Wook; Song, Boyoung; Choi, Min-Young; Kim, Mahn-Joo. Biocatalysis in Ionic Liquids: Markedly Enhanced Enantioselectivity of Lipase. *Org. Lett.*, **2001**, Vol. 3, No. 10, 1507-1509.

39. Koros, William J.; Mahajan, Rajiv. Pushing the limits on possibilities for large scale gas separation: which strategies? *Journal of Membrane Science*, **2000**, 175, 181-196.

40. Larson, Karen A.; Wiencek, John M. Liquid Ion Exchange for Mercury Removal from Water over a Wide pH Range. *Ind. Eng. Chem. Res.*, **1992**, 31, 2714-2722.

41. Lau, R. Madeira; Rantwijk, F. van; Seddon, K. R.; Sheldon, R. A. Lipase-Catalyzed Reactions in Ionic Liquids. *Organic Letters*, **2000**, Vol. 2, No. 26, 4189-4191.

42. Law, George; Watson, Philip R.; Carmichael, Adrian J.; Seddon, Kenneth R. Molecular composition and orientation at the surface of room-temperature ionic liquids: Effect of molecular structure. *Phys. Chem. Chem. Phys.*, **2001**, 3, 2879-2885.

43. Liang, Chengdu; Yuan, Ching-Yao; Warmack, Robert J.; Barnes, Craig E.; Dai, Sheng. Ionic Liquids: A New Class of Sensing Materials for Detection of Organic Vapors Based on the Use of a Quartz Crystal Microbalance. *Anal. Chem.*, **2002**, 74, 2172-2176.

44. Lozano, Pedro; Diego, Teresa de; Carrie, Daniel; Vaultier, Michel; Iborra, Jose L. Continuous green biocatalytic processes using ionic liquids and supercritical carbon dioxide. *Chem. Commun.*, **2002**, 692-693.

45. Mariz, Carl. Carbon Dioxide Recovery: Large Scale Design Trends. *Journal of Canadian Petroleum Technology*. **1998**, Vol. 37, No. 7, 1-6.

46. Morrison, Linda. Price Quotation for Ionic Liquids from Covalent Associates Inc. June 6, **2002**.

47. Morrow, Timothy I.; Maginn, Edward J. Molecular Dynamics Study of the Ionic Liquid 1-n-Butyl-3-methylimidazolium Hexafluorophosphate. *J. Phys. Chem. B*, **2002**.

48. Muldoon, Mark J.; Gordon, Charles M.; Dunkin, Ian R. Investigations of solvent-solute interactions in room temperature ionic liquids using solvatochromic dyes. J. *Chem. Soc., Perkin Trans. 2*, **2001**, 433-435.

49. Murase, K.; Nitta, K.; Hirato, T.; Awakura, Y. Electrochemical behavior of copper in trimethyl-n-hexylammonium bis((trifluoromethyl)sulfonyl)amide, an ammonium imide-type room temperature molten salt. *J. of Appl. Electrochem.*, **2001**, 31, 10, 1089-1094.

50. Najdanovic-Visak, Vesna; Esperanca, Jose M.S.S.; Rebelo, Luis P.N.; Nunes de Ponte, Manuel; Guedes, Henrique J.R.; Seddon, Kenneth R.; Szydlowski, Jerzy. Phase behaviour of room temperature ionic liquid solutions: an unusually large co-solvent effect in (water + ethanol). *Phys. Chem. Chem. Phys.*, **2002**, 4, 1702-1703.

51. Orme, Christopher J.; Harrup, Mason K.; Luther, Thomas A.; Lash, Robert P.; Houston, Kelly S.; Weinkauf, Donald H.; Stewart, Frederick F. Characterization of gas transport in selected rubbery amorphous polyphosphazene membranes. *Journal of Membrane Science*, **2001**, 186, 249-256.

52. Pereira, Bryan; Admassu, Wudneh. Effects of chemical impurities on gas permeation and diffusion in polymeric membranes. *Separation Science and Technology*, **2001**, Vol. 36, No. 14, 3121-3140.

53. Perry, Robert H.; Green, Dan W.; Maloney, James O. Perry's Chemical Engineers' Handbook: Seventh Edition. *McGraw-Hill*, **1997**.

54. Pope, Bill. Personal Communication from Air Products representative. August 27, **2002**.

55. Prausnitz, John M.; Lichtenhaler, Rudiger N.; Gomes de Azevedo, Edmundo. Molecular Thermodynamics of Fluid-Phase Equilibria: 3rd Edition. Prentice Hall PTR, **1999**, 588-603.

56. Reetz, Manfred T.; Wiesenhofer, Wolfgang; Francio, Giancarlo; Leitner, Walter. Biocatalysis in ionic liquids: batchwise and continuous flow processes using supercritical carbon dioxide as the mobile phase. *Chem. Commun.*, **2002**, 992-993.

57. Ricco, Antonio J.; Crooks, Richard M.; Osbourn, Gordon C. Surface acoustic wave chemical sensor arrays: new chemically sensitive interfaces combined with novel cluster analysis to detect volatile organic compounds and mixtures. *Acc. Chem. Res.*, **1998**, 31, 289-296.

58. Rodahl, Michael; Kasemo, Bengt. Frequency and dissipation-factor responses to localized liquid deposits on a QCM electrode. *Sensors and Actuators B*, **1996**, 37, 111-116.

59. Schafer, Thomas; Rodrigues, Carla, M.; Afonso, Carlos A.M.; Crespo, Joao G. Selective recovery of solutes from ionic liquids by pervaporation- a novel approach for purification and green processing. *Chem. Commun.*, **2001**, 1622-1623.

60. Schofer, Sonja H.; Kaftzik, Nicole; Wasserscheid, Peter; Kragl, Udo. Enzyme catalysis in ionic liquids: lipase catalysed kinetic resolution of 1-phenylethanol with improved enantioselectivity. *Chem. Commun.*, **2001**, 425-426.

61. Scovazzo, Paul; Visser, Ann E.; Davis, James H., Jr.; Rogers, Robin D.; Koval, Carl A.; Dubois, Dan L.; Noble, Richard D. Supported Ionic Liquid Membranes (SILMs) and Facilitated Ionic Liquid Membranes (FILMs), **2002**.

62. Scurto, Aaron M.; Aki, Sudhir N.V.K.; Brennecke, Joan F. CO_2 as a Separation Switch for Ionic Liquid/ Organic Mixtures. *J. Am. Chem. Soc.*, **2002**, 124, 10276-10277.

63. Seddon, Kenneth R.; Stark, Annegret; Torres, Maria-Jose. Influence of chloride, water, and organic solvents on the physical properties of ionic liquids. *Pure Appl. Chem.*, **2000**, Vol. 72, No. 12, 2275-2287.

64. SEEN (Sustainable Energy and Economy Network) website: http://www.seen.org December 6, **2002**.

65. Shah, Jindal K.; Brennecke, Joan F.; Maginn, Edward J. Thermodynamic properties of the ionic liquid 1-n-butyl-3-methylimidizolium hexafluorophosphate from Monte Carlo simulations. *Green Chemistry*, **2002**, 4, 112-118.

66. Sheldon, Roger A.; Madeira Lau, Rute; Sorgedrager, Menno J.; van Rantwijk, Fred. Biocatalysis in Ionic Liquids. *Green Chemistry*, **2002**, 4, 147-151.

67. Simbeck, Dale R. CO_2 Mitigation Economics for Existing Coal-Fired Power Plants. *First National Conference on Carbon Sequestration*, May 14-17, **2001**.

68. Singh, D.J.; Croiset, E.; Douglas, P.L.; Douglas, M.A. CO_2 capture options for an existing coal fired power plant: O_2/CO_2 recycle combustion vs. amine scrubbing. CANMET Energy Technology Center, **2001**.

69. Singh, Rajendra P.; Manandhar, Sudha; Shreeve, Jean'ne. New dense fluoroalkyl-substituted imidazolium ionic liquids. *Tetrahedron Letters*, **2002**, 43, 9497-9499.

70. Song, Choong Eui; Roh, Eun Joo. Practical method to recycle a chiral (salen)Mn epoxidation catalyst by using an ionic liquid. *Chem. Commun.*, **2000**, 837-838.

71. Soria, R. Overview on industrial membranes. *Catalysis Today*, **1995**, 25, 285-290.

72. Stevens, Malcolm P. Polymer Chemistry: An Introduction: 3rd Edition. Oxford University Press, **1999**.

73. Sun, J.; Forsyth, M.; MacFarlane, D.R. Room-Temperature Molten Salts Based on the Quaternary Ammonium Ion. *J. Phys. Chem. B* **1998**, 102, 8858-8864.

74. Swatloski, Richard P.; Visser, Ann E.; Reichert, W. Matthew; Broker, Grant A.; Farina, Lindsy M.; Holbrey, John D.; Rogers, Robin D. On the solubilization of water with ethanol in hydrophobic hexafluorophosphate ionic liquids. *Green Chemistry*, **2002**, 4, 81-87.

75. Swatloski, Richard P.; Visser, Ann E.; Reichert, W. Matthew; Broker, Grant A.; Farina, Lindsy M.; Holbrey, John D.; Rogers, Robin D. Solvation of 1-butyl-3-methylimidazolium hexafluorophosphate in aqueous ethanol- a green solution for dissolving 'hydrophobic' ionic liquids. *Chem. Commun.*, **2001**, 2070-2071.

76. Tsionsky, V.; Gileadi, E. Use of the Quartz Crystal Microbalance for the Study of Adsorption from the Gas Phase. *Langmuir*, **1994**, 10, 2830-2835.

77. Ullevig, Dale M.; Evans, John F.; Albrecht, M. Grant. Effects of Stressed Materials on the Radial Sensitivity Function of the Quartz Crystal Microbalance. *Anal. Chem.*, **1982**, 54, 2341-2343.

78. Visser, Ann E.; Swatloski, Richard P.; Griffin, Scott T.; Hartman, Deborah H.; Rogers, Robin D. Liquid/Liquid Extraction of Metal Ions in Room Temperature Ionic Liquids. *Separation Science and Technology*, **2001**, 36(5&6), 785-804.

79. Visser, Ann E.; Swatloski, Richard P.; Reichert, W. Matthew; Griffin, Scott T.; Rogers, Robin. Traditional Extractants in Nontraditional Solvents: Groups 1 and 2 Extraction by Crown Ethers in Room-Temperature Ionic Liquids. *Ind. Eng. Chem. Res.* **2000**, 39, 3596-3604.

80. Visser, Ann E.; Swatloski, Richard P.; Reichert, W. Matthew; Mayton, Rebecca; Sheff, Sean; Wierzbicki, Andrzej; Davis, James H., Jr.; Rogers, Robin D. Task-specific ionic liquids for the extraction of metal ions from aqueous solutions. *Chem. Commun.*, **2001**, 135-136.

81. Visser, Ann E.; Swatloski, Richard P.; Rogers, Robin D. pH-Dependent partitioning in room temperature ionic liquids provides a link to traditional solvent extraction behavior. *Green Chemistry*, **2000**, 2, 1-3.

82. Von Solms, N.; Nielsen, J.K.; Hassager, O.; Rubin, A.; Dandekar, A.Y.; Andersen, S.I.; Stenby, E.H. Direct Measurement of Gas Solubilities in Polymers Using a High-Pressure Microbalance. *Submitted to Journal of Applied Polymer Science*, **2003**, May be viewed at: 192.38.89.7/IVC-SEP/nvs/Articles/HP_balance_HDPE.pdf.

83. Vu, De Q.; Koros, William J. High Pressure CO_2/CH_4 Separation Using Carbon Molecular Sieve Hollow Fiber Membranes. *Ind. Eng. Chem. Res.*, **2002**, 41, 367-380.

84. Wasserscheid, Peter; Gordon, Charles M,; Hilgers, Claus; Muldoon, Mark J.; Dunkin, Ian R. Ionic Liquids: polar, but weakly coordinating solvents for the first biphasic oligomerisation of ethane to higher alpha-olefins with cationic Ni complexes. *Chem. Commun.*, **2001**, 1186-1187.

85. Welton, Thomas. Room-Temperature Ionic Liquids. Solvents for Synthesis and Catalysis. *Chem. Rev.*, **1999**, 99, 2071-2083.

86. Westney, Richard E. The Engineer's Cost Handbook: Tools for Managing Project Costs. *Westney Consultants International Inc.*, **1997**.

87. Wilkes, John S. A short history of ionic liquids-from molten salts to neoteric solvents. *Green Chemistry*, **2002**, 4, 73-80.

88. Zellers, Edward T.; Batterman, Stuart A.; Han, Mingwei; Patrash, Samual J. Optimal Coating Selection for the Analysis of Organic Vapor Mixtures with Polymer-Coated Surface Acoustic Wave Sensor Arrays. *Anal. Chem.*, **1995**, 67, 1092-1106.

89. Zhang, Jianmin; Yang, Chunhe; Hou, Zhenshan; Han, Buxing; Jiang, Tao; Li, Xiaohong; Zhao, Guoying; Li, Yongfang; Liu, Zhimin, Zhao, Dongbin; Kou,

Yuan. Effect of dissolved CO_2 on the conductivity of the ionic liquid [bmim][PF6]. *New J. Chem.*, **2003**, 27, 333-336.

90. Zhang, S.; Chen, Z. K.; Bao, G. W.; Li, F. Y. Organic vapor detection by quartz crystal microbalance modified with mixed multilayer Langmuir-Blodgett Films. *Talanta*, **1998**, 45, 727-733.

Appendices

Appendix A: QCM Gas Density Affects

The following data illustrate the buoyancy effect observed when a clean quartz crystal is exposed to gases of different molecular weight at various concentrations. The largest frequency shift corresponds to 100 % analyzed gas.

Background Gas: Nitrogen
Analyzed Gas: Carbon Dioxide

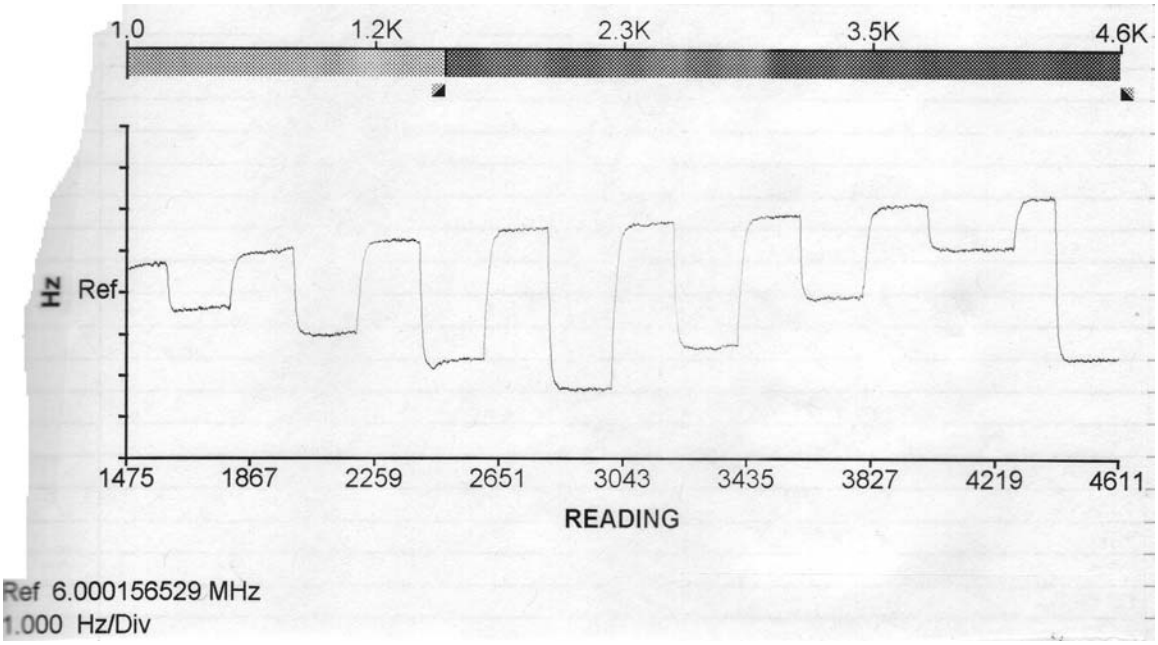

Background Gas: Nitrogen
Analyzed Gas: Helium

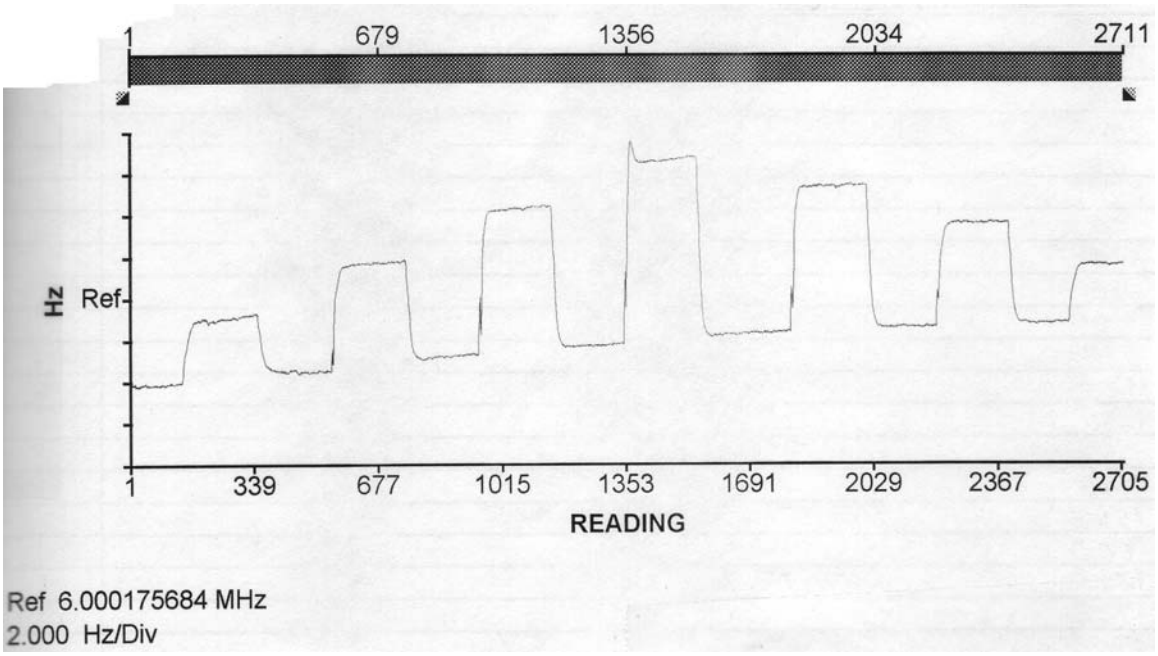

Background Gas: Nitrogen

Analyzed Gas: Argon

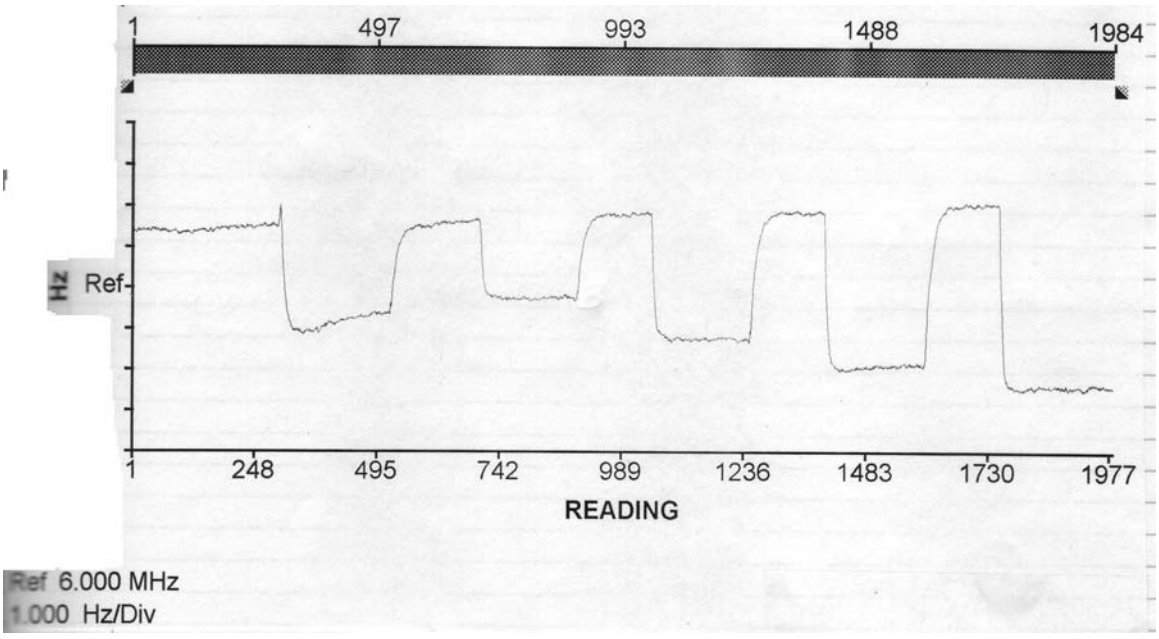

Background Gas: Argon and Nitrogen

Analyzed Gas: Carbon Dioxide

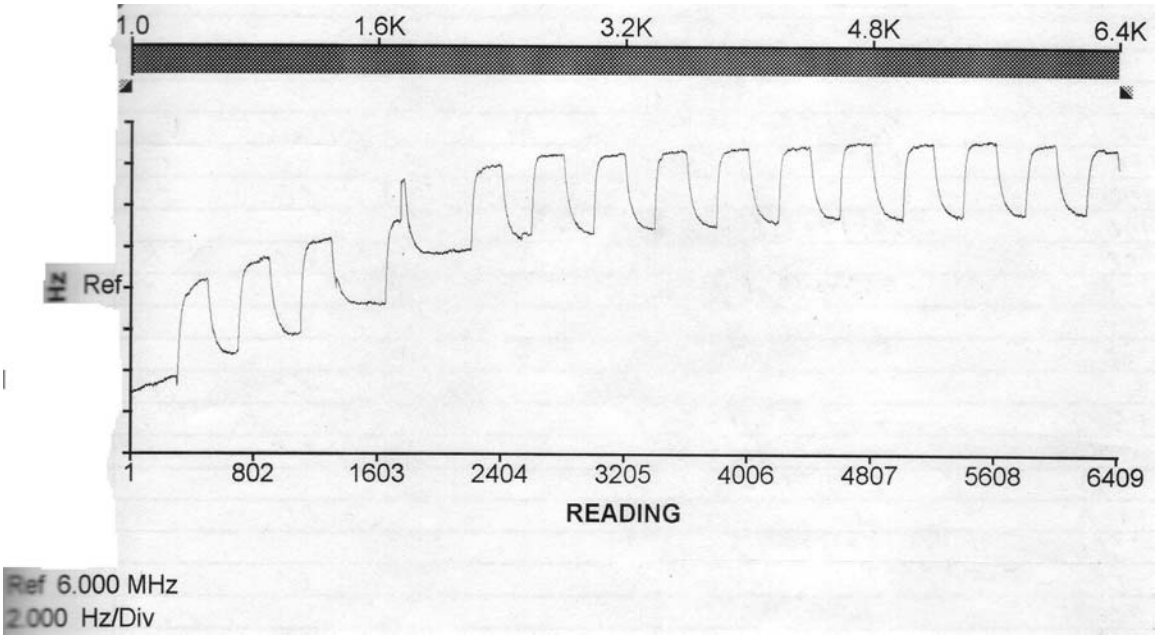
1.0
1.6K
3.2K
4.8K
6.4K
Hz
Ref
1
802
1603
2404
3205
4006
4807
5608
6409
READING
Ref 6.000 MHz
2.000 Hz/Div

Appendix B: QCM Responses to Ionic Liquid with CO_2

The following data illustrate the results from QCM experiments for the ionic liquids response to CO_2 studied in this project. These graphs were used to determine the Henry's Law values of the ionic liquids.

Ionic Liquid: [OctMeIm] Tf_2N

IL Frequency Shift: 562 Hz

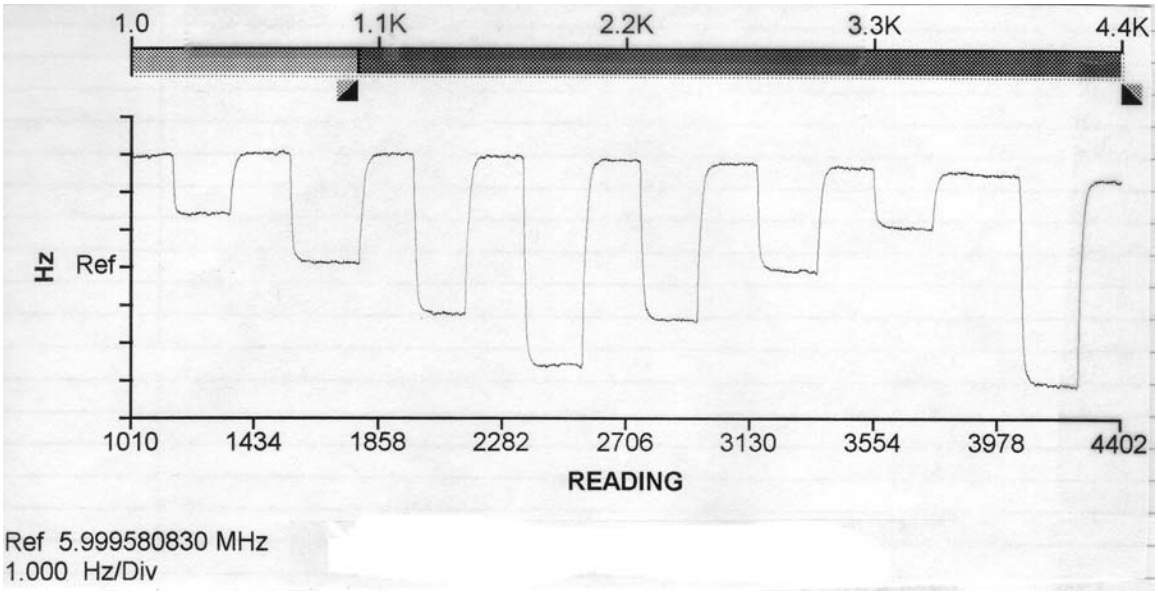

Ionic Liquid: [BuMeIm] Tf_2N

IL Frequency Shift: 579 Hz

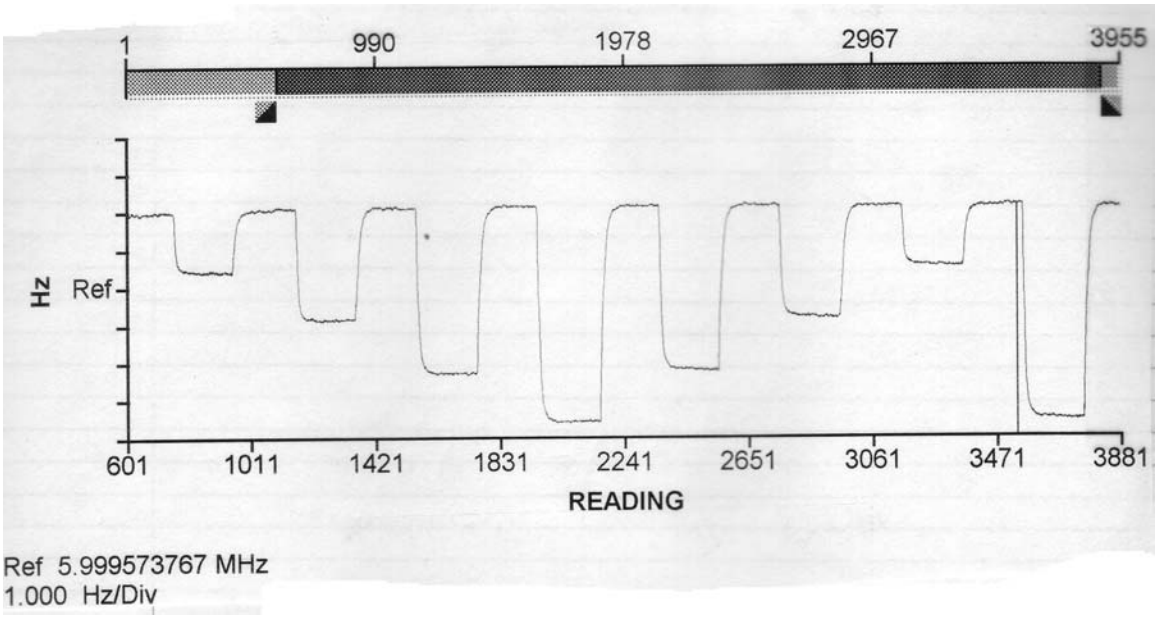

Ionic Liquid: [PrMeIm] Tf_2N

IL Frequency Shift: 569 Hz

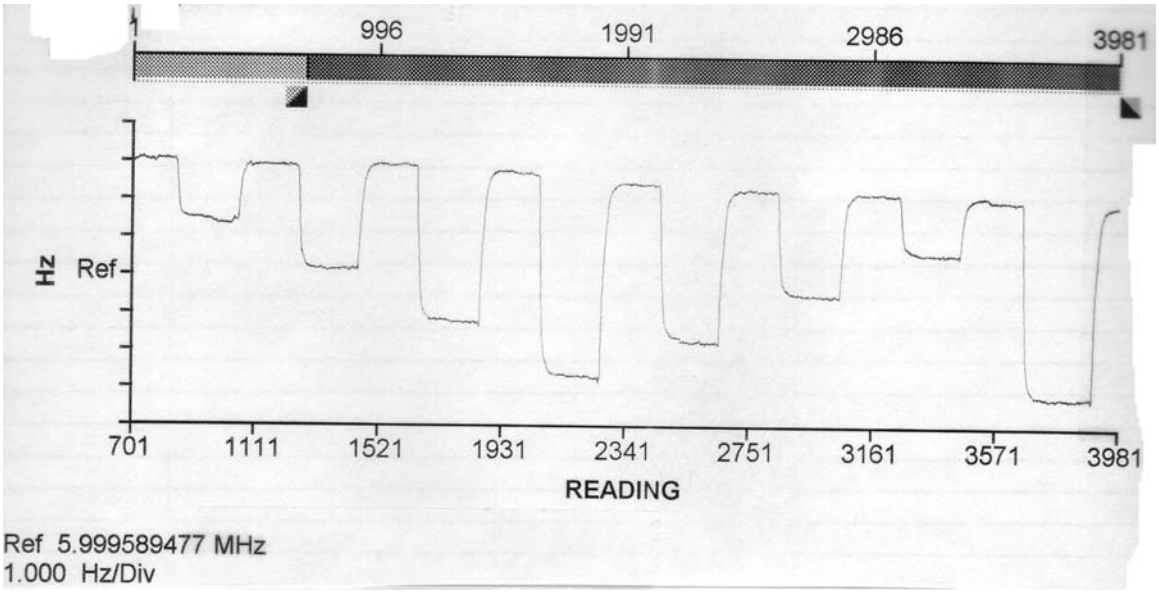

Ionic Liquid: [HexMeIm] Tf_2N

IL Frequency Shift: 430 Hz

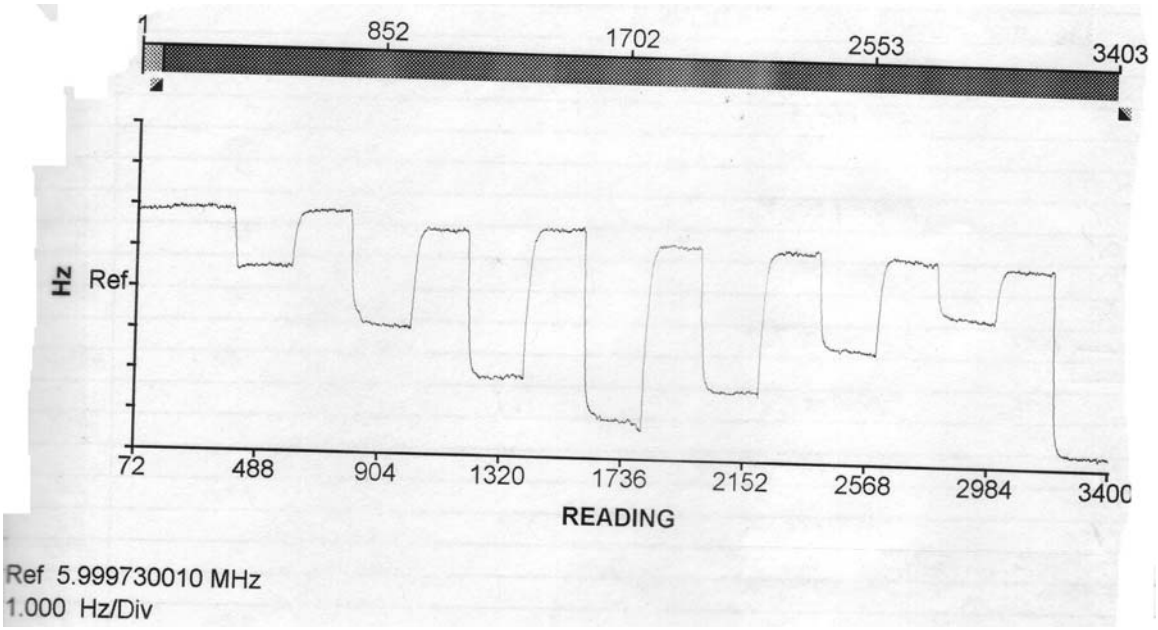

Ionic Liquid: [PrMeIm] PF_6

IL Frequency Shift: 379 Hz

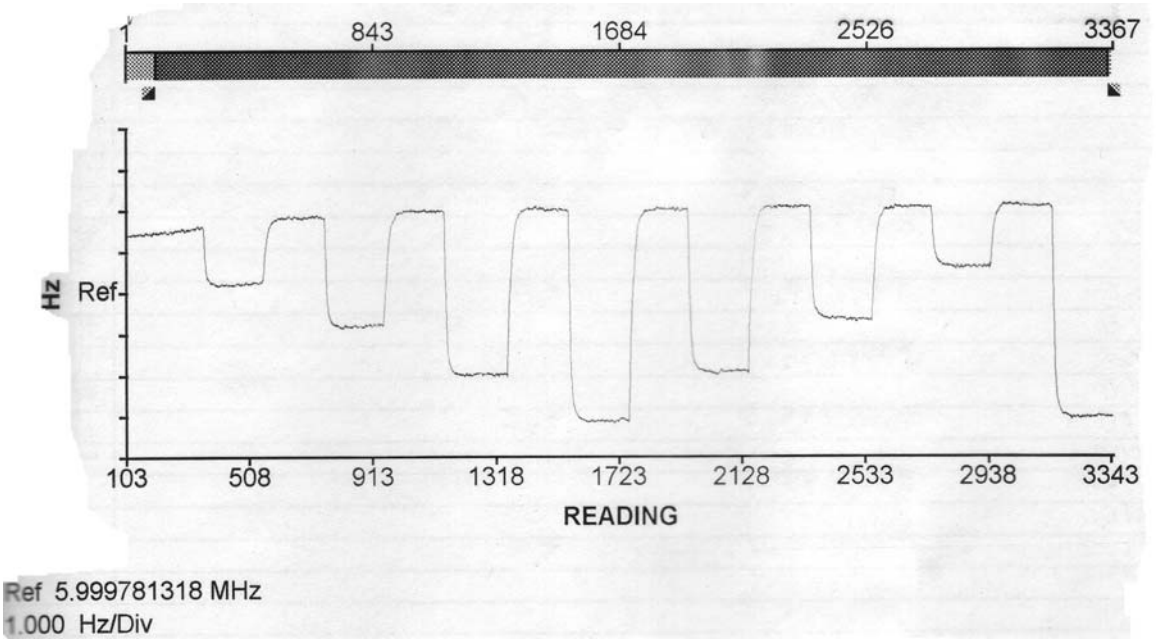

Ionic Liquid: [BuMeIm] Tf_2N with Polyethylenimine

IL Frequency Shift: 642 Hz

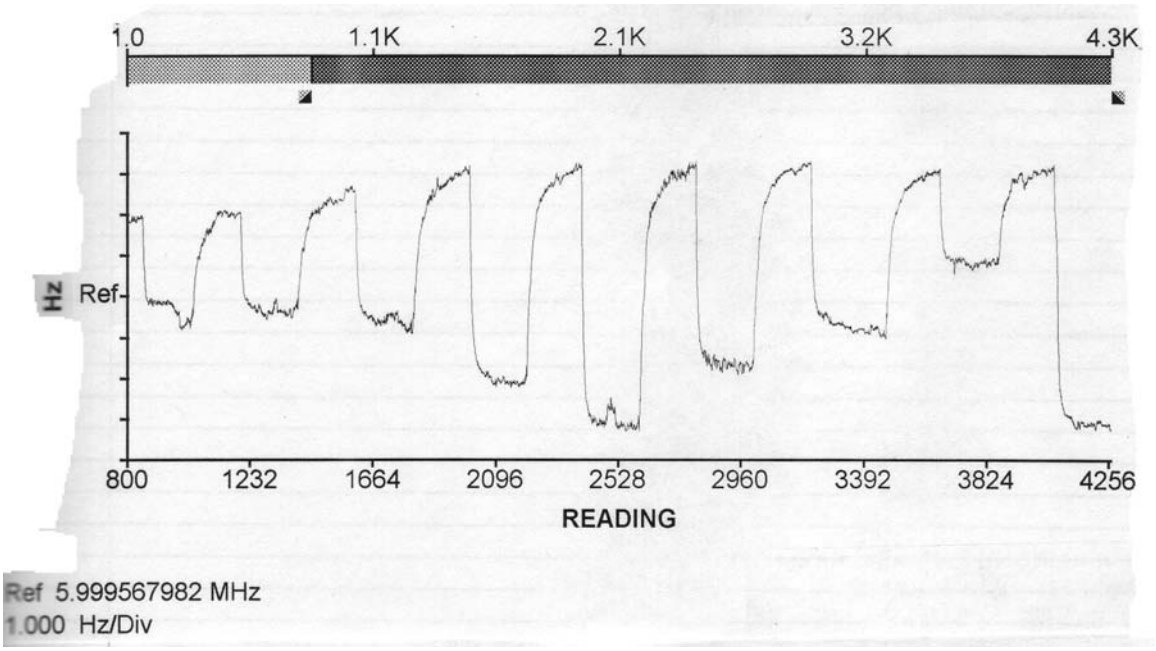

Ionic Liquid: [OctMeIm] Tf_2N with 13 F in place of H on the octyl ligand

IL Frequency Shift: 277 Hz

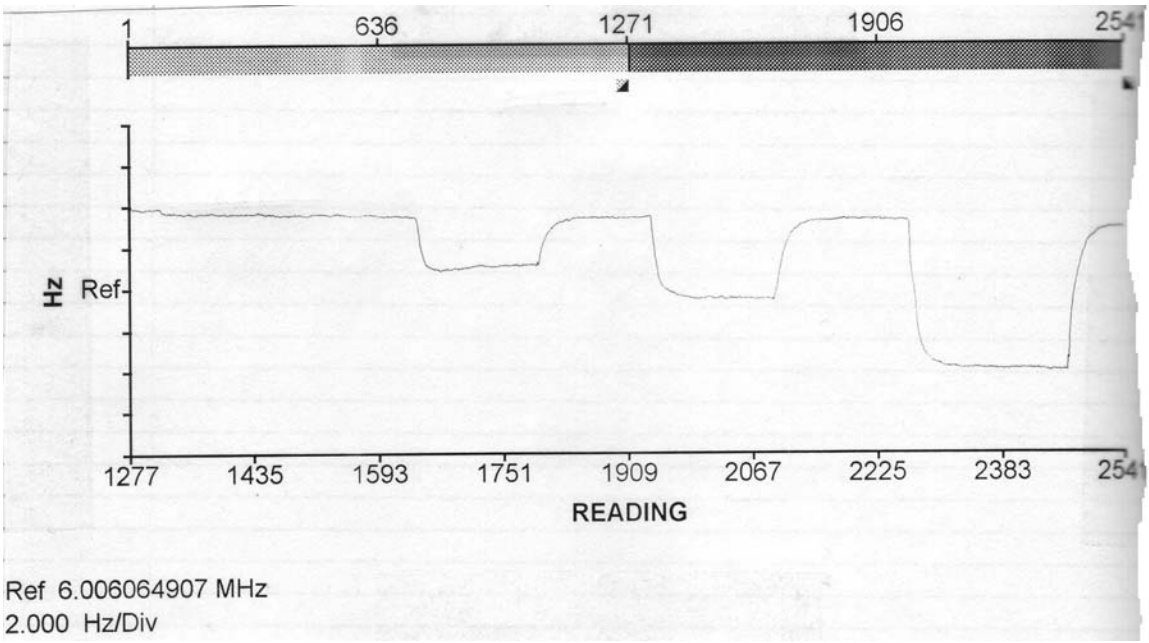

Appendix C: DBT / Ionic Liquid GC Results

The following two GC plots illustrate the manner in which the amount of DBT removed from octane was determined. The first plot shows DBT in octane that was not contacted with ionic liquid. The second plot shows the same DBT in octane solution after contact with the ionic liquid. The decrease in the DBT peak area corresponds to the amount of DBT absorbed by the ionic liquid, because the octane phase is tested each time. The DBT peak elutes around 6 minutes and the peak area is listed on the plots.

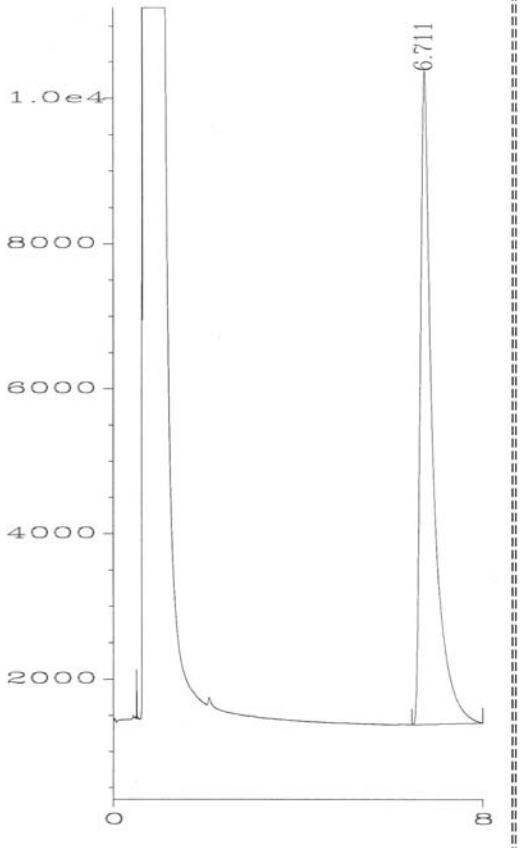


```
================================================================================
                        Area Percent Report
================================================================================

Data File Name   : C:\HPCHEM\1\DATA\091101tk\001F0101.D
Operator         : ktk                      Page Number      : 1
Instrument       : 5890 GC                  Vial Number      : 1
Sample Name      : DBT                      Injection Number : 1
Run Time Bar Code:                          Sequence Line    : 1
Acquired on      : 08 Jan 02  03:04 PM      Instrument Method: AUTO.MTH
Report Created on: 08 Jan 02  03:15 PM      Analysis Method  : AUTO.MTH
Sample Info      :


Sig. 1 in C:\HPCHEM\1\DATA\091101tk\001F0101.D
   Pk#  Ret Time     Area        Height      Type   Width    Area %
  |---|----------|----------|----------|----|---------|----------|
     1    6.711     168830        9002   BBA    0.252    100.0000

Total area = 168830
```

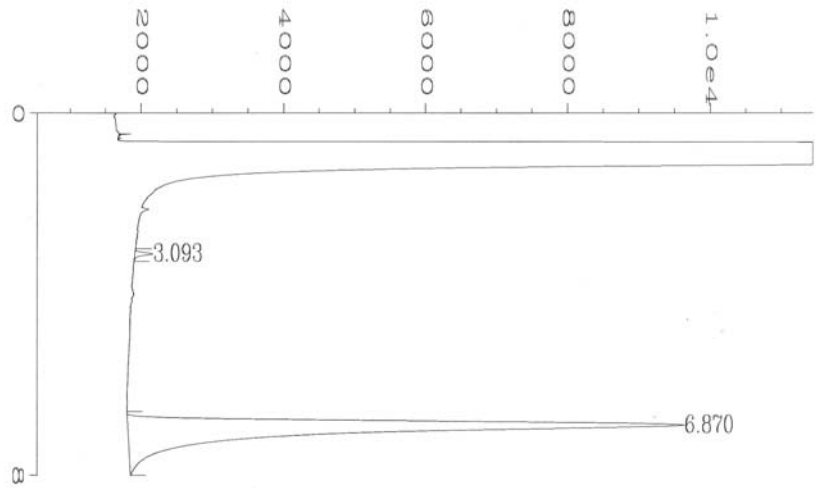

==========

Area Percent Report

==========

Data File Name : C:\HPCHEM\1\DATA\091101tk\002F0101.D
Operator : ktk
Instrument : 5890 GC
Sample Name : DBT+Old IL
Run Time Bar Code:
Acquired on : 08 Jan 02 03:56 PM
Report Created on: 08 Jan 02 04:06 PM
Sample Info :

Page Number : 1
Vial Number : 2
Injection Number : 1
Sequence Line : 1
Instrument Method: AUTO.MTH
Analysis Method : AUTO.MTH

Sig. 1 in C:\HPCHEM\1\DATA\091101tk\002F0101.D

Pk#	Ret Time	Area	Height	Type	Width	Area %
1	3.093	1107	257	BB	0.065	0.7733
2	6.870	142009	7830	BBA	0.241	99.2267

Total area = 143116

Appendix D: QCM Data Obtained for CO_2 Solubility in Ionic Liquids

Ionic Liquid: PrMeIm Tf_2N

Mole Fraction CO_2	Partial P_{CO2} atm	f_{IL}	$(f_{IL}-f_{CC})/\Delta f_{IL}*MW_{IL}/MW_g+1$
0.256	0.256	1.552	0.389
0.488	0.488	2.959	0.472
0.745	0.745	4.515	0.716
1.000	1.000	6.063	0.851
0.745	0.745	4.515	0.728
0.488	0.488	2.959	0.503
0.256	0.256	1.552	0.320
1.000	1.000	6.063	0.763
0.256	0.256	1.552	0.269
0.488	0.488	2.959	0.395
0.745	0.745	4.515	0.642
1.000	1.000	6.063	0.712
0.745	0.745	4.515	0.656
0.488	0.488	2.959	0.448
0.256	0.256	1.552	0.296
1.000	1.000	6.063	0.830
0.256	0.256	1.552	0.257
0.488	0.488	2.959	0.498
0.745	0.745	4.515	0.687
1.000	1.000	6.063	0.874
0.745	0.745	4.515	0.750
0.488	0.488	2.959	0.562
0.256	0.256	1.552	0.314
1.000	1.000	6.063	0.874
0.256	0.256	1.552	0.284
0.488	0.488	2.959	0.621
0.745	0.745	4.515	0.905
1.000	1.000	6.063	1.166
0.745	0.745	4.515	0.929
0.488	0.488	2.959	0.659
0.256	0.256	1.552	0.352
1.000	1.000	6.063	1.187

H (atm)	**error (+/-)**
36.8	**7.0**

SUMMARY OUTPUT

Regression Statistics	
Multiple R	0.900796515
R Square	0.811434362
Adjusted R Square	0.805148841
Standard Error	0.124824493
Observations	32

ANOVA

	df	*SS*	*MS*	*F*	*Significance F*
Regression	1	2.011461477	2.011461477	129.0957947	2.1576E-12
Residual	30	0.467434624	0.015581154		
Total	31	2.478896101			

	Coefficients	*Standard Error*	*t Stat*	*P-value*	*Lower 95%*	*Upper 95%*
Intercept	-0.04131404	0.062421358	-0.661857439	0.513114828	-0.168795328	0.086167248
X Variable 1	38.95259951	3.428312468	11.36203304	2.1576E-12	31.9510586	45.95414043

Ionic Liquid: BuMeIm Tf_2N

Mole Fraction CO_2	Partial P_{CO2} atm	f_{IL}	$(f_{IL}-f_{CC})/\Delta f_{IL} * MW_{IL}/MW_g + 1$
0.256	0.256	1.375	0.336
0.488	0.488	2.621	0.617
0.745	0.745	4.000	0.876
1.000	1.000	5.372	1.074
0.745	0.745	4.000	0.852
0.488	0.488	2.621	0.641
0.256	0.256	1.375	0.342
1.000	1.000	5.372	1.068
0.256	0.256	1.375	-0.004
0.488	0.488	2.621	0.562
0.745	0.745	4.000	0.677
1.000	1.000	5.372	0.801
0.745	0.745	4.000	0.777
0.488	0.488	2.621	0.482
0.256	0.256	1.375	0.312
1.000	1.000	5.372	0.822
0.256	0.256	1.375	0.452
0.488	0.488	2.621	0.485
0.745	0.745	4.000	0.662
1.000	1.000	5.372	0.796
0.745	0.745	4.000	0.677
0.488	0.488	2.621	0.539
0.256	0.256	1.375	0.388
1.000	1.000	5.372	0.654

H (atm)	**error (+/-)**
37.0	**3.4**

SUMMARY OUTPUT

Regression Statistics	
Multiple R	0.862414019
R Square	0.74375794
Adjusted R Square	0.700279679
Standard Error	0.143919978
Observations	24

ANOVA

	df	*SS*	*MS*	*F*	*Significance F*
Regression	1	1.382773994	1.382773994	66.75887883	4.15125E-08
Residual	23	0.476398082	0.02071296		
Total	24	1.859172076			

	Coefficients	*Standard Error*	*t Stat*	*P-value*	*Lower 95%*	*Upper 95%*
Intercept	0	#N/A	#N/A	#N/A	#N/A	#N/A
X Variable 1	36.9551072	1.628084986	22.69851238	3.01216E-17	33.58716139	40.32305301

Ionic Liquid: HexMeIm Tf_2N

Mole Fraction CO_2	Partial P_{CO2} atm	f_{IL}	$(f_{IL}-f_{CC})/\Delta f_{IL} * MW_{IL}/MW_g + 1$
0.256	0.256	1.700	0.442
0.488	0.488	3.040	0.717
0.745	0.745	4.460	0.976
1.000	1.000	5.640	1.088
0.745	0.745	4.440	0.964
0.488	0.488	2.990	0.685
0.256	0.256	1.720	0.455
1.000	1.000	5.680	1.114
0.256	0.256	1.400	0.295
0.488	0.488	2.570	0.490
0.745	0.745	3.840	0.683
1.000	1.000	4.740	0.604
0.745	0.745	3.720	0.593
0.488	0.488	2.580	0.498
0.256	0.256	1.490	0.362
1.000	1.000	4.850	0.687
0.256	0.256	1.360	0.285
0.488	0.488	2.780	0.699
0.745	0.745	3.570	0.518
1.000	1.000	4.710	0.628
0.745	0.745	3.510	0.470
0.488	0.488	2.410	0.400
0.256	0.256	1.360	0.285
1.000	1.000	4.530	0.482

H (atm)	**error (+/-)**
34.2	**5.1**

SUMMARY OUTPUT

Regression Statistics	
Multiple R	0.608758751
R Square	0.370587217
Adjusted R Square	0.327108956
Standard Error	0.225560815
Observations	24

ANOVA

	df	*SS*	*MS*	*F*	*Significance F*
Regression	1	0.688985406	0.688985406	13.54199697	0.001312194
Residual	23	1.17018667	0.050877681		
Total	24	1.859172076			

	Coefficients	*Standard Error*	*t Stat*	*P-value*	*Lower 95%*	*Upper 95%*
Intercept	0	#N/A	#N/A	#N/A	#N/A	#N/A
X Variable 1	34.20828161	2.442717817	14.00418885	9.56114E-13	29.15514169	39.26142153

Ionic Liquid: OctMeIm Tf_2N

Mole Fraction CO_2	Partial P_{CO2} atm	f_{IL}	$(f_{IL}-f_{CC})/\Delta f_{IL} * MW_{IL}/MW_g + 1$
0.256	0.256	1.650	0.013
0.488	0.488	2.840	0.018
0.745	0.745	4.160	0.024
1.000	1.000	5.530	0.032
0.745	0.745	4.150	0.024
0.488	0.488	2.810	0.018
0.256	0.256	1.510	0.010
1.000	1.000	5.550	0.032
0.256	0.256	1.570	0.011
0.488	0.488	2.910	0.019
0.745	0.745	4.250	0.025
1.000	1.000	5.520	0.030
0.745	0.745	4.240	0.025
0.488	0.488	2.870	0.018
0.256	0.256	1.590	0.011
1.000	1.000	5.590	0.032
0.256	0.256	1.570	0.013
0.488	0.488	2.570	0.015
0.745	0.745	3.860	0.021
1.000	1.000	5.200	0.028
0.745	0.745	3.950	0.023
0.488	0.488	2.740	0.019
0.256	0.256	1.400	0.009
1.000	1.000	5.420	0.033
1.000	2.361	8.100	0.073
1.000	2.361	8.300	0.077
1.000	2.361	8.500	0.080
1.000	3.042	11.900	0.106
1.000	3.042	11.500	0.099
1.000	3.042	11.100	0.092
1.000	3.723	14.800	0.123
1.000	3.723	14.000	0.110
1.000	3.723	14.500	0.118

H (atm)	**error (+/-)**
31.9	**1.0**

SUMMARY OUTPUT

Regression Statistics

Multiple R	0.996192189
R Square	0.992398878
Adjusted R Square	0.992153681
Standard Error	0.003229257
Observations	33

ANOVA

	df	*SS*	*MS*	*F*	*Significance F*
Regression	1	0.042206114	0.042206114	4047.34545	2.03197E-34
Residual	31	0.000323271	1.04281E-05		
Total	32	0.042529385			

	Coefficients	*Standard Error*	*t Stat*	*P-value*	*Lower 95%*	*Upper 95%*
Intercept	0.001708132	0.000845533	2.020183009	0.052077576	-1.63455E-05	0.003432609
X Variable 1	0.031340374	0.000492628	63.61875077	2.03197E-34	0.030335653	0.032345096

Ionic Liquid: PrMeIm PF_6

Mole Fraction CO_2	Partial P_{CO2} atm	f_{IL}	$(f_{IL}-f_{CC})/\Delta f_{IL} * MW_{IL}/MW_g + 1$
0.256	0.256	1.650	0.388
0.488	0.488	2.840	0.558
0.745	0.745	4.160	0.744
1.000	1.000	5.530	0.964
0.745	0.745	4.150	0.738
0.488	0.488	2.810	0.540
0.256	0.256	1.510	0.304
1.000	1.000	5.550	0.976
0.256	0.256	1.570	0.378
0.488	0.488	2.910	0.668
0.745	0.745	4.250	0.887
1.000	1.000	5.520	1.066
0.745	0.745	4.240	0.881
0.488	0.488	2.870	0.641
0.256	0.256	1.590	0.392
1.000	1.000	5.590	1.113
0.256	0.256	1.360	0.262
0.488	0.488	2.340	0.314
0.745	0.745	3.450	0.386
1.000	1.000	4.350	0.309
0.745	0.745	3.410	0.356
0.488	0.488	2.390	0.351
0.256	0.256	1.270	0.195
1.000	1.000	4.400	0.346

H (atm)	**error (+/-)**
47.6	**7.8**

SUMMARY OUTPUT

Regression Statistics	
Multiple R	0.489996208
R Square	0.240096283
Adjusted R Square	0.196618023
Standard Error	0.247842146
Observations	24

ANOVA

	df	*SS*	*MS*	*F*	*Significance F*
Regression	1	0.446380306	0.446380306	7.266992384	0.013204315
Residual	23	1.41279177	0.061425729		
Total	24	1.859172076			

	Coefficients	*Standard Error*	*t Stat*	*P-value*	*Lower 95%*	*Upper 95%*
Intercept	0	#N/A	#N/A	#N/A	#N/A	#N/A
X Variable 1	47.62334643	3.782843919	12.58929722	8.44009E-12	39.79794822	55.44874464

Appendix E: Derivation of Equation for Distribution Coefficient

Definition of Distribution Coefficient:

$$K_D = \frac{C_{IL}}{C_f}$$

Material Balance:

$$N_{DBT} = C_i\, V_{Oct} = C_f\, V_{Oct} + C_{IL}\, V_{IL}$$

Solving the material balance for C_{IL} yields:

$$C_{IL} = (C_i - C_f)\,\frac{V_{Oct}}{V_{IL}}$$

Substituting this equation for C_{IL} into the definition of K_D yields Equation (2-1):

$$K_D = \frac{(C_i - C_f)}{C_f}\,\frac{V_{Oct}}{V_{IL}} = \left(\frac{(C_i)}{(C_f)} - 1\right)\frac{V_{Oct}}{V_{IL}}$$

Appendix F: Derivation of Henry's Law Equation from Sauerbrey Equation

General definition of Henry's Law value:

$$H\ x = y\ P$$

For pure gases Henry's Law can be simplified into:

$$H = \frac{P}{x}$$

Sauerbrey Equation:

$$\Delta f = \frac{-2 \cdot \Delta m n f_o^2}{A\sqrt{\mu_q \rho_q}}$$

The Sauerbrey Equation can be simplified to the following form when comparing two frequency shifts (the shift associated with applying the ionic liquid to the QCM and the shift when the QCM is exposed to gas.

$$\frac{\Delta f_g}{\Delta f_{IL} + \Delta f_g} = \frac{\Delta m_g}{\Delta m_{IL} + \Delta m_g} \qquad \text{where } \Delta f_g = f_{IL} - f_{CC}$$

This expression can be converted to a mole fraction of gas in the ionic liquid using the following equation:

$$x = \frac{\frac{(f_{IL} - f_{CC})}{MW_g}}{\frac{\Delta f_{IL}}{MW_{IL}} + \frac{(f_{IL} - f_{CC})}{MW_g}} = \frac{\frac{\Delta m_g}{MW_g}}{\frac{\Delta m_{IL}}{MW_{IL}} + \frac{\Delta m_g}{MW_g}}$$

Plugging this value for *x* into the simplified Henry's Law equation yields the following equation which is equal to Equation (3-1):

$$H = \left(\frac{\frac{\Delta f_{IL}}{MW_{IL}} + \frac{(f_{IL} - f_{CC})}{MW_g}}{\frac{(f_{IL} - f_{CC})}{MW_g}} \right) P = \left(1 + \frac{\Delta f_{IL}\ MW_g}{(f_{IL} - f_{CC})\ MW_{IL}} \right) P$$

Appendix G: Derivation of Equation for Gas Permeance

Definition of Permeance:

$$Permeance = \frac{CO_2\ Flux}{\Delta P_{CO_2}} = \frac{\frac{dN_{CO2}}{dt}\frac{1}{A}}{P_{up} - P_{CO2}} = \frac{\frac{V}{R\ T\ A}\frac{dP}{dt}}{P_{up} - P_{CO2}}$$

Equation for pressure (P):

$$P_{CO2} = P\ y_{CO2} = P\frac{N_{CO2}}{N} = P\left[\frac{N - N_o}{N}\right] = P - P_o$$

Rearranging this equation and plugging back into the original permeance equation yields:

$$\frac{dP}{dt} = \frac{A\ R\ T\ Permeance}{V}\left(P_{up} + P_o - P\right)$$

Rearranging this equation yields the following:

$$\int_{P_o}^{P} \frac{dP}{\left(P_{up} + P_o - P\right)} = \int_0^t \frac{A\ R\ T\ Permeance}{V} dt$$

Integrating both sides of this equation yields:

$$\ln\left(P_{up} + P_o - P\right) - \ln(P_{up} + P_o - P_o) = \frac{A\ R\ T\ Permeance\ t}{V}$$

The left side of the equation can be further simplified:

$$\ln\left(P_{up} + P_o - P\right) - \ln(P_{up}) = \ln\frac{P_{up} + P_o - P}{P_{up}} = \ln\frac{P - P_{up} - P_o}{-P_{up}}$$

Using this simplification, Equation (3-3) is shown:

$$\ln\frac{P - P_{up} - P_o}{-P_{up}} = \frac{A\ R\ T\ Permeance\ t}{V}$$

Vita

Benjamin Culbertson was born in Birmingham, Alabama on February 12, 1978. He attended The Webb School in Bell Buckle, Tennessee for high school. He then moved on to study Chemistry at the University of the South in Sewanee, Tennessee, where he received a Bachelors in Science in Chemistry. Following his graduation, Benjamin entered the Masters' program in Chemical Engineering at the University of Tennessee, Knoxville. He conducted his graduate research at the Oak Ridge National Laboratory.